

Supporting Information

Groups 1, 2 and Zn(II) Heterodinuclear Catalysts for Exopoxide/CO₂ Ring Opening Copolymerization.

Arron C. Deacy, Christopher B. Durr, Jennifer A. Garden, Andrew J. P. White and Charlotte K. Williams*

*Department of Chemistry, University of Oxford, Oxford, OX1 3TA, UK

Part A: Experimental Section.....	4
Part B: Characterisation.....	7
Part C: X – Ray Crystallographic Data.....	47
Figure S1: ¹ H NMR of 1 (<i>d</i> ₈ -THF, 298 K).....	7
Figure S2: 2D HSQC NMR of 1 (<i>d</i> ₈ -THF, 298 K).....	7
Figure S3: 2D COSY NMR of 1 (<i>d</i> ₈ -THF, 298 K).....	8
Figure S4: ¹³ C NMR of 1 (<i>d</i> ₈ -THF, 298 K).....	8
Figure S5: ⁷ Li NMR of 1 (<i>d</i> ₈ -THF, 298 K).....	9
Figure S6: ¹ H NMR of 2 (<i>d</i> ₈ -THF, 298 K).....	9
Figure S7: 2D HSQC NMR of 2 (<i>d</i> ₈ -THF, 298 K).....	10
Figure S8: 2D COSY NMR of 2 (<i>d</i> ₈ -THF, 298 K)	10
Figure S9: ¹³ C NMR of 2 (<i>d</i> ₈ -THF, 298 K).....	11
Figure S10: ¹ H NMR of 3 (<i>d</i> ₈ -THF, 298 K).....	11
Figure S11: 2D HSQC NMR of 3 (<i>d</i> ₈ -THF, 298 K).....	12
Figure S12: 2D COSY NMR of 3 (<i>d</i> ₈ -THF, 298 K)	12
Figure S13: ¹³ C NMR of 3 (<i>d</i> ₈ -THF, 298 K).....	13
Figure S14: ORTEP representation of the molecular structure of 1 , with disorder and hydrogen atoms (excluding N-H) omitted for clarity and thermal ellipsoids represented at 30 % probability.	14
Figure S15: ORTEP representation of the molecular structure of 2 , with disorder and hydrogen atoms (excluding N-H) omitted for clarity with thermal ellipsoide represented at 30 % probability.....	15
Figure S16: 2D DOSY of 1 (<i>d</i> ₈ -THF, 298 K)	16
Figure S17: 2D DOSY of 2 (<i>d</i> ₈ -THF, 298 K)	16
Figure S18: 2D DOSY of 3 (<i>d</i> ₈ -THF, 298 K)	16
Figure S19: ¹ H NMR of 4a (<i>d</i> ₈ -THF, 298 K).....	17
Figure S20: ¹ H NMR of 4a (<i>d</i> ₂ -TCE, 403 K).....	17
Figure S21: ¹³ C NMR of 4a (<i>d</i> ₂ -TCE, 403 K).....	18
Figure S22: ¹ H NMR of 4b (<i>d</i> ₈ -THF, 298 K)	18
Figure S23: ¹ H NMR of 4b (<i>d</i> ₂ -TCE, 403 K).....	19
Figure S24: ¹³ C NMR of 4b (<i>d</i> ₂ -TCE, 403 K). Unfortunately, aromatic quaternary carbons were not able to be observed in the ¹³ C NMR as previously reported with a dinuclear zinc phenyl catalyst. ¹ ...	19
Figure S25: ¹⁹ F NMR of 4b (<i>d</i> ₂ -TCE, 403 K).....	20

Figure S26: 2D DOSY NMR of complex 4a (d_8 -THF, 298 K).....	20
Figure S27: 2D DOSY NMR of complex 4b (d_8 -THF, 298 K)	21
Figure S28: MALDI-ToF mass spectrum of 4a . An m/z of 808 was observed and assigned to the complex cation $[LZn_2(I)]^+$	21
Figure S29: MALDI-ToF mass spectrum of 4b . An m/z of 868 was obseereved and assigned to the complex cation $[LZn_2(OBzpCF_3)]^+$	22
Figure S30: ORTEP representation of the molecular structure of 4a , with disorder and hydrogen atoms (excluding N-H) omitted for clarity with thermal ellipsoids represented at 30 % probability. .	23
Figure S31: ORTEP representation of the molecular structure of 4b , with disorder and hydrogen atoms (excluding N-H) omitted for clarity with thermal ellipsodies represented at 30 % probability.	24
Figure S32: Metal redistribution reaction between 1 and 4a (d_8 -THF).	25
Figure S33: Metal redistribution reaction between 3 and 4a (d_8 -THF).	25
Figure S34: COSY NMR of product formed from metal redistribution reaction between 1 and 4a (d_8 -THF).....	26
Figure S35: Metal redistribution reaction between 2 and 4a . (d_8 -THF).	26
Figure S36: 1H NMR of complex 5a prepared through sequential metatlation (d_8 -THF, 298 K).....	27
Figure S37: 1H NMR of complex 7a prepared through sequential metatlation. (d_8 -THF, 298 K).....	27
Figure S38: 1H NMR spectrum of 5a (d_5 -pyridine, 403 K).	28
Figure S39: COSY NMR of complex 5a (d_5 -pyridine, 403 K).	28
Figure S40: 1H NMR of complex 6a (d_8 -THF, 298 K).....	29
Figure S41: COSY NMR of complex 6a (d_8 -THF, 298 K).	29
Figure S42: Metal redistribution of complex 6a towards complexes 2 and 4a as observed in 1H NMR (d_8 -THF, 298 K)	30
Figure S43: 1H NMR of complex 5b (d_8 -dioxane, 403 K).	30
Figure S44: COSY NMR of complex 5b (d_8 -dioxane, 403 K).	31
Figure S45: 1H NMR of complex 7b (d_8 -THF, 298 K).....	31
Figure S46: HSQC NMR of complex 7b (d_8 -THF, 298 K).	32
Figure S47: COSY NMR of complex 7b (d_8 -THF, 298K).....	32
Figure S48: ^{13}C NMR of complex 7b (d_8 -THF, 298 K).....	33
Figure S49: ^{19}F NMR of complex 7b (d_8 -THF, 298 K).	33
Figure S50: 2D DOSY NMR of complex 7b (d_8 -THF, 298 K).	34
Figure S51: MALDI-ToF mass spectrum of complex 5a	34
Figure S52: MALDI-ToF mass spectrum of complex 5b	35
Figure S53: MALDI-ToF mass spectrum of complex 7a	35
Figure S54: MALDI-ToF mass spectrum of complex 7b	36
Figure S55: ORTEP representation of the molecular structure of 5b , with disorder and hydrogen atoms (excluding N-H) omitted for clarity with thermal elipsoids represented at 30 %.....	37
Figure S56: 1H NMR of 8a (d_8 -THF, 298 K).....	38
Figure S57: 2D COSY NMR of 8a (d_8 -THF, 298 K).	38
Figure S58: HSQC NMR of complex 8a (d_8 -THF, 298 K).....	39
Figure S59: ^{13}C NMR of 8a (d_8 -THF, 298 K).....	39
Figure S60: 1H NMR of 9a (d_8 -THF, 298 K).....	40
Figure S61: 2D HSQC NMR of 9a (d_8 -THF, 298 K).....	40
Figure S62: 2D COSY NMR of 9a (d_8 -THF, 298 K).	41
Figure S63: ^{13}C NMR of complex 9a (d_8 -THF, 298 K)	41

Figure S64: 2D DOSY NMR of 8a (d_8 -THF, 298 K).....	42
Figure S65: 2D DOSY NMR of 9a (d_8 -THF, 298 K).....	42
Figure S66: MALDI-ToF of complex 8a	43
Figure S67: MALDI-ToF mass spectrum of 9a	43
Figure S68: ORTEP representation of the molecular structure of 8a , with disorder and hydrogen atoms (excluding N-H) omitted for clarity with thermal ellipsoids represented at 30 %.....	44
Figure S69: ORTEP representation of the molecular structure of 9a , with disorder and hydrogen atoms (excluding N-H) omitted for clarity with thermal ellipsoids represented at 30 %.....	45
Figure S70: Representative example of ^1H NMR spectrum of a typical CO ₂ -CHO ring opening copolymerisation forming both poly(cyclohexene oxide) and <i>trans</i> -cyclic carbonate (CDCl ₃ , 298 K). ..	46
Figure S71: Representative example of ^1H NMR spectrum of a typical CO ₂ -CHO reaction forming the <i>cis</i> -cyclic carbonate (CDCl ₃ , 298 K).....	46

Part A: Experimental Section

General Experimental

All experimental manipulations were performed using a dual-manifold nitrogen-vacuum Schlenk line or in a nitrogen filled glovebox. All solvents and reagents were obtained from commercial sources and used as received unless stated otherwise. THF and pentane were obtained from an SPS system, degassed by several freeze-pump-thaw cycles, further dried with 3 Å molecular sieves and stored under nitrogen. Cyclohexene oxide was dried over calcium hydride, overnight, and purified via fractional distillation prior to use and stored under an inert atmosphere. Research-grade carbon dioxide was dried through a drierite column and two additional drying columns (Micro Torr, Model number: MC1-804FV) in series before use in copolymerisation studies. ¹H, ⁷Li, ¹³C, ¹⁹F and 2D NMR (COSY, HSQC and DOSY) spectra were obtained using a Bruker AV 400 MHz spectrometer, at 298 K, unless stated otherwise. MALDI-ToF analysis was performed on a Micromass MALDI micro MX spectrometer. The matrix used was trans-2-[3-(4-tert-butylphenyl)-2-methyl-2-propenylidene]-malonitrile. The samples were prepared as follows: 19 mg/mL THF solutions of complex and matrix were mixed together. This mixture (2 µL) was then spotted on the MALDI-plate and allowed to dry. All sample preparations were carried out in a nitrogen filled glovebox. Gel permeation chromatography analysis was carried out on a two mixed bed PSS SDV linear S column in series, with THF as the eluent at a flow rate of 1mL/min on a Shimadzu LC-20AD instrument at 40 °C. Polymer molecular weight (M_n) was determined by comparison against polystyrene standards. The polymer samples were dissolved in HPLC-grade THF (10 mg/mL) and filtered through a 0.20 µm porous filter frit prior to analysis. Elemental analysis was determined by Mr. Stephen Boyer at London Metropolitan University.

General Procedure for LM₂ where M = Li, Na, K.

MN(SiMe₃)₂ (1.81 mmol) was added to a solution of H₂L (0.50 g, 0.91 mmol) in THF (10 mL) and stirred for 16 h. The solution was reduced in vacuo to dryness and the crude product was washed with pentane (3 x 5 mL) to afford a white solid.

Complex 1: (0.42 g, 0.75 mmol, 83 %). ¹H NMR (d₈-THF, 400.20 MHz, 298 K) 6.87 (s, 4H, PhH) 3.57 (s, 8H, Ph-CH₂-NH) 2.46 (d, 8H, ³J = 7.37 Hz, CH₂-C(CH₃)₂) 1.41 (q, 4H, ³J = 6.27 Hz, NH) 1.22 (s, 18H, C(CH₃)₃) 0.89 (s, 12H, C(CH₃)₂). ⁷Li NMR (155.52 MHz, d₈-THF, 298K) 1.07 ppm. ¹³C NMR (125.81 MHz, d₈-THF, 298K) 166.7 (ipso-Ph) 131.2 (ortho-Ph) 126.8 (para-Ph) 125.6 (meta-Ph) 59.9 (Ph-CH₂-NH) 56.3 (CH₂-C(CH₃)₂) 34.3 (C(CH₃)₃) 33.8 (C(CH₃)₂) 32.3 (C(CH₃)₃) 26.4 (C(CH₃)₂). Elemental Analysis for C₃₄H₅₄Li₂N₄O₂ (564.46 gmol⁻¹): Calculated; C, 72.3; H, 9.6; N, 9.9 %. Found: C, 72.0; H, 9.3; N, 9.9 %.

Complex 2: (0.41 g, 0.68 mmol, 75 %). ¹H NMR (d₈-THF, 400.20 MHz, 298 K) 6.91 (s, 4H, PhH) 4.42 (t, 4H, ³J = 9.91 Hz, Ph-CH₂-NH) 3.14 (d, 4H, ³J = 9.61 Hz, Ph-CH₂-NH) 2.44 (d, 4H, NH-CH₂-C(CH₃)₂) 2.37 (t, 4H, ³J = 10.08 Hz, NH-CH₂-C(CH₃)₃) 1.20 (s, 18H, C(CH₃)₃) 0.94 (br. 4H, NH) 0.91 (s, 6H, C(CH₃)₂) 0.78 (s, 6H, C(CH₃)₂). ¹³C NMR (125.81 MHz, d₈-THF, 298K) 167.9 (ipso-Ph) 131.7 (ortho-Ph) 128.7 (para-Ph) 126.3 (meta-Ph) 62.0 (Ph-CH₂-NH) 55.6 (CH₂-C(CH₃)₂) 34.6 (C(CH₃)₃) 33.7 (C(CH₃)₂) 32.2 (C(CH₃)₃) 28.1 (C(CH₃)₂) 23.3 (C(CH₃)₂). Elemental Analysis for C₃₄H₅₄N₄Na₂O₂ (596.40 gmol⁻¹): Calculated; C, 68.4; H, 9.1; N, 9.4 %. Found: C, 68.7; H, 8.9; N, 9.1 %.

Complex 3: (0.44 g, 0.71 mmol, 78 %). ¹H NMR (d₈-THF, 400.20 MHz, 298 K) 6.81 (s, 4H, PhH) 3.60 (s, 8H, Ph-CH₂-NH) 2.25 (s, 8H, CH₂-C(CH₃)₂) 1.44 (br. 4H, NH) 1.17 (s, 18H, C(CH₃)₃) 0.82

(s, 12H, C(CH₃)₂). ¹³C NMR (125.81 MHz, d₈-THF, 298 K) 166.8 (*ipso-Ph*) 130.0 (*ortho-Ph*) 127.3 (*para-Ph*) 126.3 (*meta-Ph*) 58.8 (Ph-CH₂-NH) 55.0 (CH₂-C(CH₃)₂) 34.9 (C(CH₃)₃) 33.7 (C(CH₃)₂) 32.3 (C(CH₃)₃) 25.8 (C(CH₃)₂). Elemental Analysis for C₃₄H₅₄K₂N₄O₂ (628.35 gmol⁻¹): Calculated; C, 64.9; H, 8.7; N, 8.9 %. Found: C, 64.8; H, 8.7; N, 9.0 %.

General Sequential Mono – Metalation (Thermodynamic) Synthetic Procedure

ZnEt₂ (0.11 g, 0.91 mmol) was added dropwise to a solution of H₂L (0.50 g, 0.91 mmol) in THF (10 mL) and stirred for 16 h at 25 °C. MX_n (0.91 mmol) (**5a**, LiI; **5b**, LiOBzpCF₃; **7a**, KI; **7b**, KOBzpCF₃; **8a**, MgI₂; **9a**, CaI₂) was added and heated to 100 °C for 16 h. The solvent was removed in *vacuo* to afford a white solid.

General Sequential Metalation (Kinetic) Synthetic Procedure

ZnEt₂ (0.11 g, 0.91 mmol) was added dropwise to a solution of H₂L (0.50 g, 0.91 mmol) in THF (10 mL) and stirred for 16 h at 25 °C. MX_n (0.905 mmol) (where MX_n = NaI; **6**) was added dropwise to a stirring solution of LZn at -78 °C and stirred for 2 h. The solvent was removed in *vacuo* to afford a white solid.

Complex 4a: (0.64 g, 0.69 mmol, 76 %) ¹H NMR (d₂-TCE, 400.20 MHz, 403 K) 7.00 (s, 4H, PhH) 4.79 (s, 4H, Zn-HN-CH₂-Ph) 3.34 (s, 4H, Zn-HN-CH₂-Ph) 2.95 (s, 4H, Zn-NH) 2.88 (s, 4H, Zn-HN-CH₂-C(CH₃)₂) 2.46 (s, 4H, Zn-HN-CH₂-C(CH₃)₂) 1.35 (s, 18 H, C(CH₃)₃) 1.31 (s, 6H, C(CH₃)₂) 1.06 (s, 6H, C(CH₃)₂). ¹³C NMR (d₂-TCE, 125.81 MHz, 403 K) 160.6 (*ipso-Ph*) 140.0 (*para-Ph*) 128.4 (*meta-Ph*) 125.4 (*ortho-Ph*) 65.0 (Zn-HN-CH₂-C(CH₃)₂) 58.3 (Zn-HN-CH₂-Ph) 34.9 (C(CH₃)₂) 32.9 (C(CH₃)₃) 29.4 (C(CH₃)₂) 23.0 (C(CH₃)₂). Elemental Analysis for C₃₄H₅₄I₂N₄O₂Zn₂ (932.09 gmol⁻¹): Calculated; C, 43.7; H, 5.8; N, 6.0 %. Found; C, 43.5; H, 5.9; N, 6.1 %. MS (MALDI-ToF): m/z 808 [LZnZnI]⁺ (90 %).

Complex 4b: (0.91 g, 0.86 mmol, 95 %) ¹H NMR (d₂-TCE, 500.20 MHz, 403 K) 8.23 (d, 4H, ³J = 7.8 Hz, *ortho*-OBzpCF₃) 7.78 (d, 4H, ³J = 7.8 Hz, *meta*-OBzpCF₃) 7.00 (s, 4H, PhH) 4.80 (br., 4H, Ph-CH₂-NH) 3.35 (br., 4H, Ph-CH₂-NH) 2.97 (br., 4H, NH) 2.87 (br., 4H, CH₂-C(CH₃)₂) 2.48 (br. 4H, CH₂-C(CH₃)₂) 1.35 (s, 18H, C(CH₃)₃) 1.32 (s, 6H, C(CH₃)₂) 1.07 (s, 6H, C(CH₃)₂). ¹³C NMR (d₂-TCE, 125.81 MHz, 403 K) 130.1 (*ortho*-OBz) 127.0 (*meta*-OPh) 125.2 (*meta*-OBz) 63.4 (CH₂-C(CH₃)₂) 56.5 (Ph-CH₂-NH) 33.5 (C(CH₃)₂) 33.3 (C(CH₃)₃) 31.3 (C(CH₃)₃) 27.9 (C(CH₃)₂) 21.3 (C(CH₃)₂). Quarterny carbons were not observed. ¹⁹F NMR (d₂-TCE, 376.64 MHz, 403 K): -61.6 (s, CF₃). Elemental Analysis for C₅₀H₆₂F₆N₄O₆Zn₂ (1056.32 gmol⁻¹): Calculated; C, 56.7; H, 5.9; N, 5.3 %. Found; C, 56.8; H, 6.0; N, 5.4 %. MS (MALDI-ToF): m/z 869 [LZn₂(OBzpCF₃)]⁺ (100 %).

Complex 7b: (0.53 g, 0.63 mmol, 70 %). ¹H NMR (d₈-THF, 400.20 MHz, 298 K) 8.22 (d, 2H, ³J = 7.5 Hz, *ortho*-OBzpCF₃) 7.63 (d, 2H, ³J = 7.5 Hz, *meta*-OBzpCF₃) 6.96 (s, 2H, Zn-PhH) 6.78 (s, 2H, K-PhH) 4.38 (t, 2H, ³J = 11.7 Hz, Zn-HN-CH₂-Ph) 3.58 (d, 2H, ³J = 10.2 Hz, K-HN-CH₂-Ph) 3.38 (t, 2H, ³J = 10.1 Hz, K-HN-CH₂-Ph) 3.25 (t, 2H, ³J = 11.8 Hz, Zn-HN-CH₂-C(CH₃)₂) 3.11 (d, 2H, ³J = 11.4 Hz, Zn-HN-CH₂-Ph) 2.67 (t, 2H, ³J = 11.9 Hz, Zn-NH) 2.60 (d, 2H, ³J = 11.9 Hz, Zn-HN-CH₂-C(CH₃)₂) 2.53-2.37 (m, 4H, K-HN-CH₂-C(CH₃)₂) 1.50 (b. s, 2H, K-NH) 1.22 (s, 18H, C(CH₃)₃) 1.21 (s, 3H, C(CH₃)₂) 1.02 (s, 3H, C(CH₃)₂) 0.94 (s, 6H, C(CH₃)₂). ¹³C NMR (125.81 MHz, d₈-THF, 298 K) 164.4 (*ipso*-Ph) 141.8 (*ipso*-OBzpCF₃) 132.3 (*para*-Ph) 131.0 (q, ²J_{C-F} = 30.85 Hz, *para*-OBzpCF₃) 129.9 (*meta*-OBzpCF₃) 127.4 (*ortho*-Ph_{Zn}) 127.0 (*meta*-Ph_{Zn}) 125.3 (*meta*-Ph_K) 124.1 (*ortho*-OBzpCF₃) 123.1 (*ortho*-Ph_K) 62.7 (Zn-HN-CH₂-C(CH₃)₂) 59.7 (K-HN-CH₂-C(CH₃)₂) 56.5 (Zn-HN-CH₂-Ph) 54.2 (K-HN-CH₂-Ph) 34.4 (quat. K-HN-CH₂-C(CH₃)₂) 33.9 (quat. Zn-HN-CH₂-C(CH₃)₂) 33.0 (C(CH₃)₃) 31.4 (C(CH₃)₃) 28.1 (K-HN-CH₂-C(CH₃)₂) 25.9 (K-HN-CH₂-C(CH₃)₂) 25.4 (Zn-HN-

$\text{CH}_2\text{-C(CH}_3)_2$ 20.9 ($\text{Zn-HN-CH}_2\text{-C(CH}_3)_2$). Quaternary carbonyl and $-\text{CF}_3$ resonances were not observed. ^{19}F NMR (d_8 -THF, 376.64 MHz, 298 K): -63.3 (s, $-\text{CF}_3$) Elemental Analysis for $\text{C}_{42}\text{H}_{58}\text{F}_3\text{KN}_4\text{O}_4\text{Zn}$ (842.33 gmol $^{-1}$): Calculated; C, 59.7; H, 6.9; N, 6.6 %. Found; C, 59.9; H, 7.0; N, 6.7 %. MS (MALDI-ToF): m/z 654 [LZnK] $^+$ (95 %)

Complex 8a: (0.63 g, 0.71 mmol, 75 %) ^1H NMR (d_8 – THF, 400.20 MHz, 298 K): 6.92 (s, 4H, $\text{Mg-PhH} + \text{Zn-PhH}$) 5.09 (t, 2H, $^3J = 11.93$ Hz, $\text{Mg-HN-CH}_2\text{-Ph}$) 4.08 (d, 2H, $^3J = 10.88$ Hz, $\text{Zn-HN-CH}_2\text{-Ph}$) 3.23 (d, 2H, $^3J = 12.63$ Hz, $\text{Zn-HN-CH}_2\text{-Ph}$) 3.10 (t, 2H, $^3J = 12.63$ Hz, $\text{Mg-HN-CH}_2\text{-C(CH}_3)_2$) 3.05 (d, 2H, $^3J = 12.98$ Hz, $\text{Mg-HN-CH}_2\text{-Ph}$) 2.86 (d, 2H, $^3J = 11.58$, Mg-NH) 2.82 (d, 2H, $^3J = 7.72$ Hz, $\text{Zn-HN-CH}_2\text{-C(CH}_3)_2$) 2.69 (t, 2H, $^3J = 10.53$ Hz, Zn-NH) 2.67 (d, 2H, $^3J = 9.47$ Hz, $\text{Zn-HN-CH}_2\text{-C(CH}_3)_2$) 2.46 (d, 2H, $^3J = 11.58$ Hz, $\text{Zn-HN-CH}_2\text{-C(CH}_3)_2$) 1.41 (s, 3H, $\text{C(CH}_3)_2$) 1.38 (s, 3H, $\text{C(CH}_3)_2$) 1.24 (s, 18H, $\text{C(CH}_3)_3$) 0.96 (s, 3H, $\text{C(CH}_3)_2$) 0.94 (s, 3H, $\text{C(CH}_3)_2$). ^{13}C NMR (d_8 – THF, 125.82 MHz, 298 K) 160.2 (*ipso-Ph*) 137.3 (*para-Ph*) 128.3 (*meta-Ph_{Mg}*) 127.9 (*meta-Ph_{Zn}*) 124.9 (*ortho-Ph_{Mg}*) 124.9 (*ortho-Ph_{Zn}*) 64.0 ($\text{Mg-NH-CH}_2\text{-C(CH}_3)_2$) 63.7 ($\text{Zn-NH-CH}_2\text{-C(CH}_3)_2$) 58.6 ($\text{Mg-NH-CH}_2\text{-Ph}$) 56.1 ($\text{Zn-NH-CH}_2\text{-Ph}$) 35.3 ($\text{Zn-NH-CH}_2\text{-C(CH}_3)_2$) 34.8 ($\text{Mg-NH-CH}_2\text{-C(CH}_3)_2$) 33.9 ($\text{C(CH}_3)_3$) 31.8 ($\text{C(CH}_3)_3$) 28.5 ($\text{C(CH}_3)_2$) 28.4 ($\text{C(CH}_3)_2$). Elemental Analysis for $\text{C}_{34}\text{H}_{54}\text{I}_2\text{MgN}_4\text{O}_2\text{Zn}$ (892.15 gmol $^{-1}$): Calculated; C, 45.7; H, 6.1; N, 6.3 %. Found; C, 45.3; H, 5.9; N, 6.1 %. MS (MALDI-ToF): m/z 765 [LZnMgI] $^+$ (100 %).

Complex 9a: (0.72 g, 0.79 mmol, 87 %). ^1H NMR (d_8 – THF, 400.20 MHz, 298 K): 6.81 (s, 2H, Zn-PhH) 6.77 (s, 2H, Ca-PhH) 4.96 (br., 2H, $\text{Zn-HN-CH}_2\text{-Ph}$) 4.39 (d, 2H, $^3J = 13.16$ Hz, $\text{Ca-HN-CH}_2\text{-Ph}$) 3.45 (br., 2H, $\text{Ca-HN-CH}_2\text{-Ph}$) 3.18 (br., 2H, $\text{Zn-HN-CH}_2\text{-C(CH}_3)_2$) 3.00 – 2.80 (br. m, 6H, $\text{Zn-HN-CH}_2\text{-Ph}$, Ca-NH , Zn-NH) 2.54 (br., 2H, $\text{Ca-HN-CH}_2\text{-C(CH}_3)_2$) 2.38 (br., 2H, $\text{Zn-HN-CH}_2\text{-C(CH}_3)_2$) 2.13 (br., 2H, $\text{Ca-HN-CH}_2\text{-C(CH}_3)_2$) 1.13 (s, 18H, $\text{C(CH}_3)_3$) 1.00 (s, 3H, $\text{C(CH}_3)_2$) 0.87 (s, 6H, $\text{C(CH}_3)_2$) 0.69 (s, 3H, $\text{C(CH}_3)_2$). ^{13}C NMR (d_8 – THF, 125.81 MHz, 298 K) 160.5 (*ipso-Ph*) 137.3 (*para-Ph*) 128.5 (*meta-Ph_{Ca}*) 127.5 (*meta-Ph_{Zn}*) 126.2 (*ortho-Ph_{Ca}*) 124.7 (*ortho-Ph_{Zn}*) 63.7 ($\text{Ca-NH-CH}_2\text{-C(CH}_3)_2$) 60.7 ($\text{Zn-NH-CH}_2\text{-C(CH}_3)_2$) 58.9 ($\text{Ca-NH-CH}_2\text{-Ph}$) 53.9 ($\text{Zn-NH-CH}_2\text{-Ph}$) 35.4 ($\text{Zn-NH-CH}_2\text{-C(CH}_3)_2$) 34.4 ($\text{Ca-NH-CH}_2\text{-C(CH}_3)_2$) 33.8 ($\text{C(CH}_3)_3$) 31.8 ($\text{C(CH}_3)_3$) 28.5 ($\text{C(CH}_3)_2$) 23.2 ($\text{C(CH}_3)_2$). Elemental Analysis for $\text{C}_{34}\text{H}_{54}\text{CaI}_2\text{N}_4\text{O}_2\text{Zn}$ (908.13 gmol $^{-1}$): Calculated; C, 44.9; H, 6.0; N, 6.2 %. Found; C, 45.0; H, 6.1; N, 6.0 %. MS (MALDI-ToF): m/z 782 [LZnCaI] $^+$ (100 %).

General procedure for CO₂-CHO ROCOP:

Catalyst (14.8 μmol , typical weight 10-15 mg) was dissolved in CHO (14.8 mmol) and placed under 1 bar CO₂ atmosphere and heated to 80 °C with a stirring rate of 350 RPM. Aliquots were taken and quenched with wet chloroform and exposed to air. Reaction conversion was determined by the ^1H NMR spectroscopy, with molecular weight measured via GPC analysis. The crude polymer was obtained by evaporating the remaining CHO under reduced pressure. This polymer was then dissolved in minimal dichloromethane, passed through a silica pad and precipitated from pentane to yield a white powder.

Part B: Characterisation Data

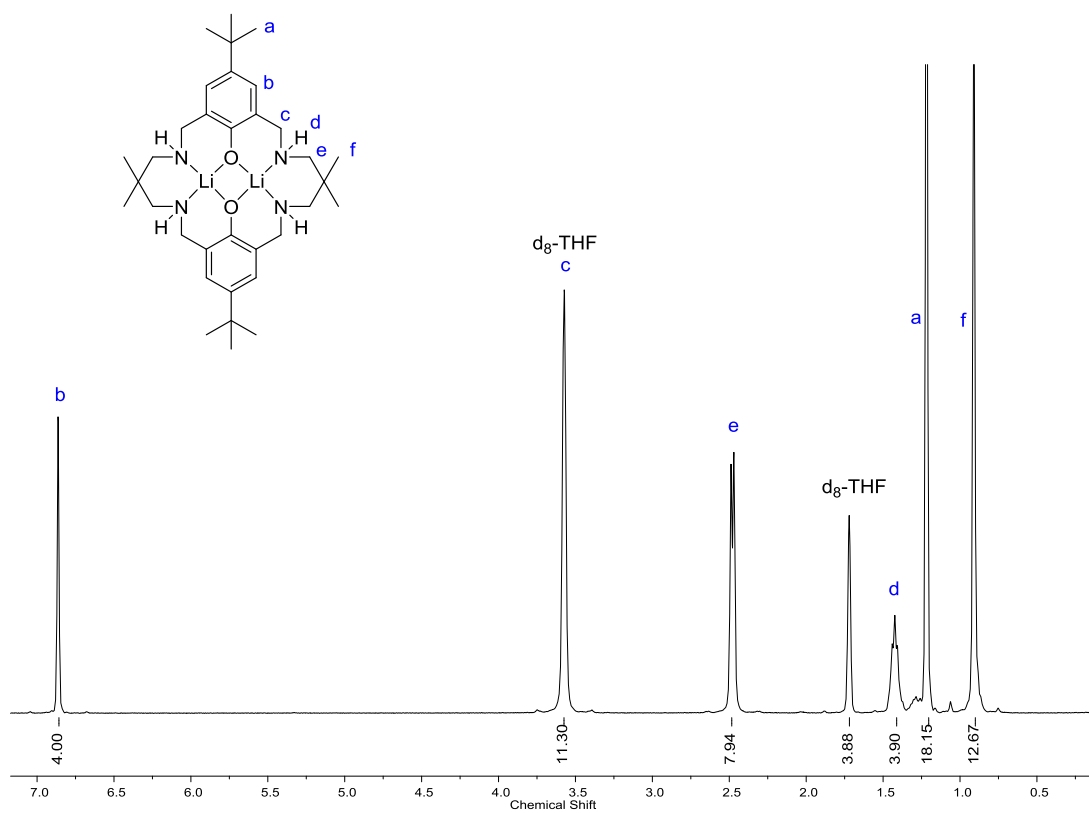


Figure S1: ^1H NMR of **1** ($d_8\text{-THF}$, 298 K).

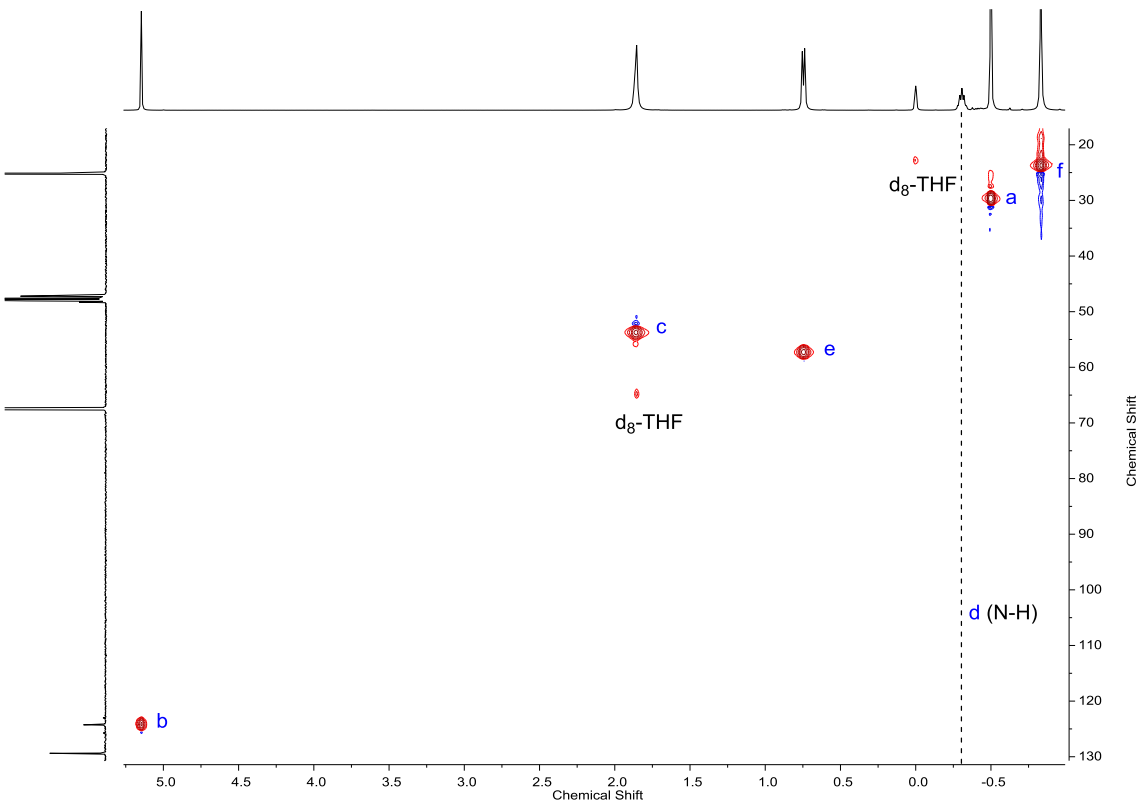


Figure S2: 2D HSQC NMR of **1** ($d_8\text{-THF}$, 298 K).

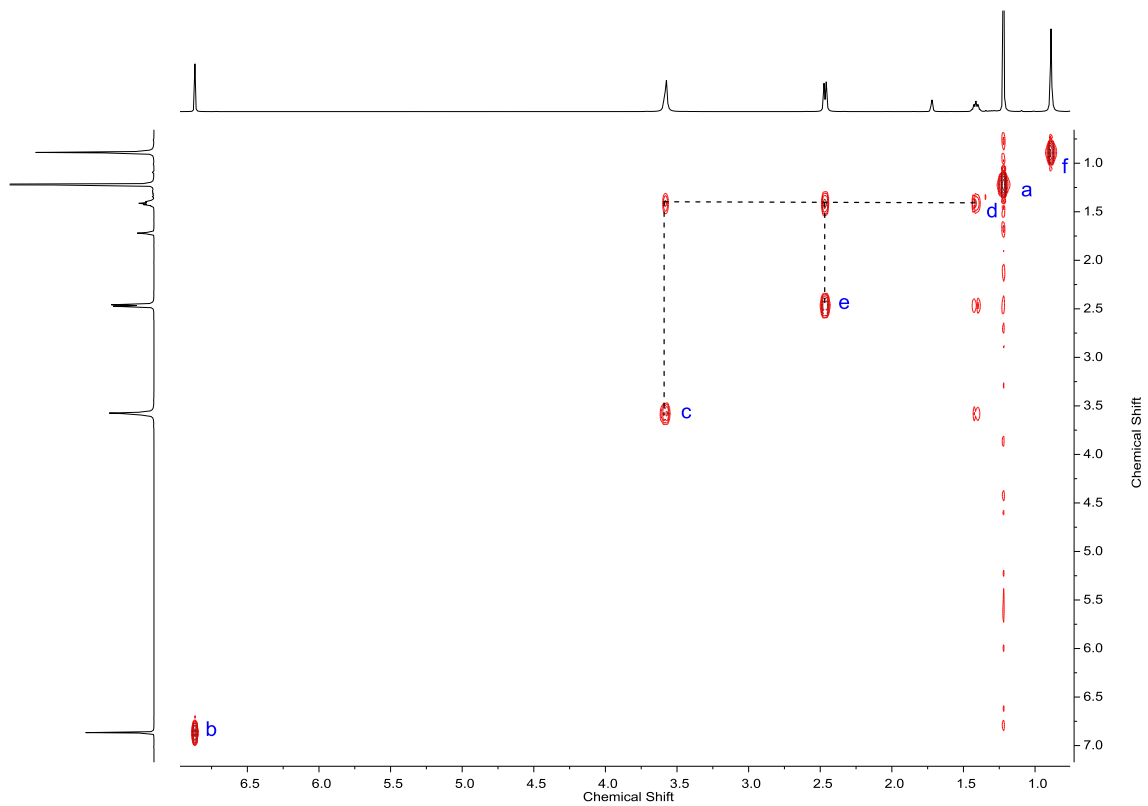


Figure S3: 2D COSY NMR of **1** (d_8 -THF, 298 K).

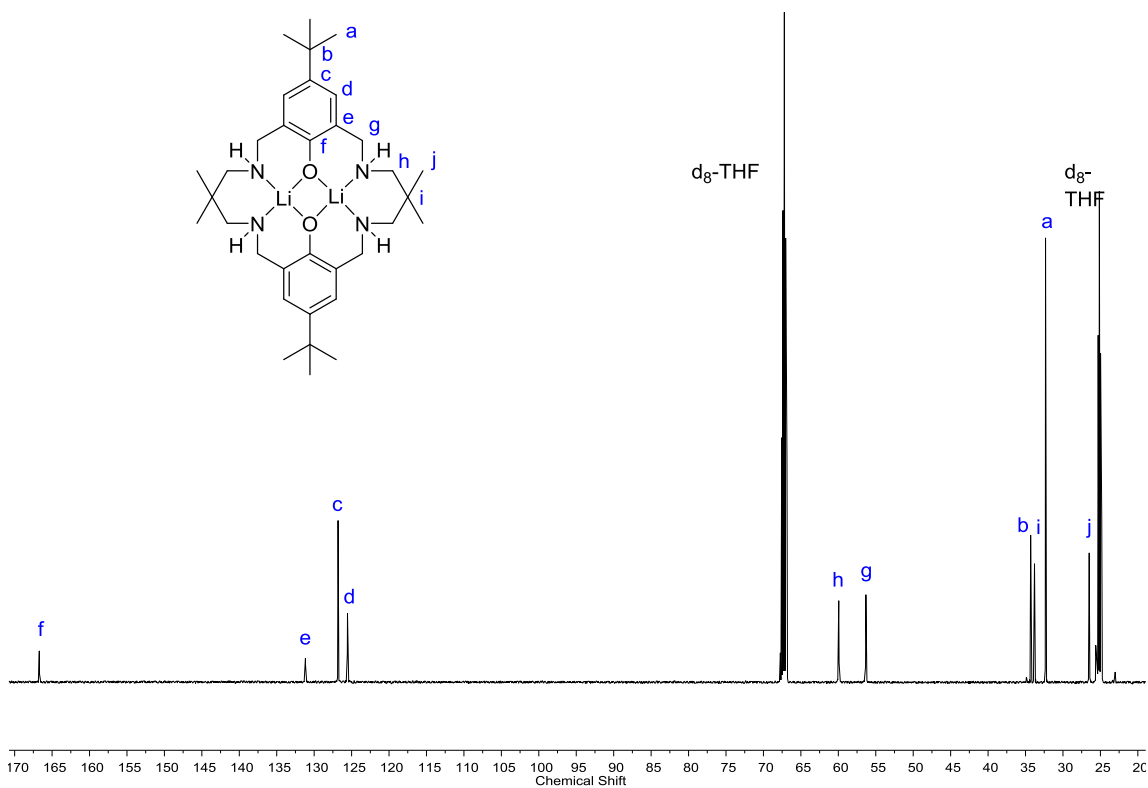


Figure S4: ^{13}C NMR of **1** (d_8 -THF, 298 K).

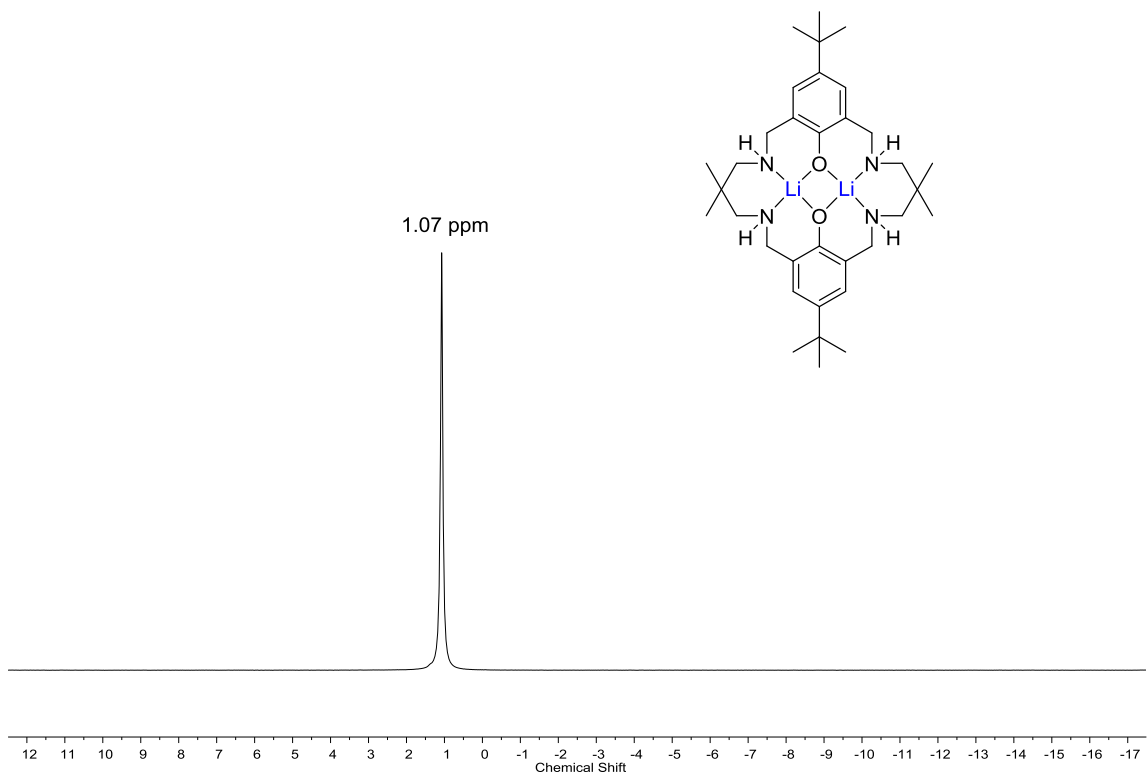


Figure S5: ^{7}Li NMR of **1** ($d_8\text{-THF}$, 298 K).

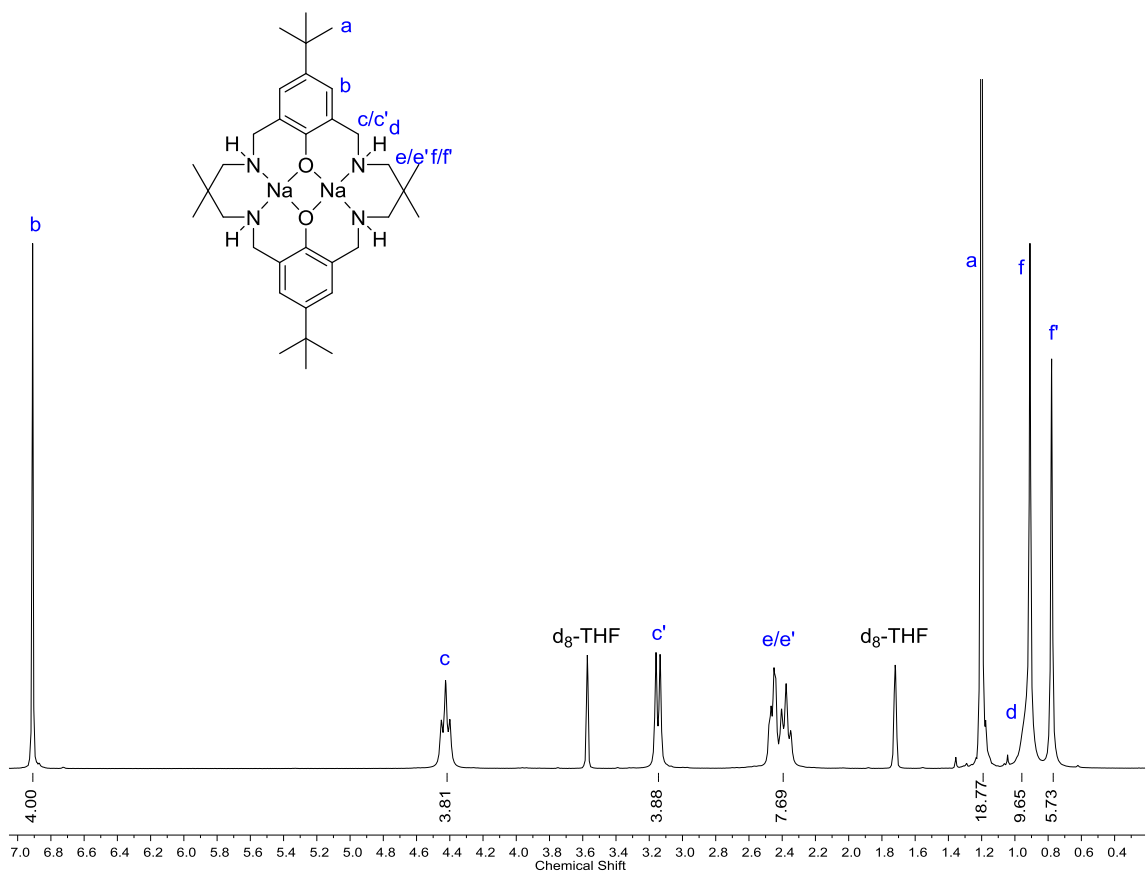


Figure S6: ^1H NMR of **2** ($d_8\text{-THF}$, 298 K).

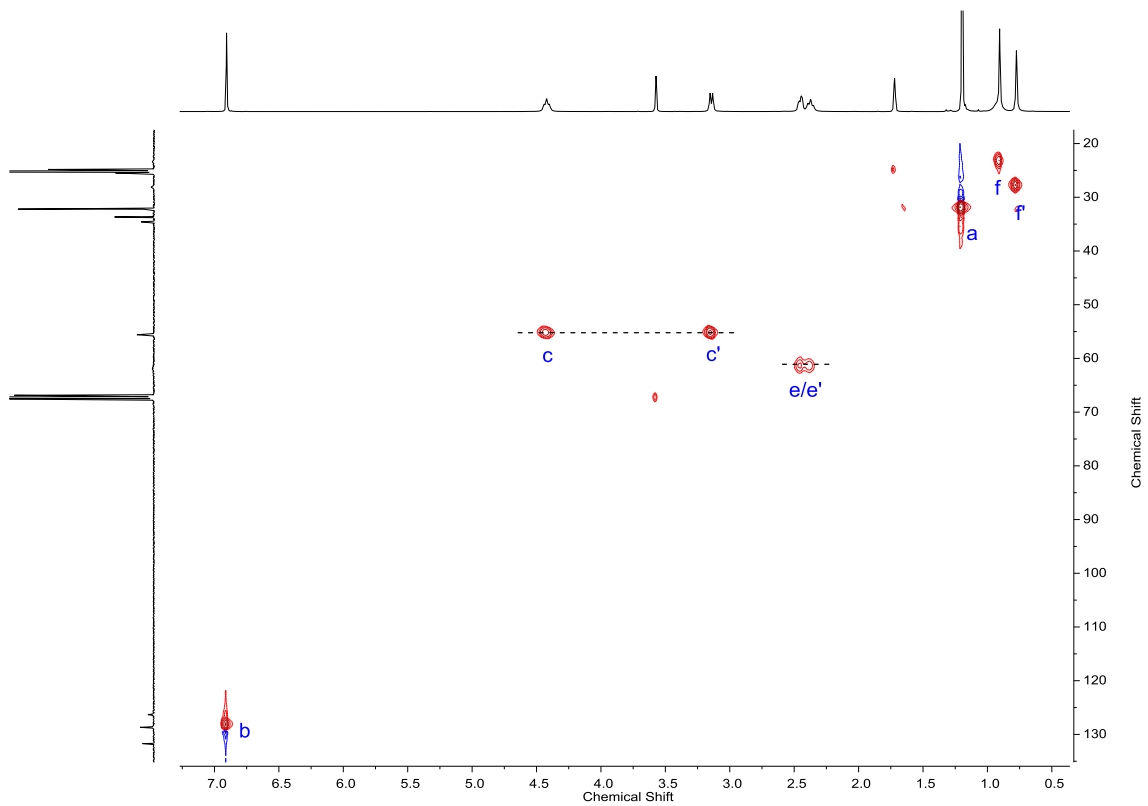


Figure S7: 2D HSQC NMR of **2** (d_8 -THF, 298 K).

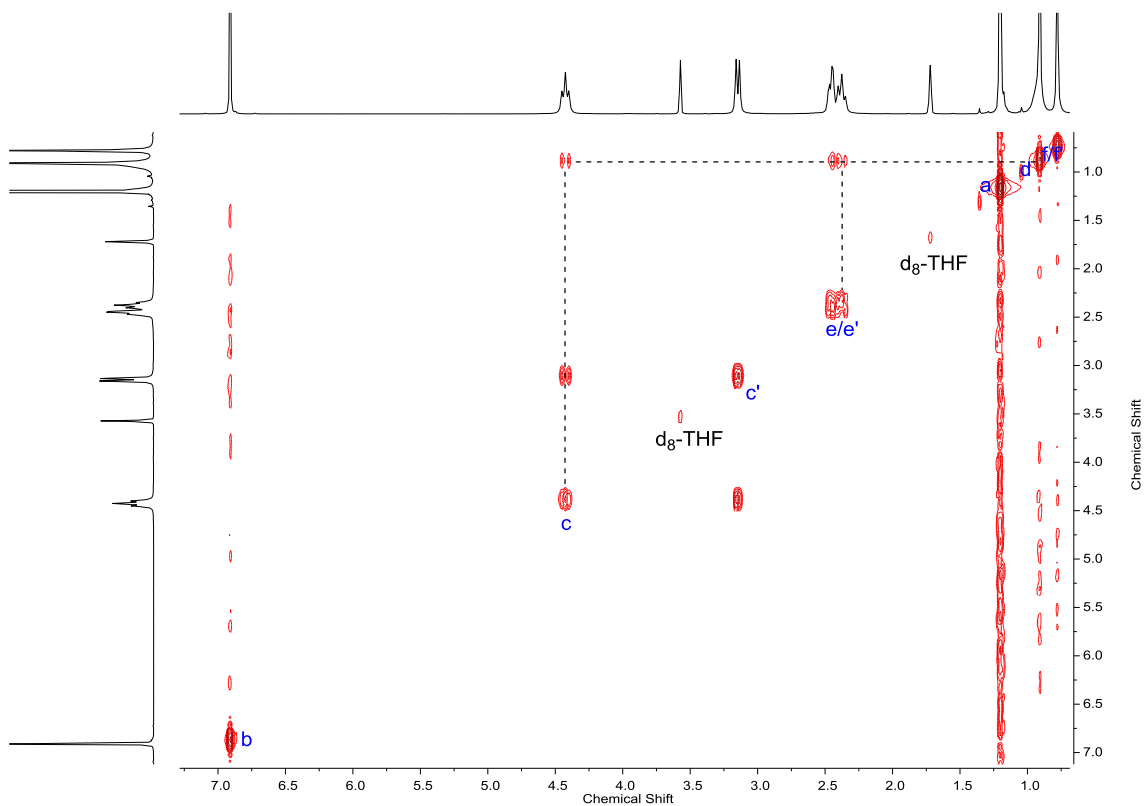


Figure S8: 2D COSY NMR of **2** (d_8 -THF, 298 K).

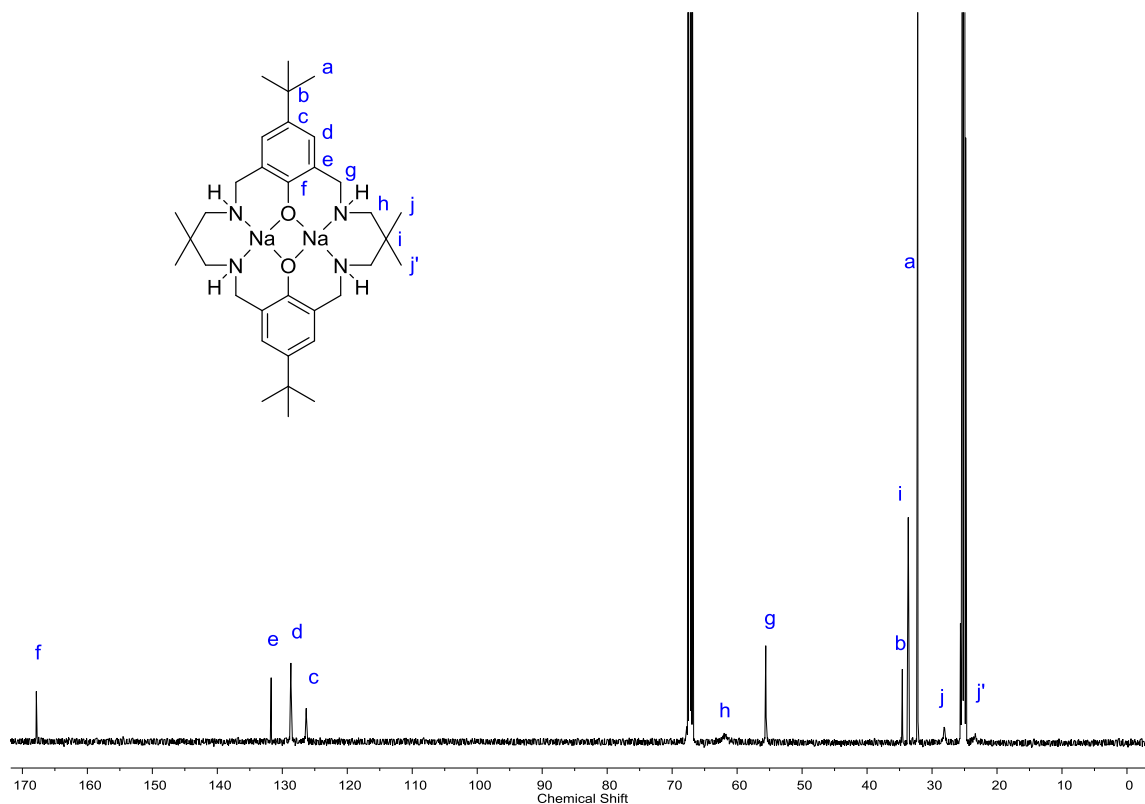


Figure S9: ^{13}C NMR of **2** ($d_8\text{-THF}$, 298 K).

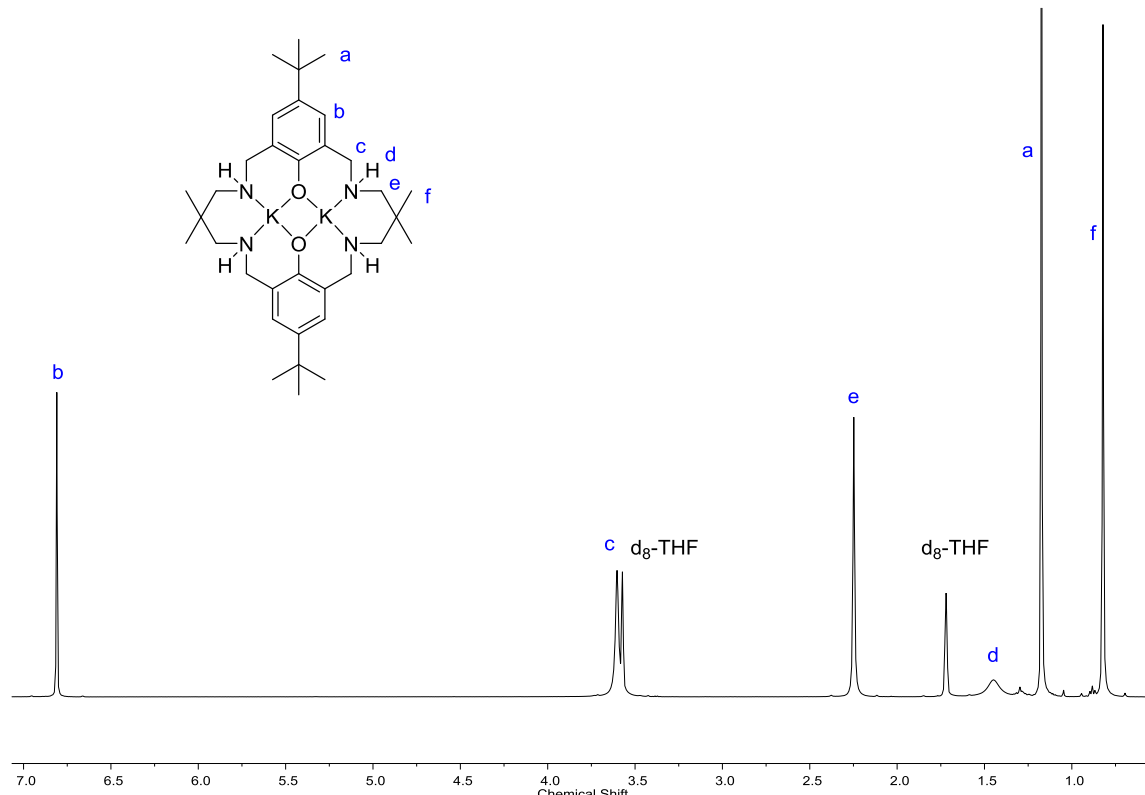


Figure S10: ^1H NMR of **3** ($d_8\text{-THF}$, 298 K).

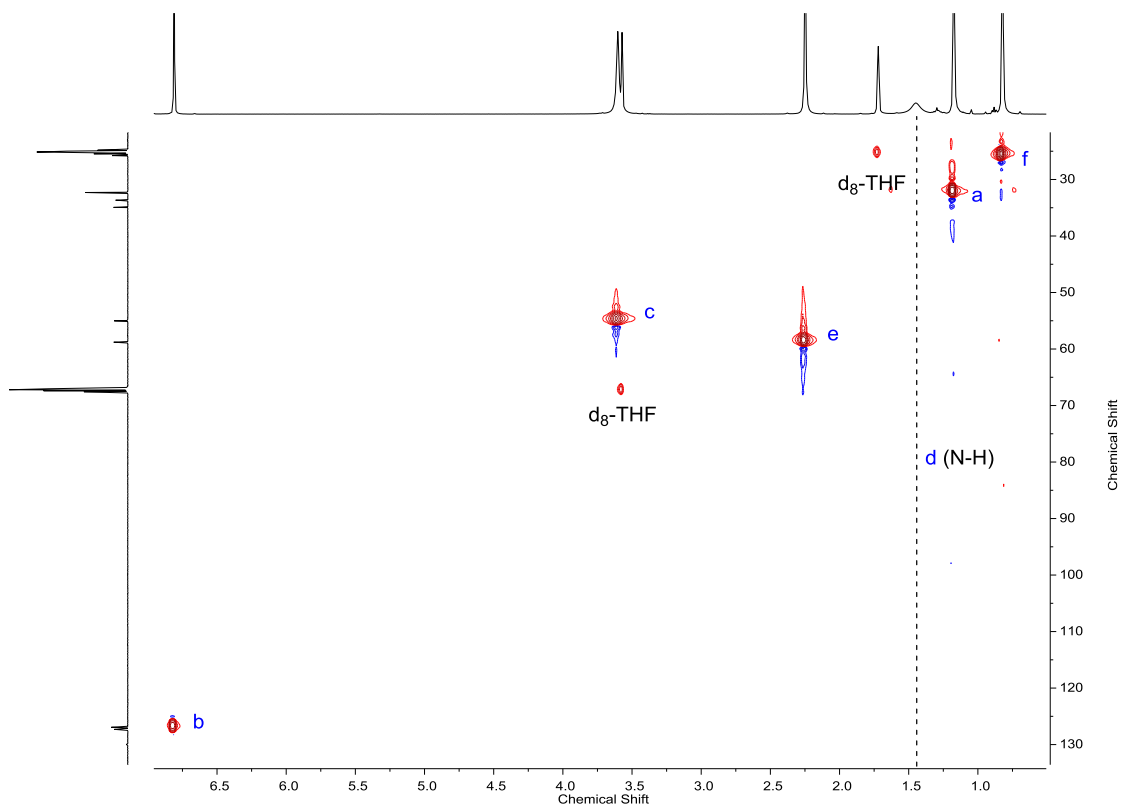


Figure S11: 2D HSQC NMR of **3** (d_8 -THF, 298 K).

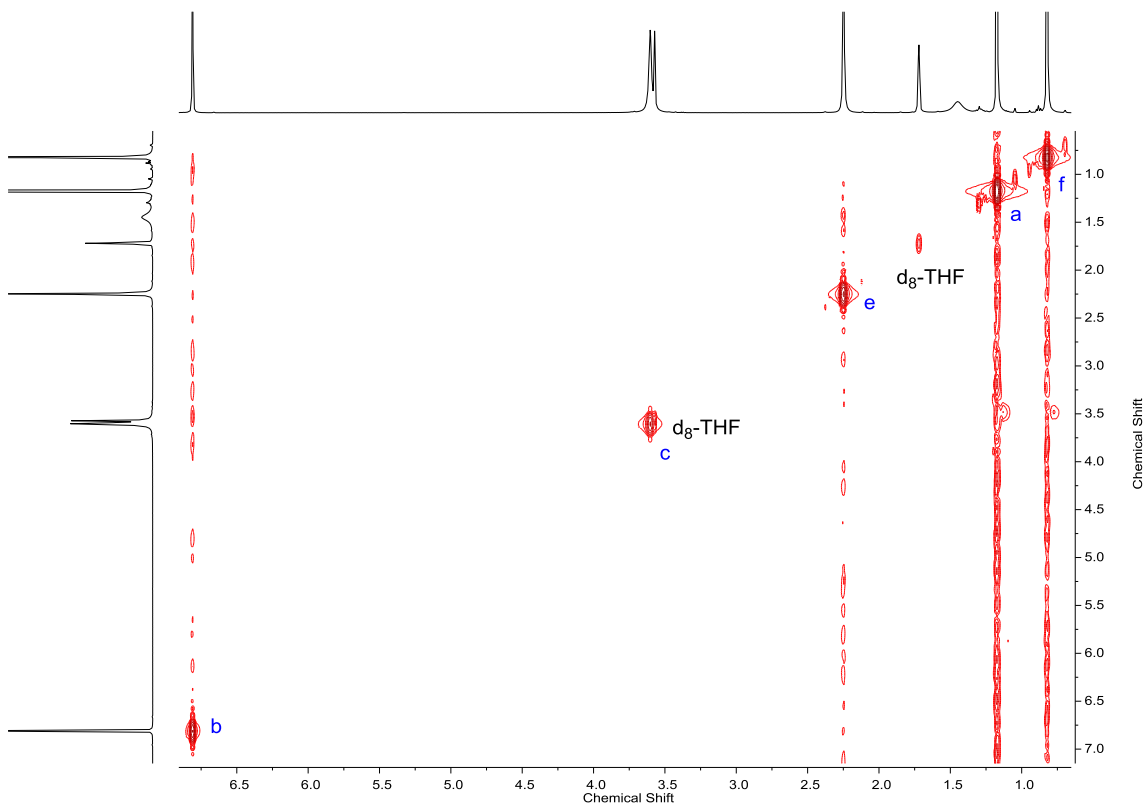


Figure S12: 2D COSY NMR of **3** (d_8 -THF, 298 K).

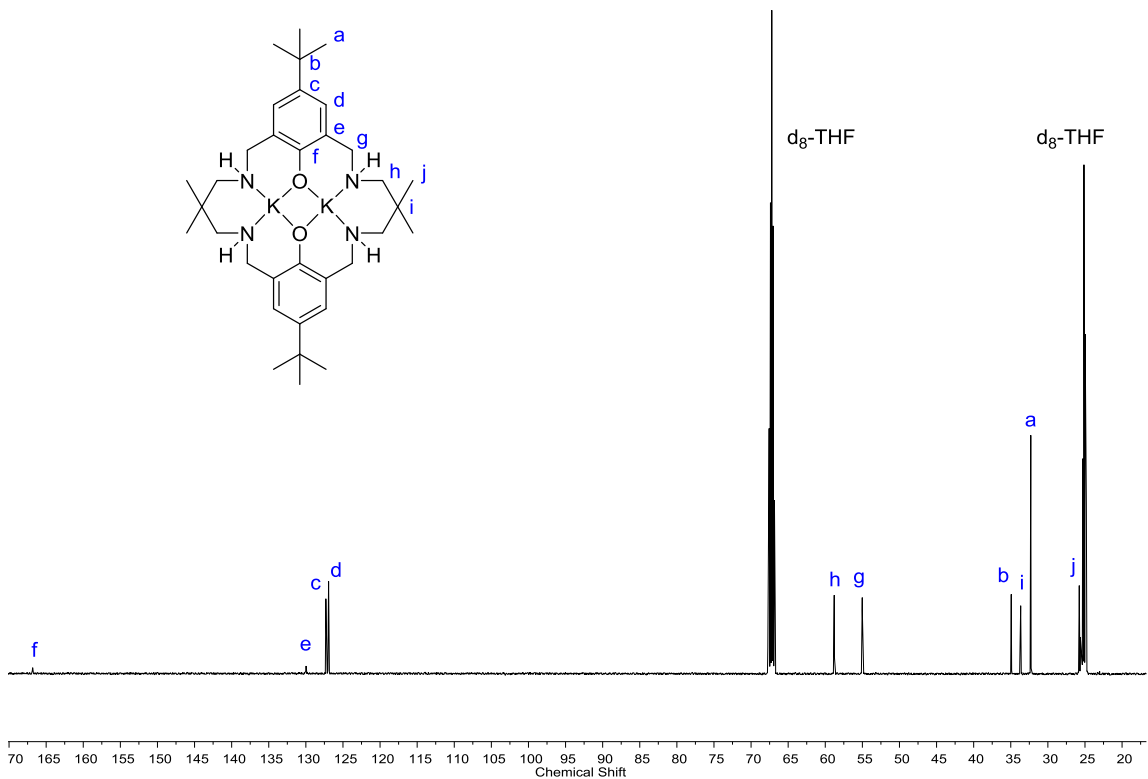


Figure S13: ^{13}C NMR of **3** ($d_8\text{-THF}$, 298 K).

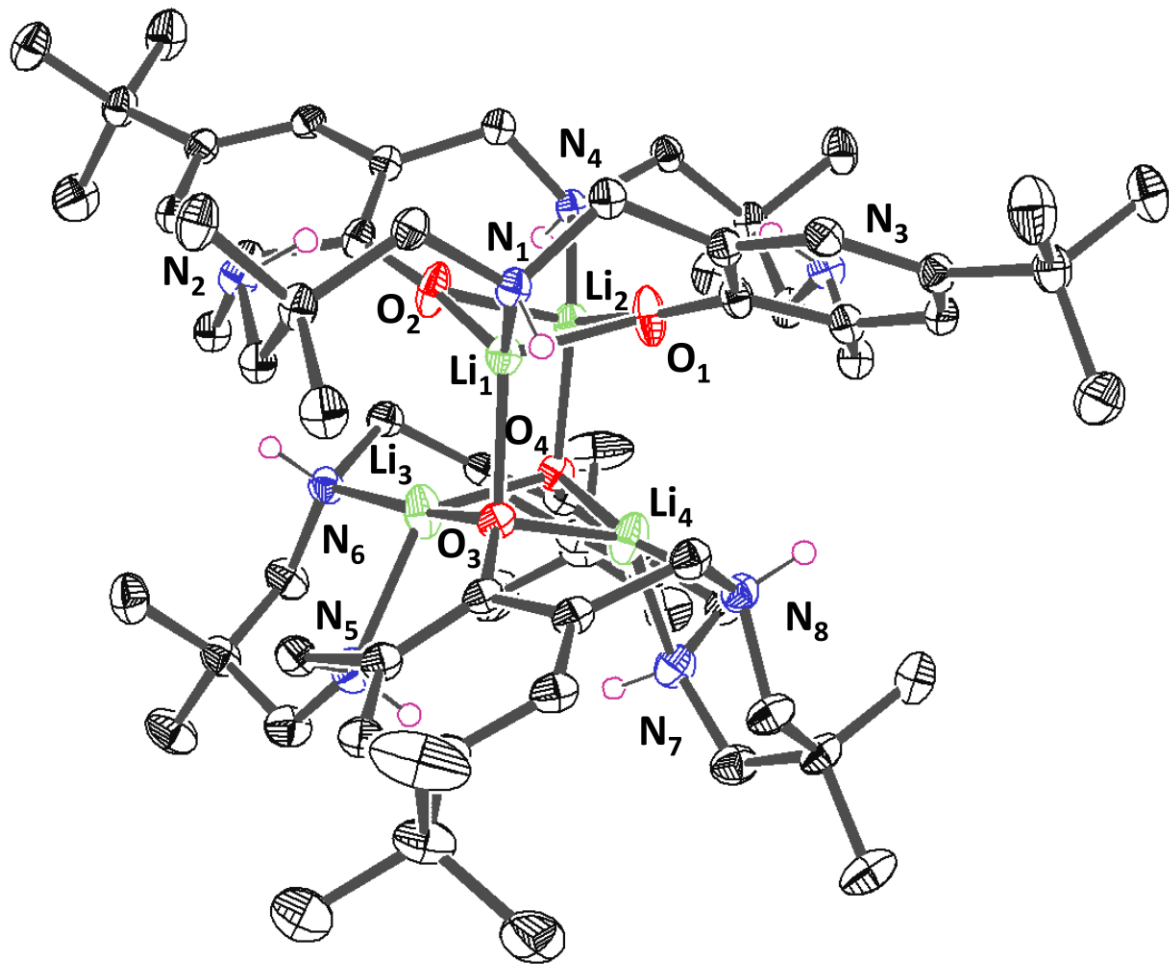


Figure S14: ORTEP representation of the molecular structure of **1**, with disorder and hydrogen atoms (excluding N-H) omitted for clarity and thermal ellipsoids represented at 30 % probability.

Table S1: Selected bond lengths (\AA) and angles ($^\circ$) for complex **1**

Bond	Bond Length (\AA)	Bond	Bond Angle ($^\circ$)
N (1) – Li (1)	2.11(9)	N (1) – Li (1) – O (2)	126.9(0)
N (2) – Li (1)	3.26(9)	N (1) – Li (1) – O (1)	101.6(1)
O (1) – Li (1)	1.93(5)	N (1) – Li (1) – O (3)	117.7(4)
O (2) – Li (1)	1.88(3)	N (7) – Li (4) – O (4)	168.6(5)
O (3) – Li (1)	1.98(1)	N (8) – Li (4) – O (3)	130.8(4)
N (7) – Li (4)	2.10(6)	N (7) – Li (4) – N (8)	93.8(0)
N (8) – Li (4)	2.16(2)		
O (3) – Li (4)	1.95(3)	Metal – Metal	
O (4) – Li (4)	1.96(5)	Li (1) – Li (2)	2.51(8)
O (1) – Li (4)	2.77(4)	Li (3) – Li (4)	2.63(0)

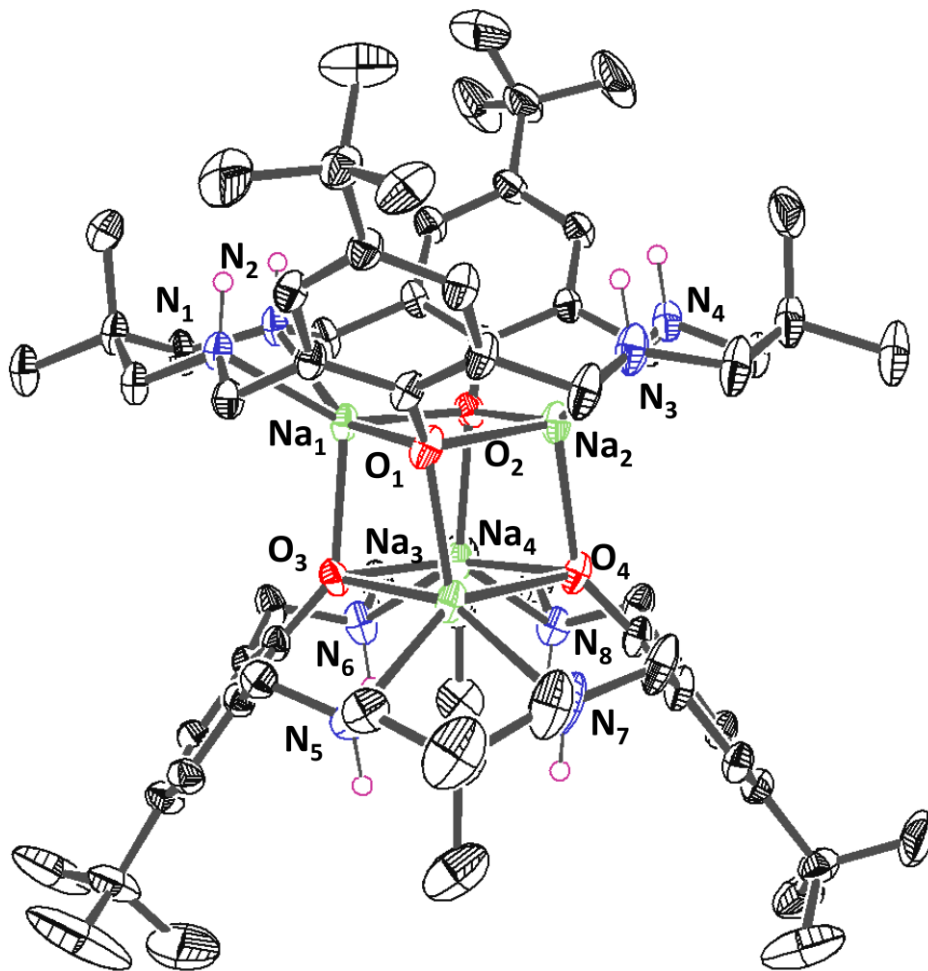


Figure S15: ORTEP representation of the molecular structure of **2**, with disorder and hydrogen atoms (excluding N-H) omitted for clarity with thermal ellipsoide represented at 30 % probability.

Table S2: Selected bond lengths (\AA) and bond angles ($^\circ$) of complex **2**.

Bond	Bond Length (\AA)	Bond	Bond Angle ($^\circ$)
N (1) – Na (1)	2.42(2)	N (1) – Na (1) – O (2)	150.3(7)
N (2) – Na (1)	2.45(3)	N (2) – Na (1) – O (1)	151.6(5)
O (1) – Na (1)	2.36(6)	N (1) – Na (1) – O (3)	114.0(7)
O (2) – Na (1)	2.34(5)	N (3) – Na (2) – O (2)	150.7(0)
O (3) – Na (1)	2.29(0)	N (4) – Na (2) – O (1)	149.1(5)
N (3) – Na (2)	2.46(9)	N (3) – Na (2) – O (4)	123.4(4)
N (4) – Na (2)	2.42(9)		
O (1) – Na (2)	2.36(3)	Metal – Metal	Distance (\AA)
O (2) – Na (2)	2.37(7)	Na (1) – Na (2)	3.13(9)
O (4) – Na (2)	2.31(4)		

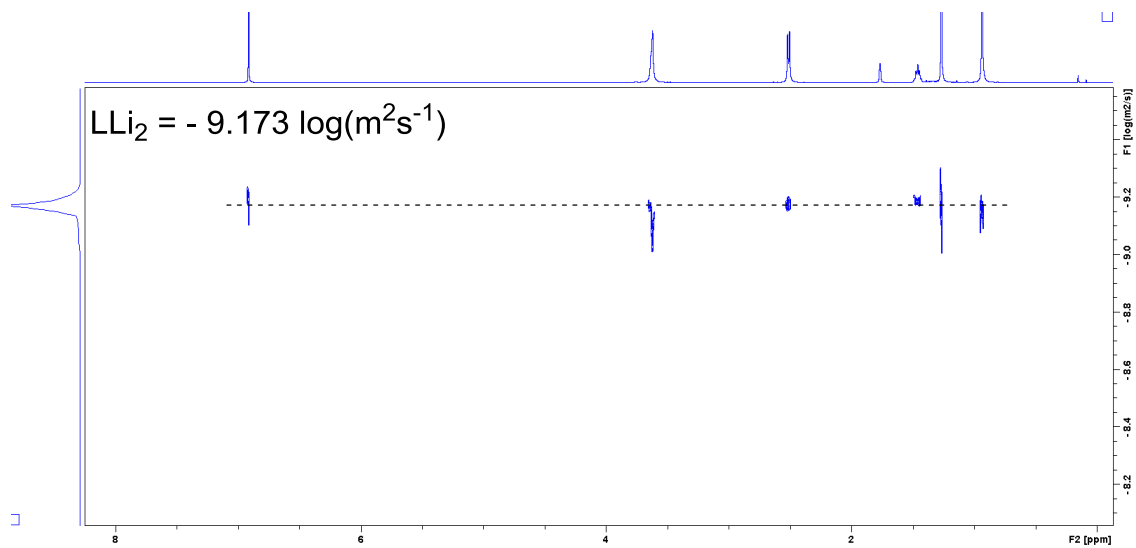


Figure S16: 2D DOSY of **1** (d_8 -THF, 298 K)

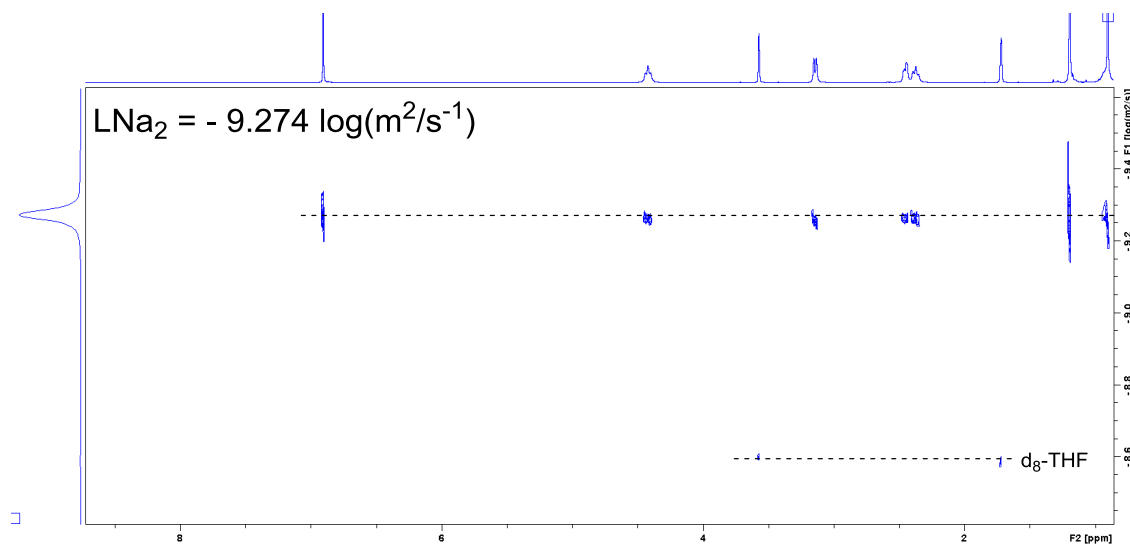


Figure S17: 2D DOSY of **2** (d_8 -THF, 298 K)

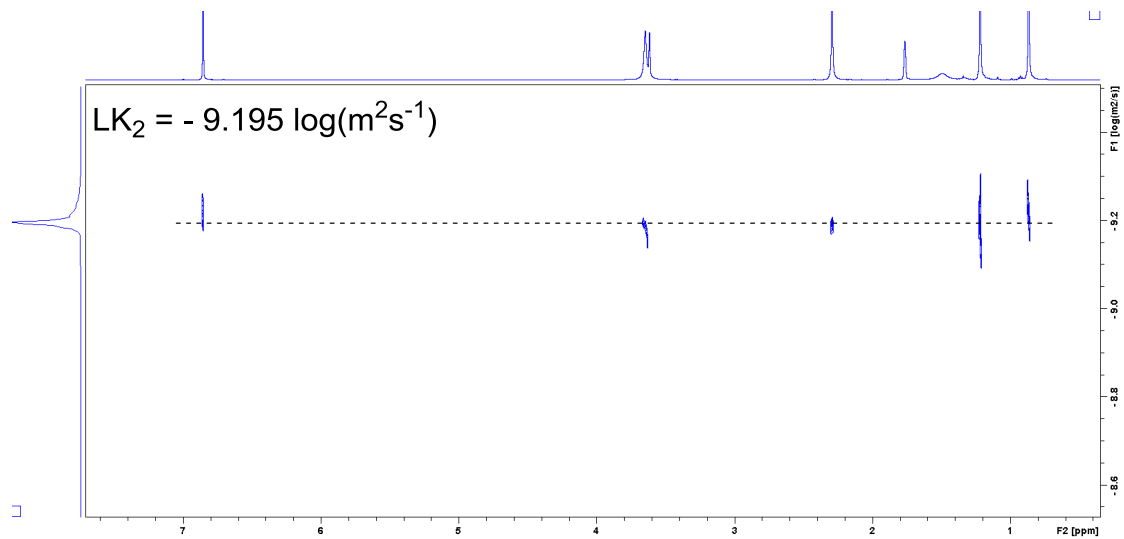


Figure S18: 2D DOSY of **3** (d_8 -THF, 298 K)

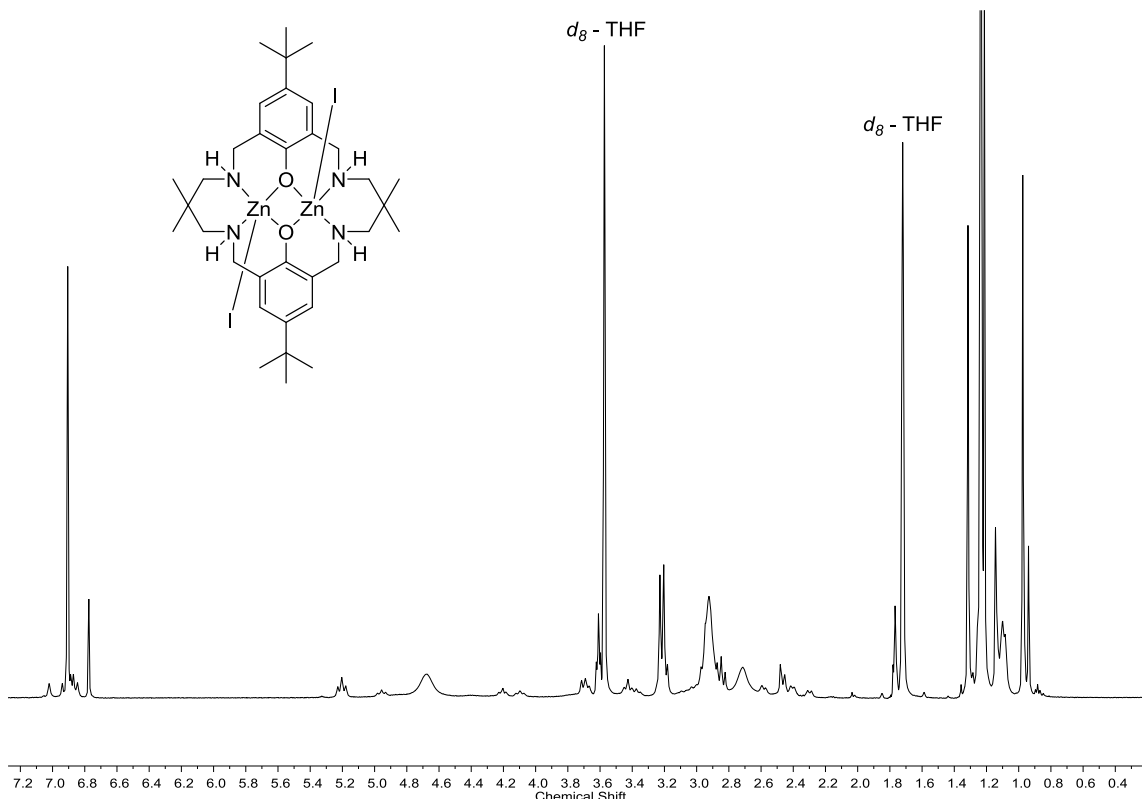


Figure S19: ^1H NMR of **4a** (d_8 -THF, 298 K).

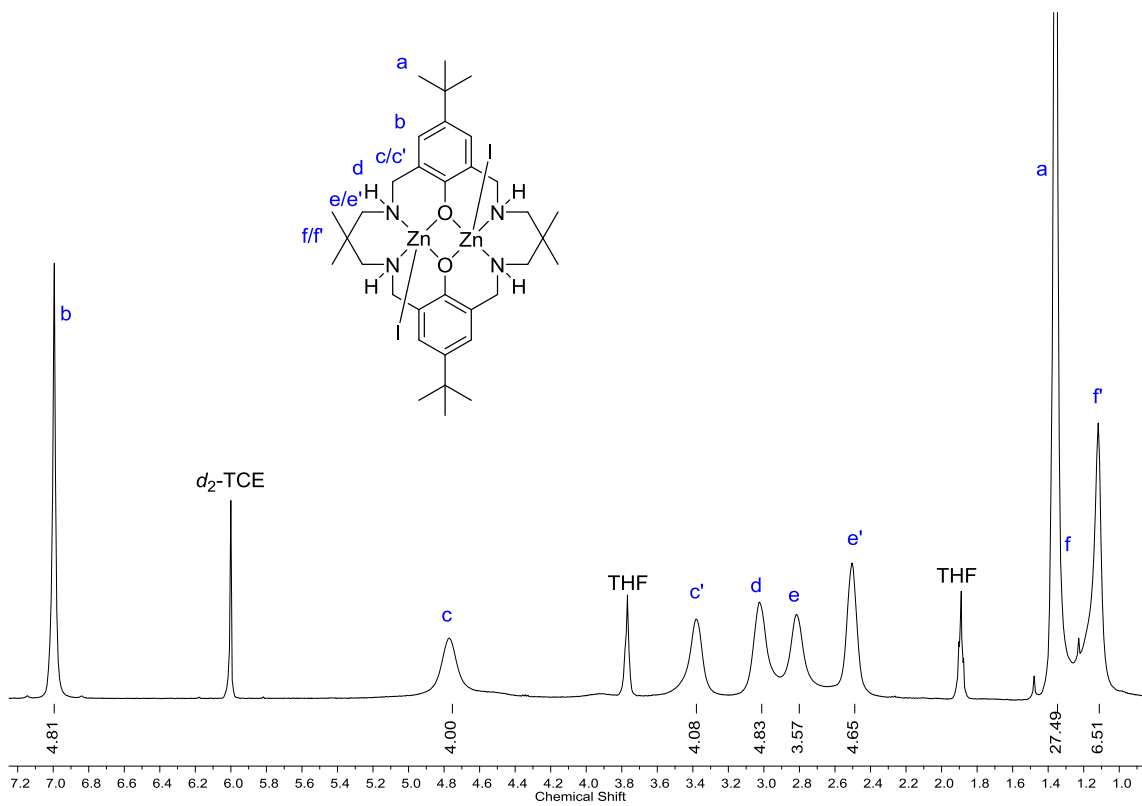


Figure S20: ^1H NMR of **4a** (d_2 -TCE, 403 K).

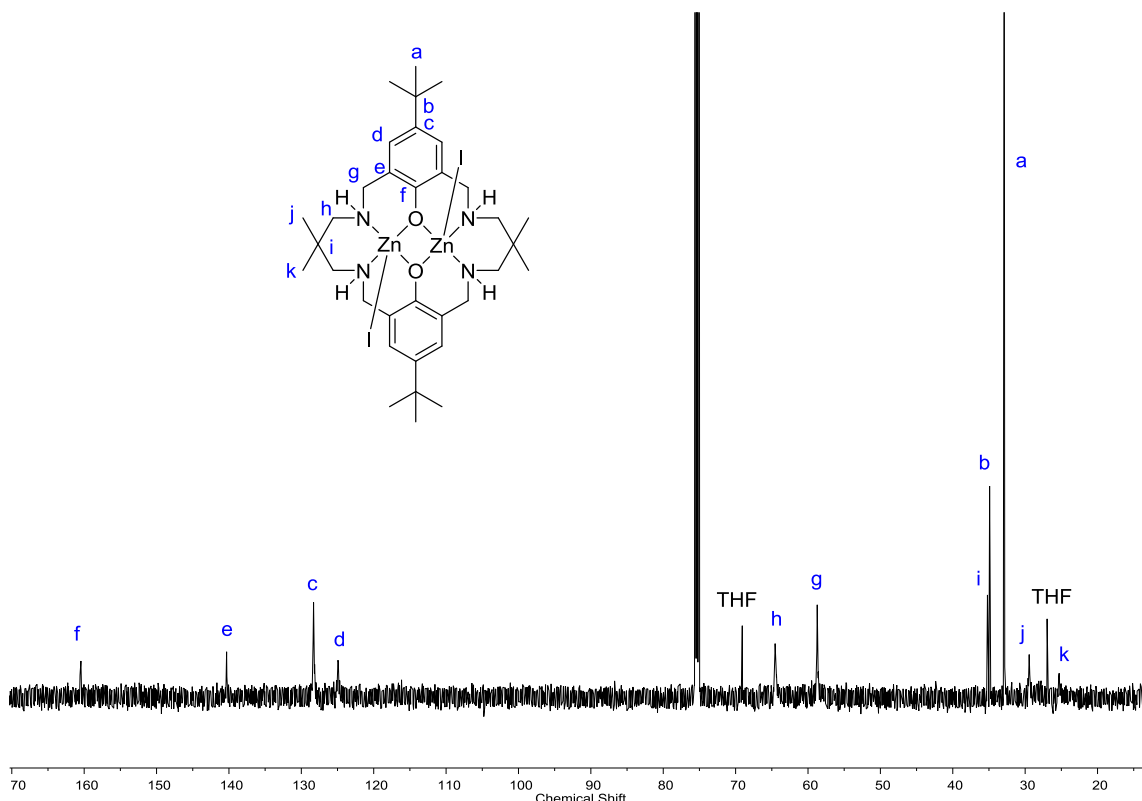


Figure S21: ^{13}C NMR of **4a** ($d_2\text{-TCE}$, 403 K).

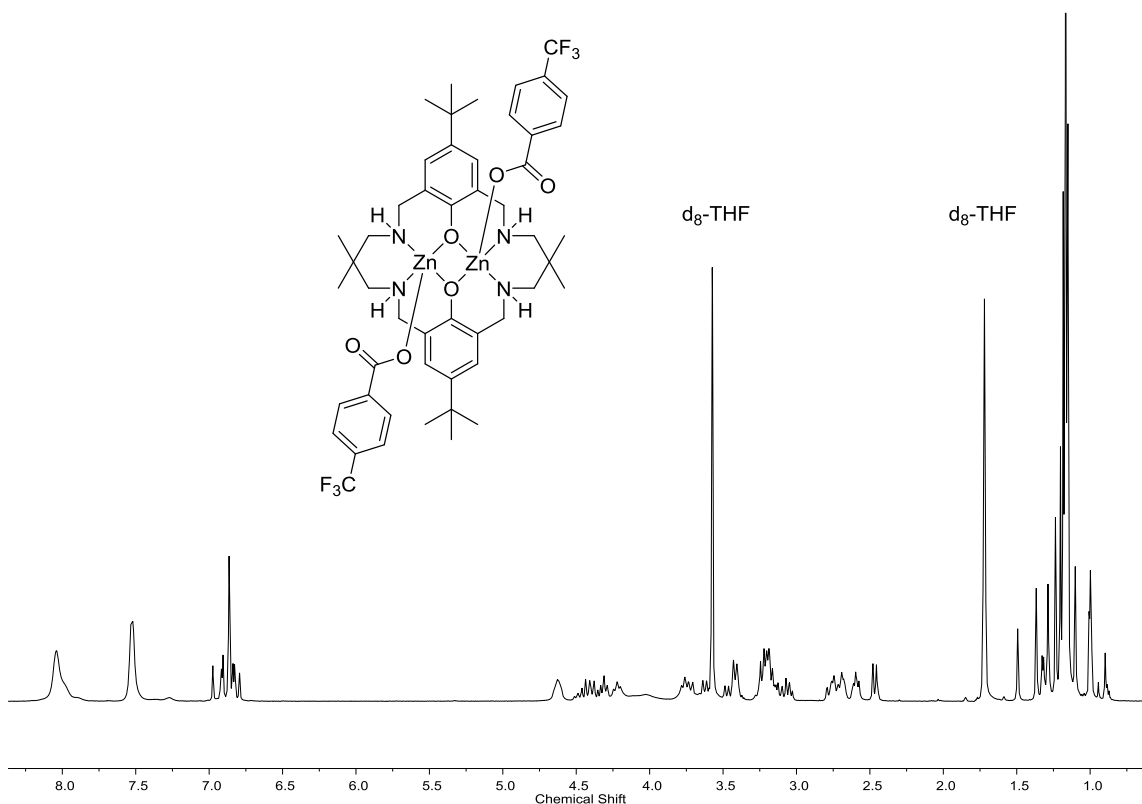
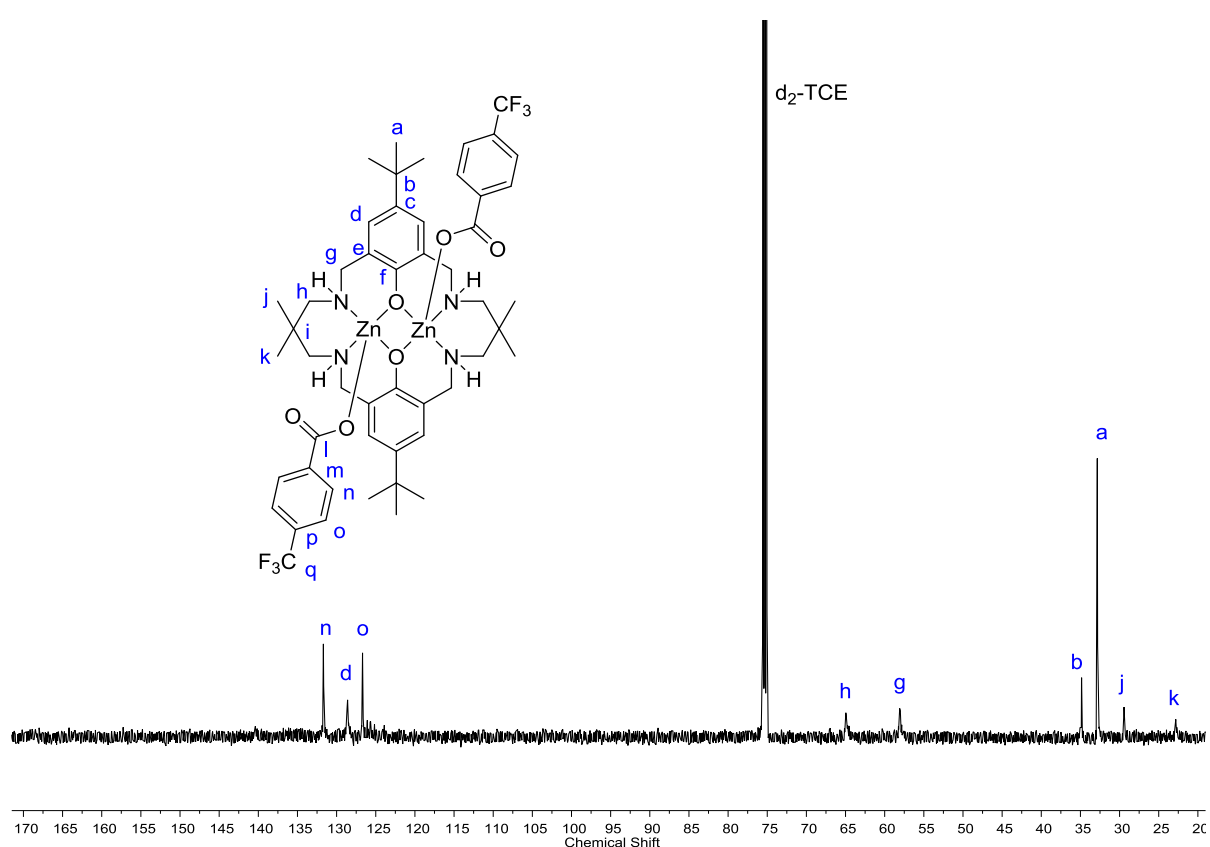
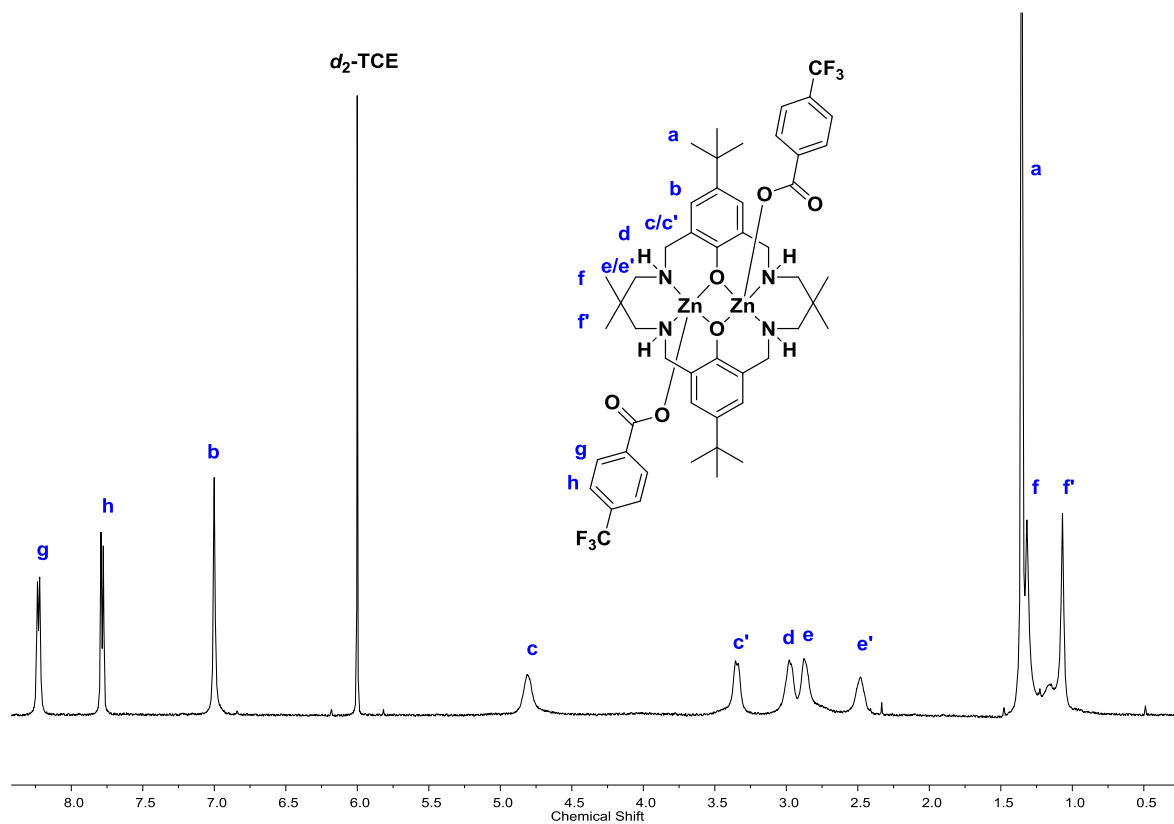


Figure S22: ^1H NMR of **4b** ($d_8\text{-THF}$, 298 K).



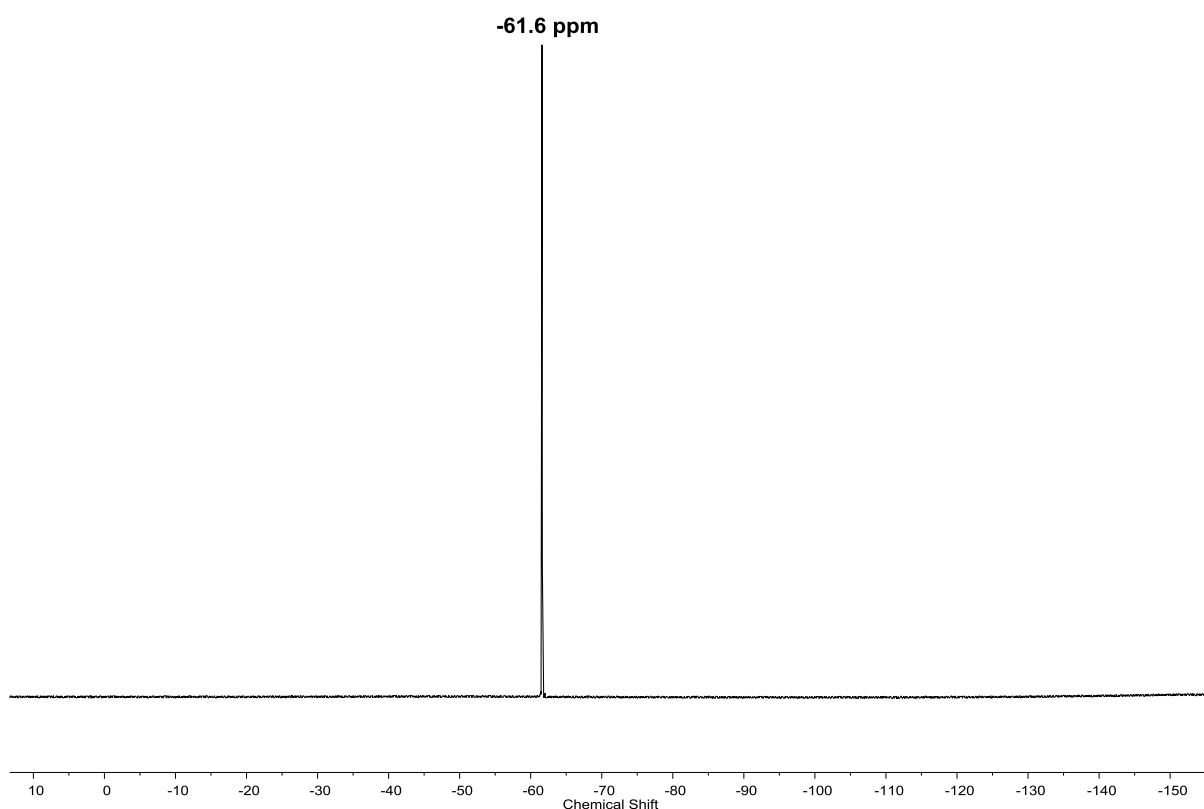


Figure S25: ^{19}F NMR of **4b** ($\text{d}_2\text{-TCE}$, 403 K).

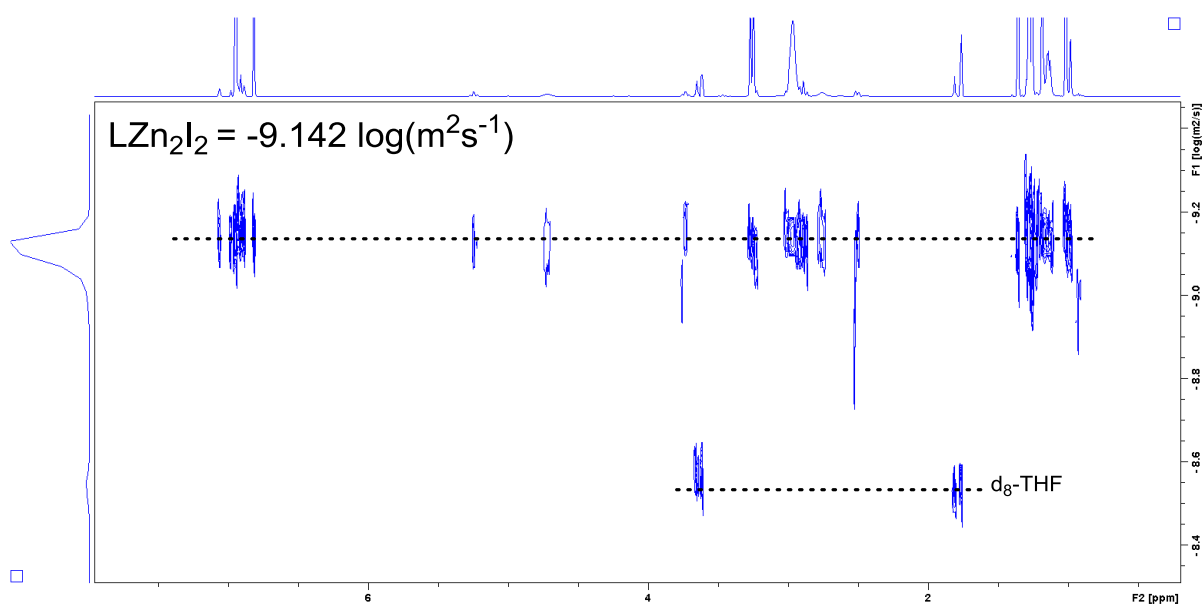


Figure S26: 2D DOSY NMR of complex **4a** ($\text{d}_8\text{-THF}$, 298 K).

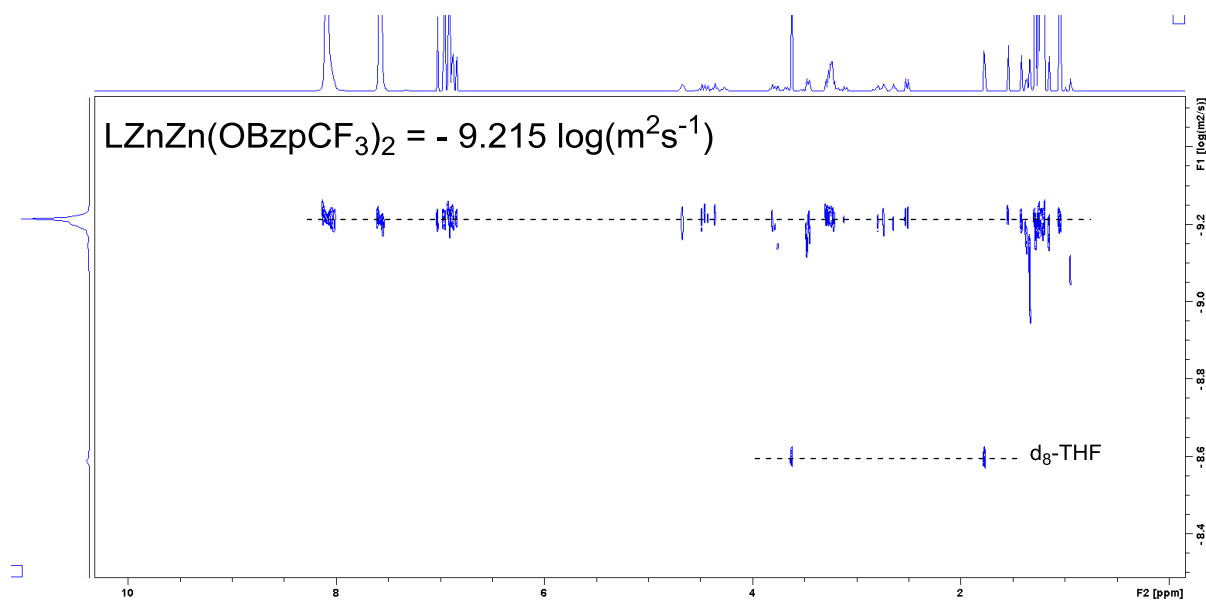


Figure S27: 2D DOSY NMR of complex **4b** (d_8 -THF, 298 K)

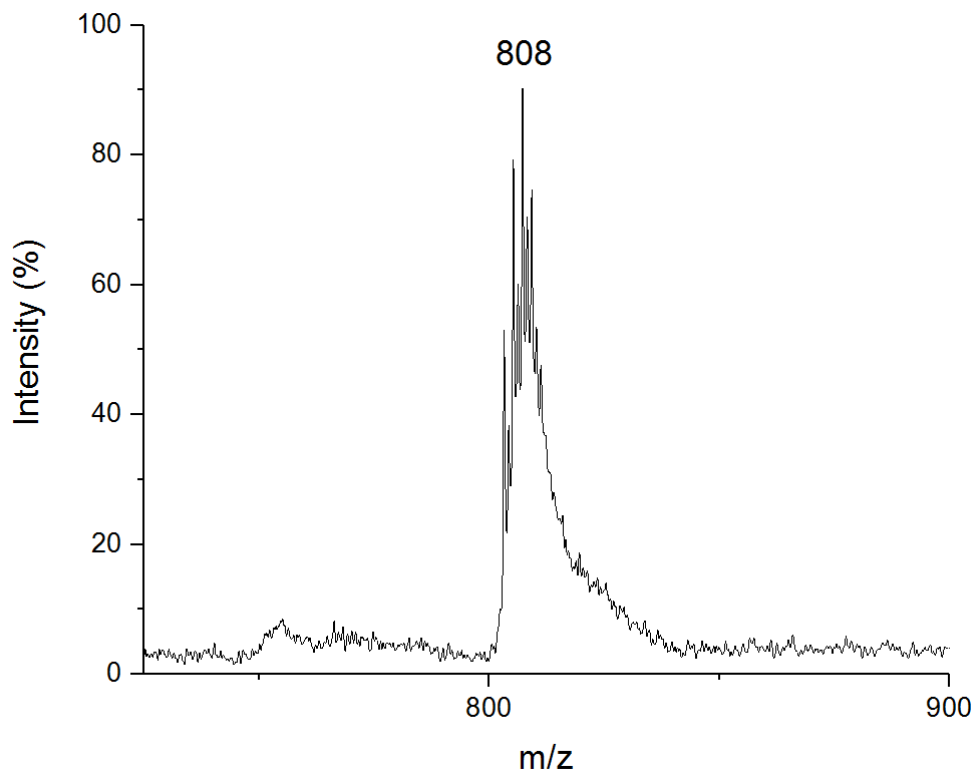


Figure S28: MALDI-ToF mass spectrum of **4a**. An m/z of 808 was observed and assigned to the complex cation $[LZn_2(I)]^+$.

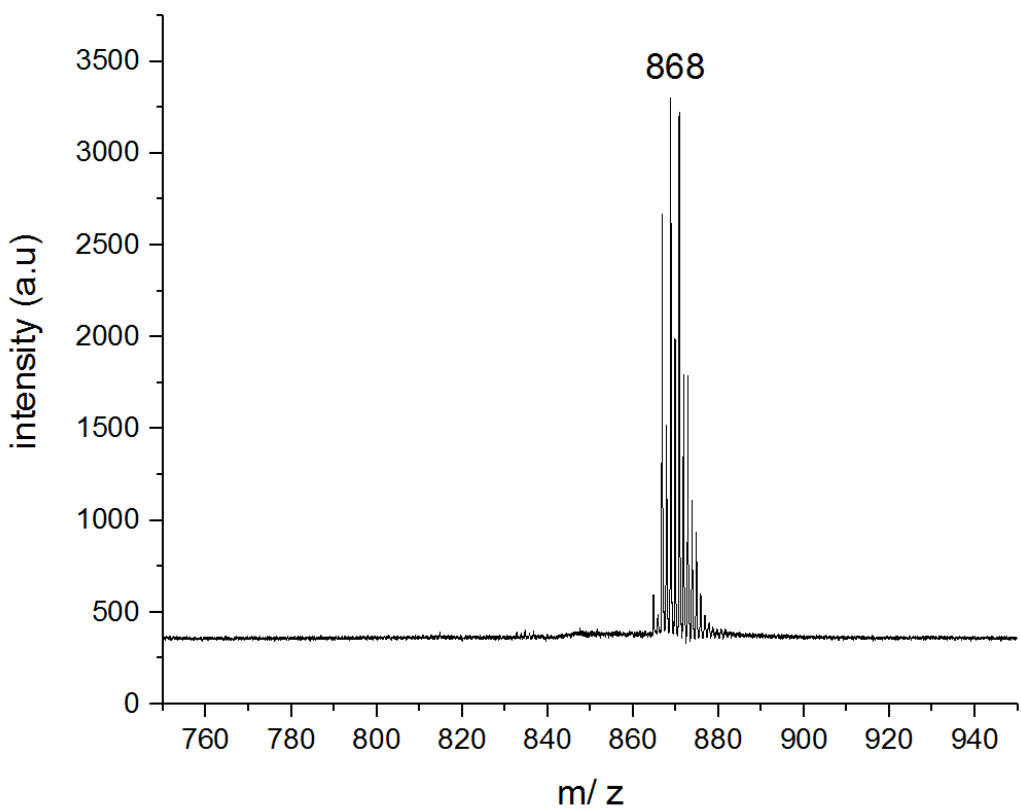


Figure S29: MALDI-ToF mass spectrum of **4b**. An m/z of 868 was observed and assigned to the complex cation $[LZn_2(OBzpCF_3)]^+$.

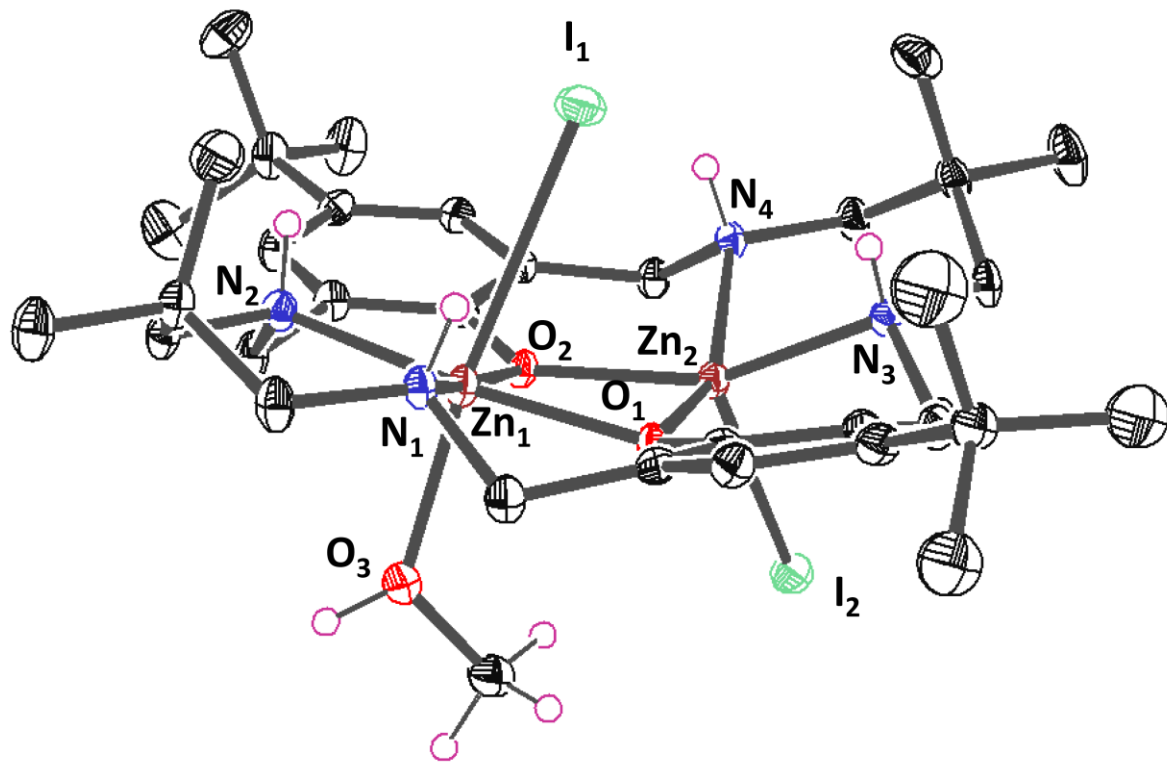


Figure S30: ORTEP representation of the molecular structure of **4a**, with disorder and hydrogen atoms (excluding N-H) omitted for clarity with thermal ellipsoids represented at 30 % probability.

Table 3: Selected bond lengths (\AA) and angles ($^\circ$) for complex **4a**.

Bond	Bond Length (\AA)	Bond	Bond Angle ($^\circ$)
N (1) – Zn (1)	2.13(1)	N (1) – Zn (1) – O (2)	151.0(7)
N (2) – Zn (1)	2.14(4)	N (2) – Zn (1) – O (1)	150.8(0)
O (1) – Zn (1)	2.08(7)	N (1) – Zn (1) – I (1)	100.9(4)
O (2) – Zn (1)	2.06(0)	N (3) – Zn (2) – O (2)	171.3(2)
I (1) – Zn (1)	2.64(2)	N (4) – Zn (2) – O (1)	171.7(6)
I (2) – Zn (1)	3.70(4)	I (2) – Zn (2) – O (1)	174.1(8)
N (3) – Zn (2)	2.10(8)		
N (4) – Zn (2)	2.10(7)		
O (1) – Zn (2)	2.05(1)		
O (2) – Zn (2)	2.05(3)		
I (2) – Zn (2)	3.13(0)		
O (3) – Zn (2)	2.13(8)		
Metal – Metal		Distance (\AA)	
		Zn (1) – Zn (2)	
		3.10(0)	

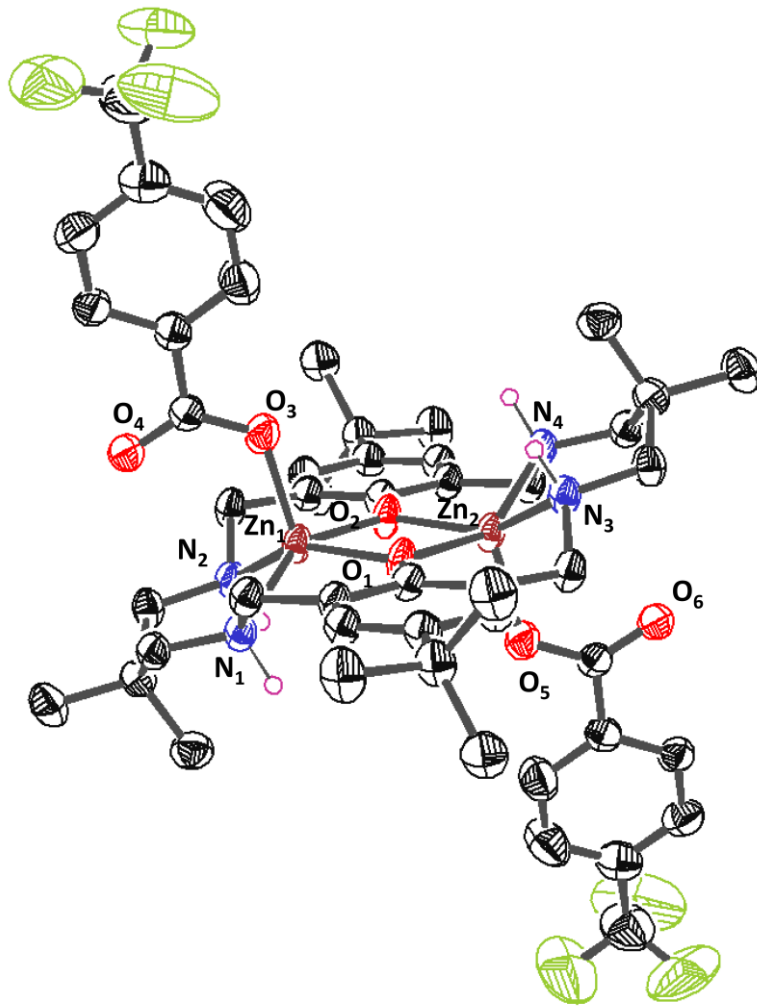


Figure S31: ORTEP representation of the molecular structure of **4b**, with disorder and hydrogen atoms (excluding N-H) omitted for clarity with thermal ellipsoids represented at 30 % probability.

Table S4: Selective bond lengths (\AA) and angles ($^\circ$) for complex **4b**.

Bond	Bond Length (\AA)	Bond	Bond Angle ($^\circ$)
N (1) – Zn (1)	2.10(6)	N (1) – Zn (1) – O (2)	148.4(7)
N (2) – Zn (1)	2.10(5)	N (2) – Zn (1) – O (1)	147.8(5)
O (1) – Zn (1)	2.06(4)	O (3) – Zn (1) – I (1)	99.6(0)
O (2) – Zn (1)	2.04(1)	N (3) – Zn (2) – O (2)	147.8(5)
O (3) – Zn (1)	1.98(7)	N (4) – Zn (2) – O (1)	148.4(7)
N (3) – Zn (2)	2.10(5)	O (5) – Zn (2) – O(1)	102.0(1)
N (4) – Zn (2)	2.10(6)		
O (1) – Zn (2)	2.04(1)	Metal – Metal	Distance (\AA)
O (2) – Zn (2)	2.06(4)	Zn (1) – Zn (2)	3.19(2)
O (5) – Zn (2)	1.98(7)		

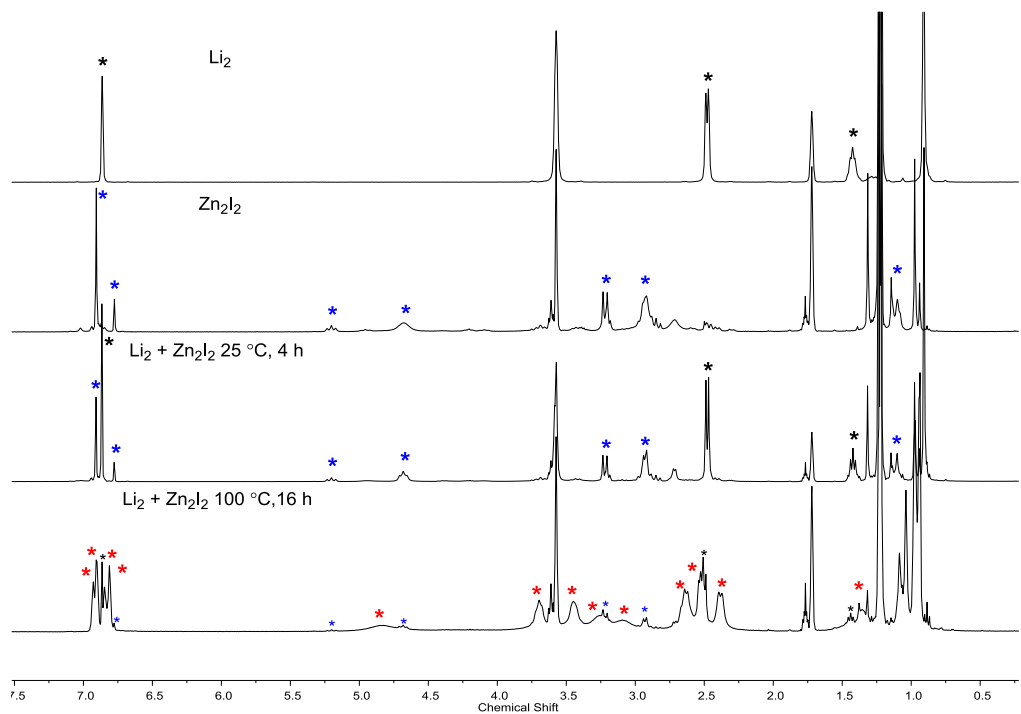


Figure S32: Metal redistribution reaction between **1** and **4a** (d_8 -THF).

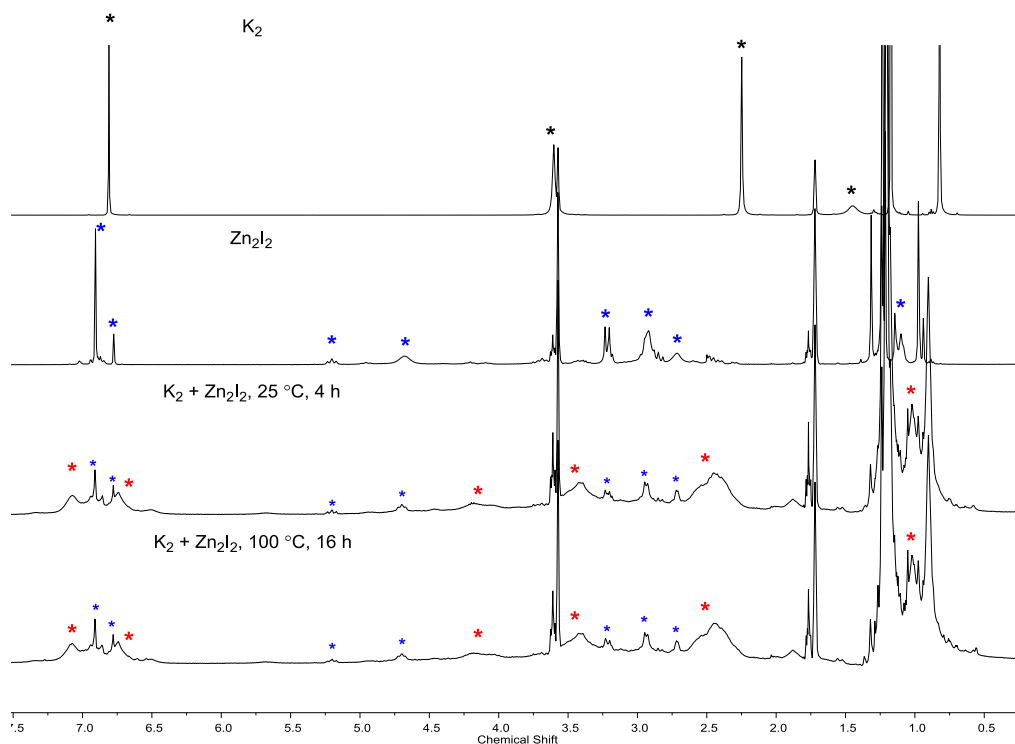


Figure S33: Metal redistribution reaction between **3** and **4a** (d_8 -THF).

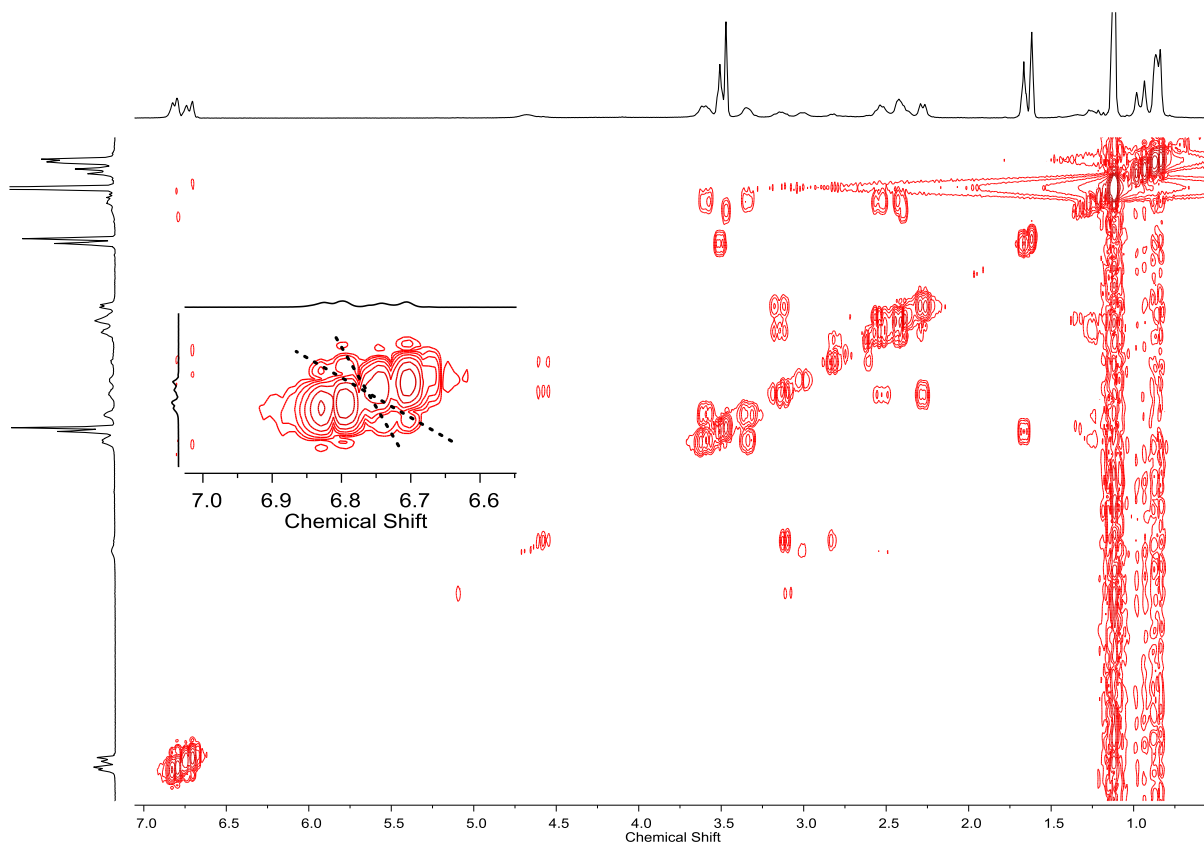


Figure S34: COSY NMR of product formed from metal redistribution reaction between **1** and **4a** (d_8 -THF).

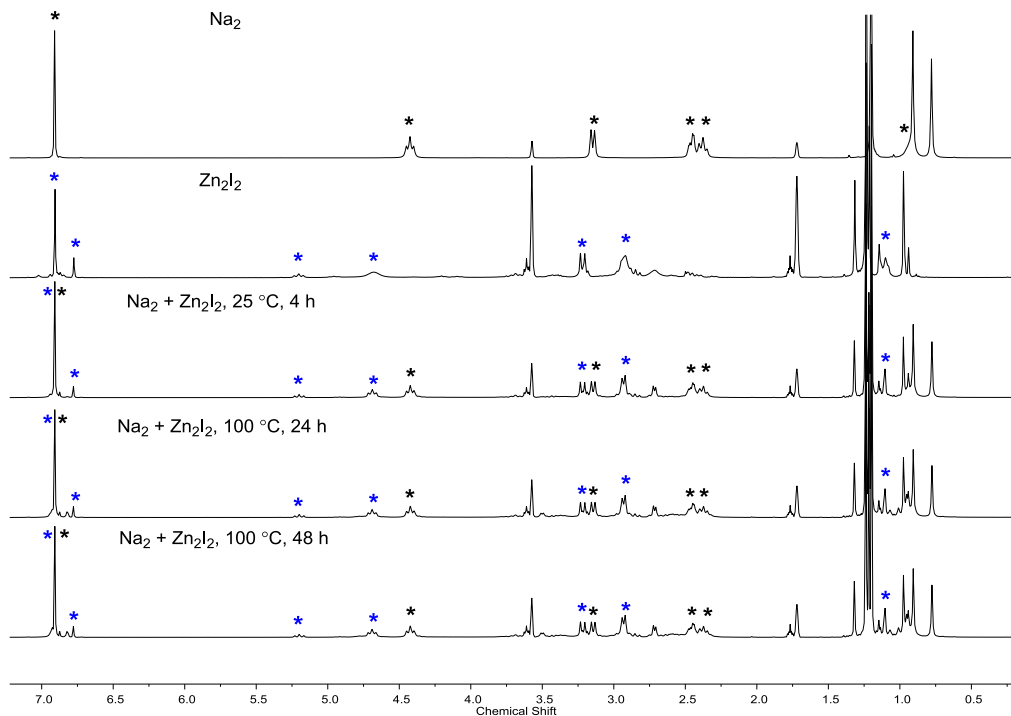


Figure S35: Metal redistribution reaction between **2** and **4a**. (d_8 -THF).

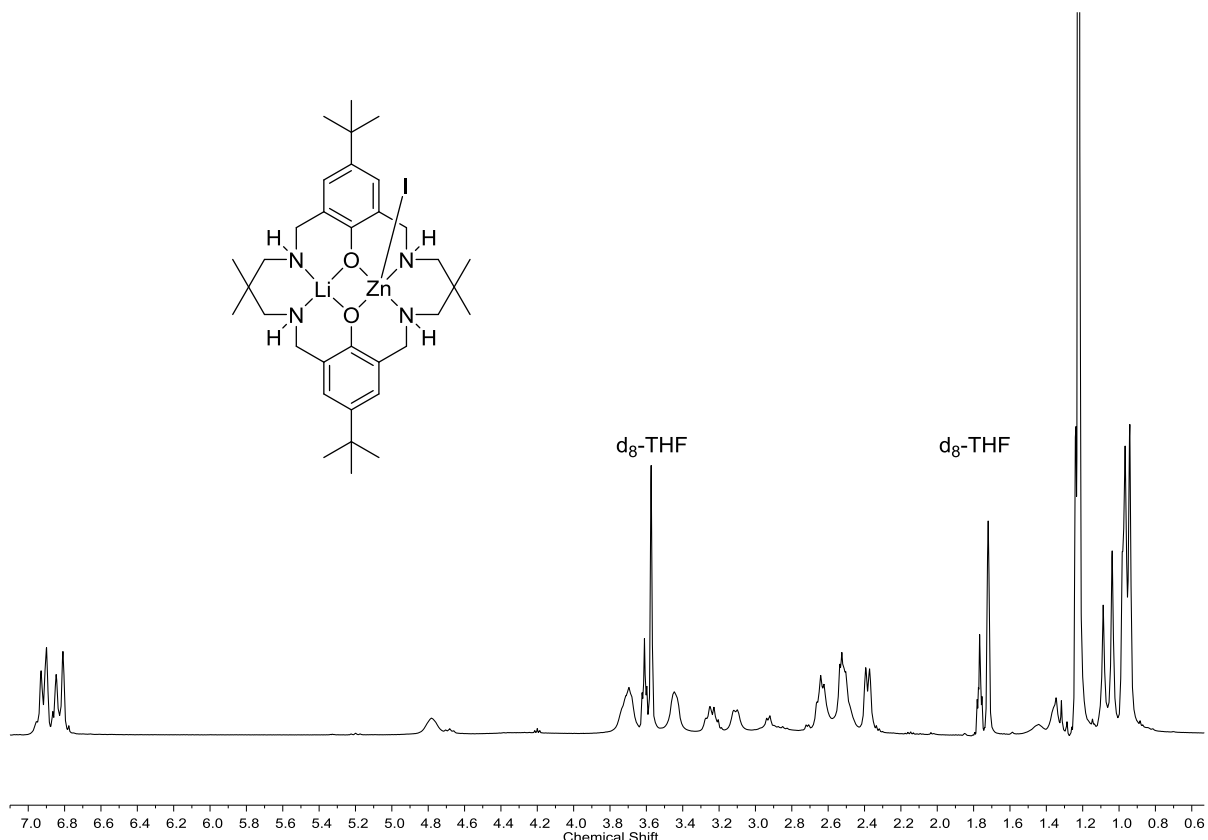


Figure S36: ^1H NMR of complex **5a** prepared through sequential metalation (d_8 -THF, 298 K).

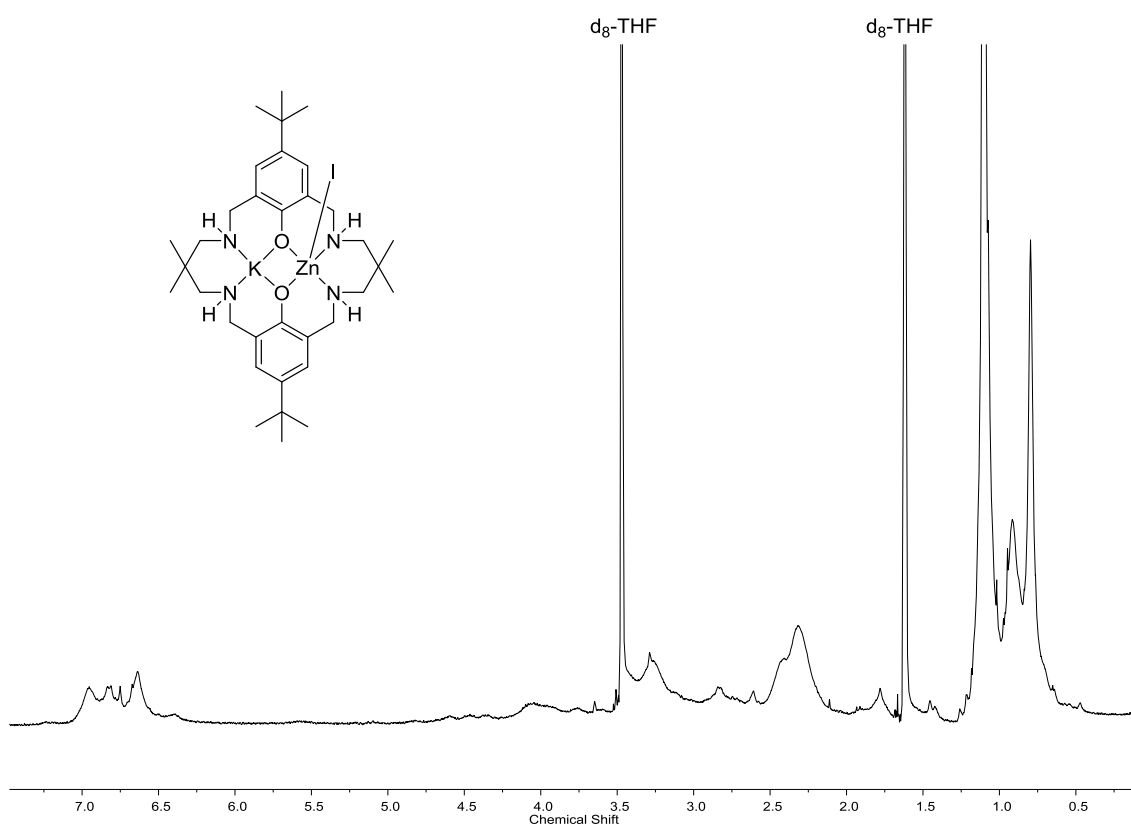


Figure S37: ^1H NMR of complex **7a** prepared through sequential metalation. (d_8 -THF, 298 K).

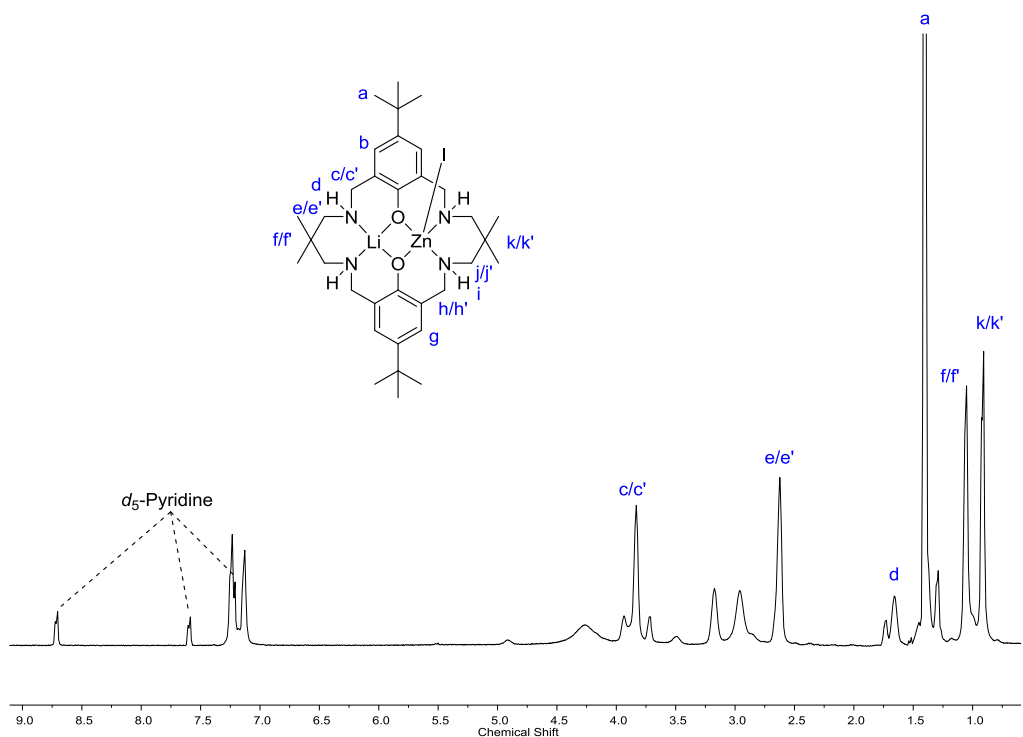


Figure S38: ^1H NMR spectrum of **5a** (d_5 -pyridine, 403 K).

Due to multiple conformations and fluxionality of complex **5a** at room temperature, the complex was analysed by ^1H NMR spectroscopy in a range of high boiling organic solvents, including toluene, dioxane, tetrachloroethane, DMSO and pyridine. Although full coalescence of the proton environments are not fully observed, coupling between the phenyl proton resonances are observed in the COSY NMR, indicating heterodinuclear complex formation. (Figure S39)

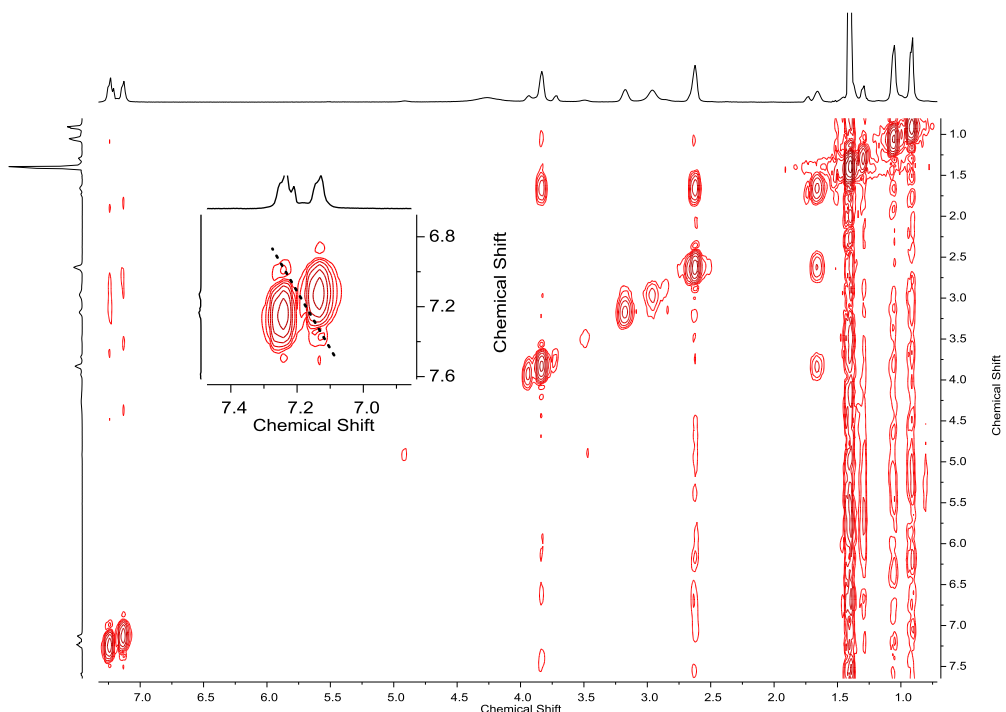


Figure S39: COSY NMR of complex **5a** (d_5 -pyridine, 403 K).

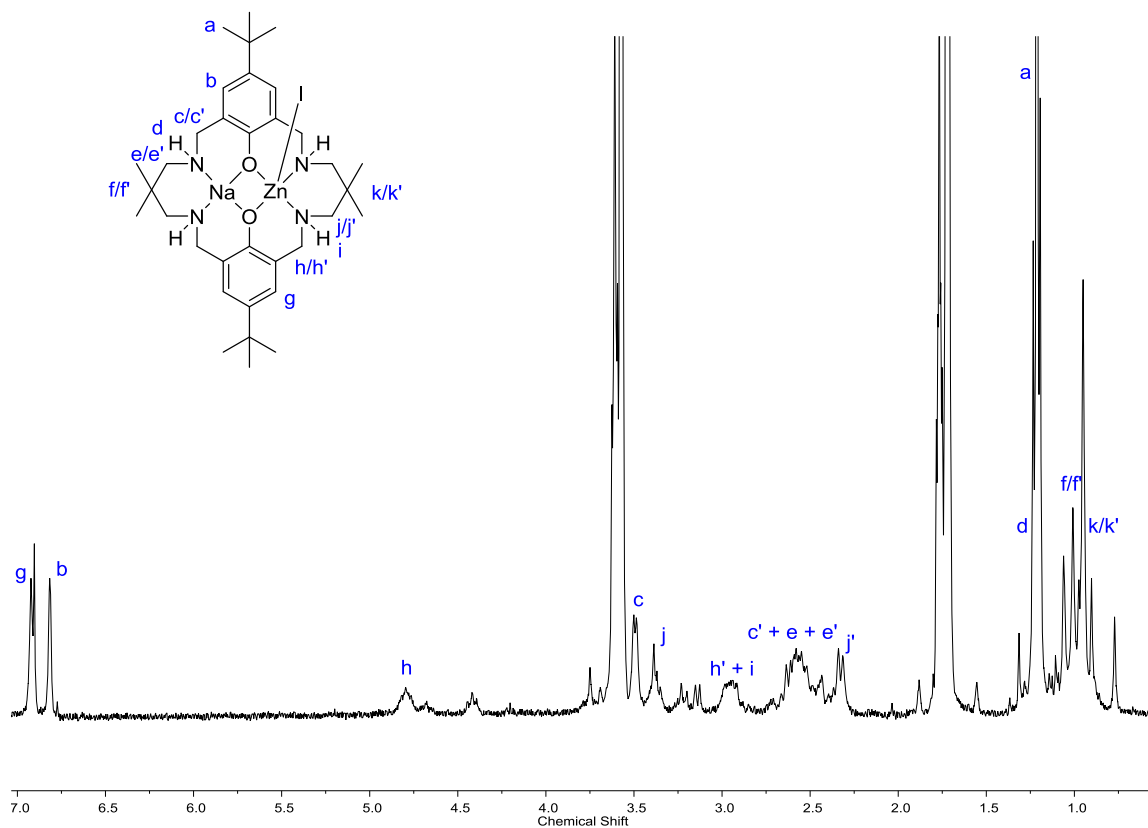


Figure S40: ^1H NMR of complex **6a** ($\text{d}_8\text{-THF}$, 298 K).

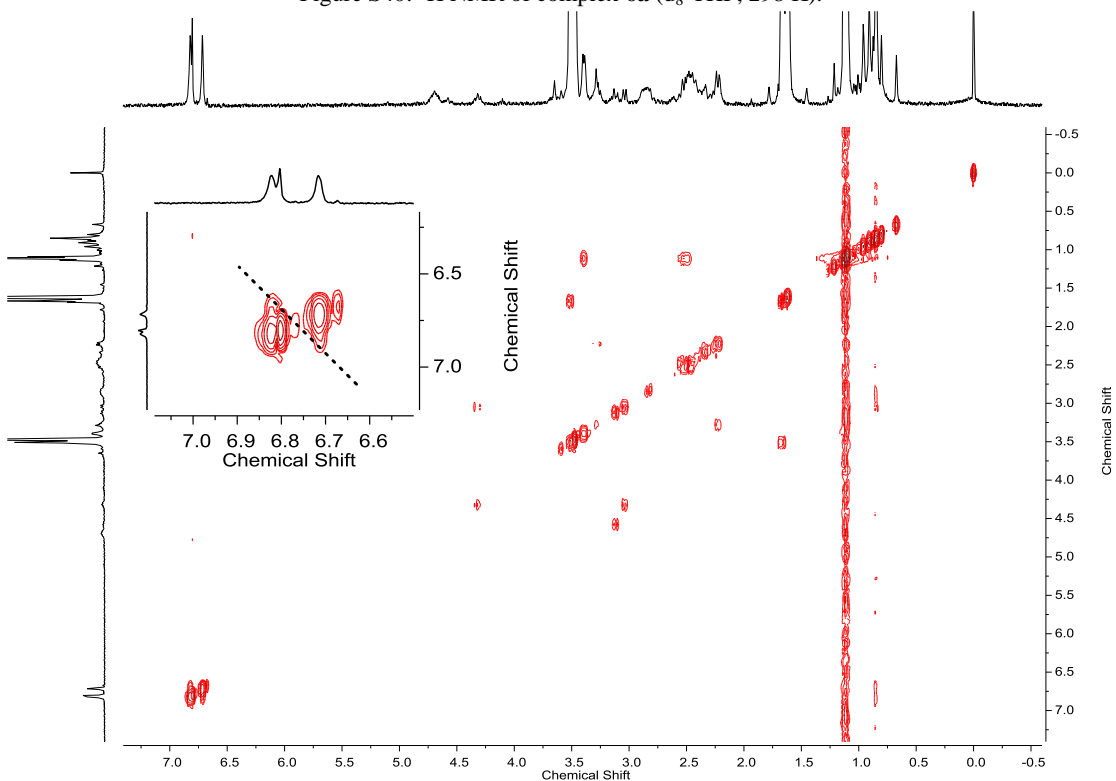


Figure S41: COSY NMR of complex **6a** ($\text{d}_8\text{-THF}$, 298 K).

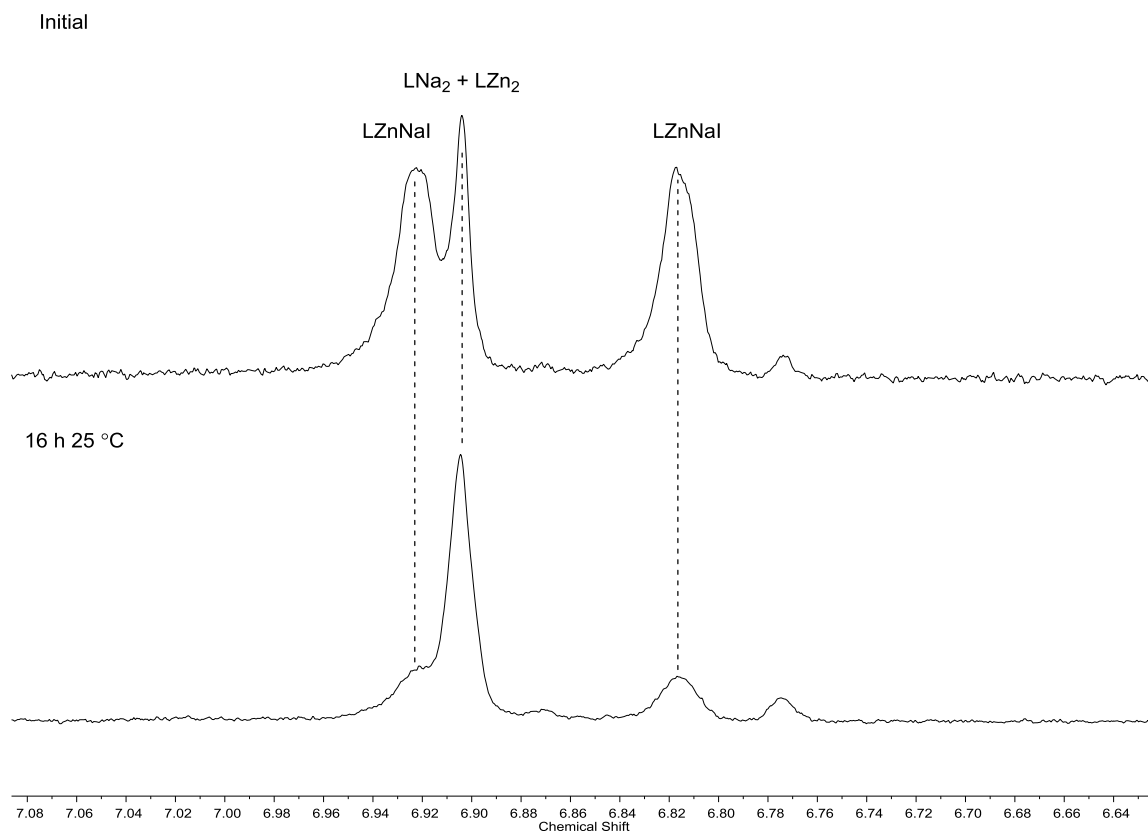


Figure S42: Metal redistribution of complex **6a** towards complexes **2** and **4a** as observed in ^1H NMR (d_8 -THF, 298 K).

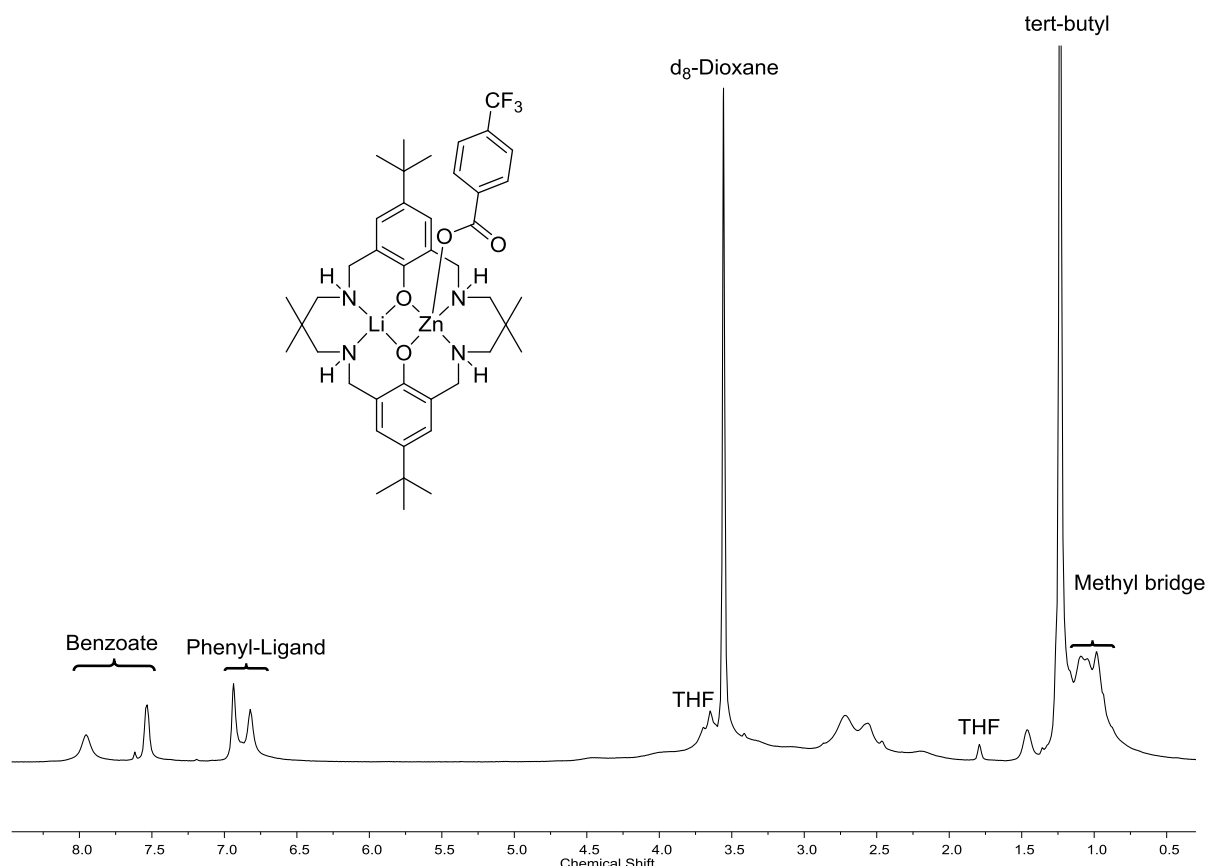


Figure S43: ^1H NMR of complex **5b** (d_8 -dioxane, 403 K).

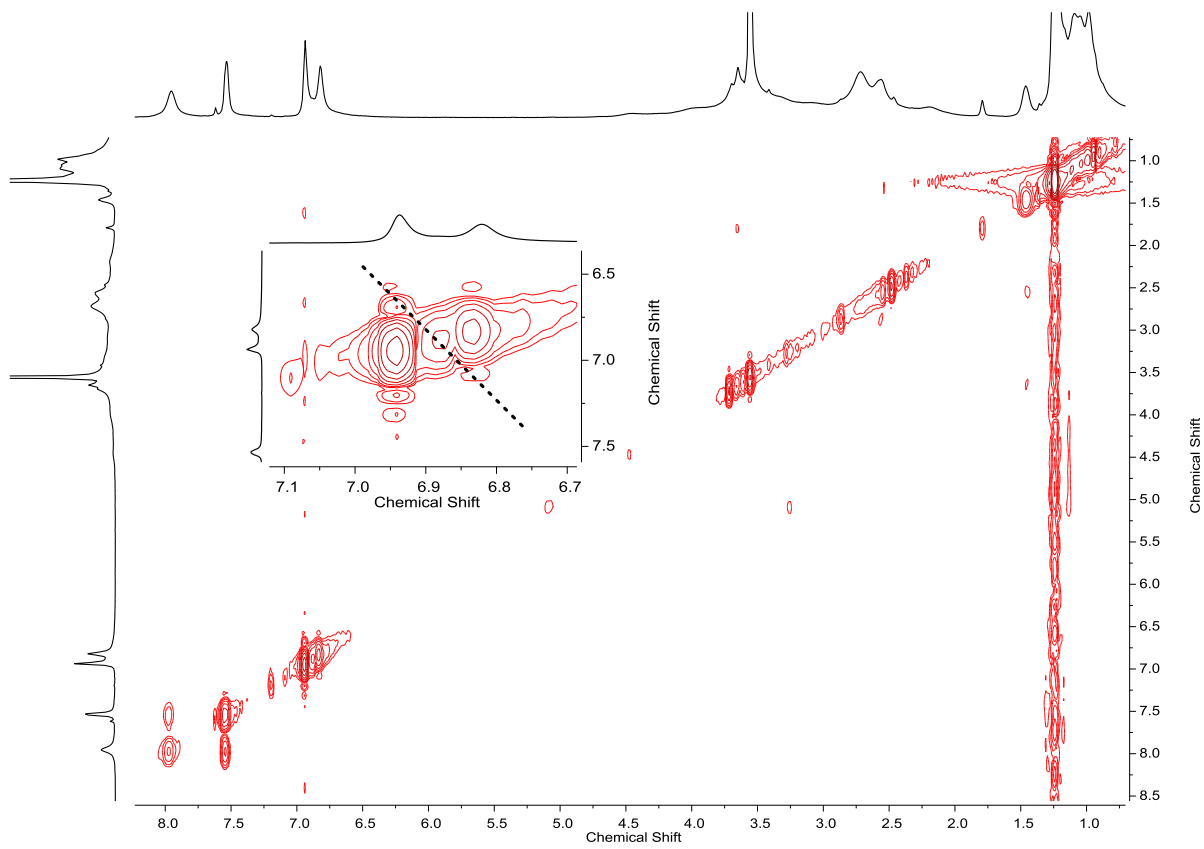


Figure S44: COSY NMR of complex **5b** (d_8 -dioxane, 403 K).

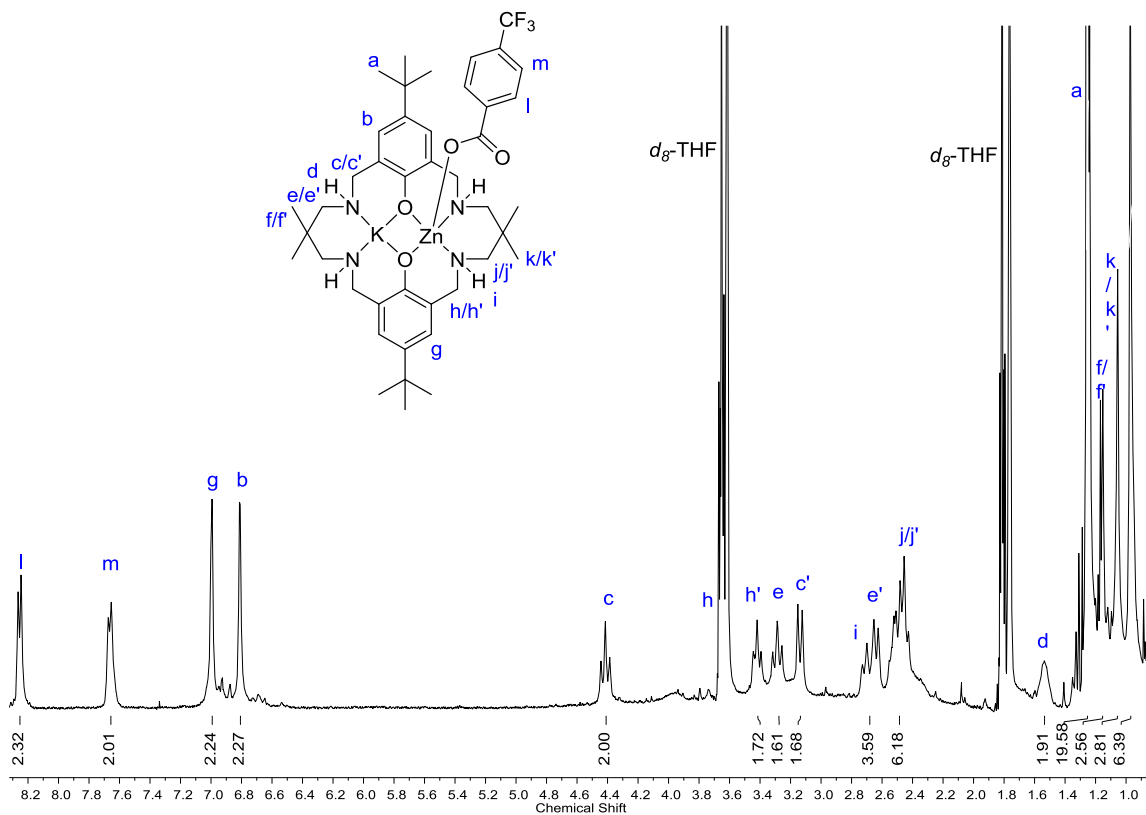


Figure S45: ^1H NMR of complex **7b** (d_8 -THF, 298 K).

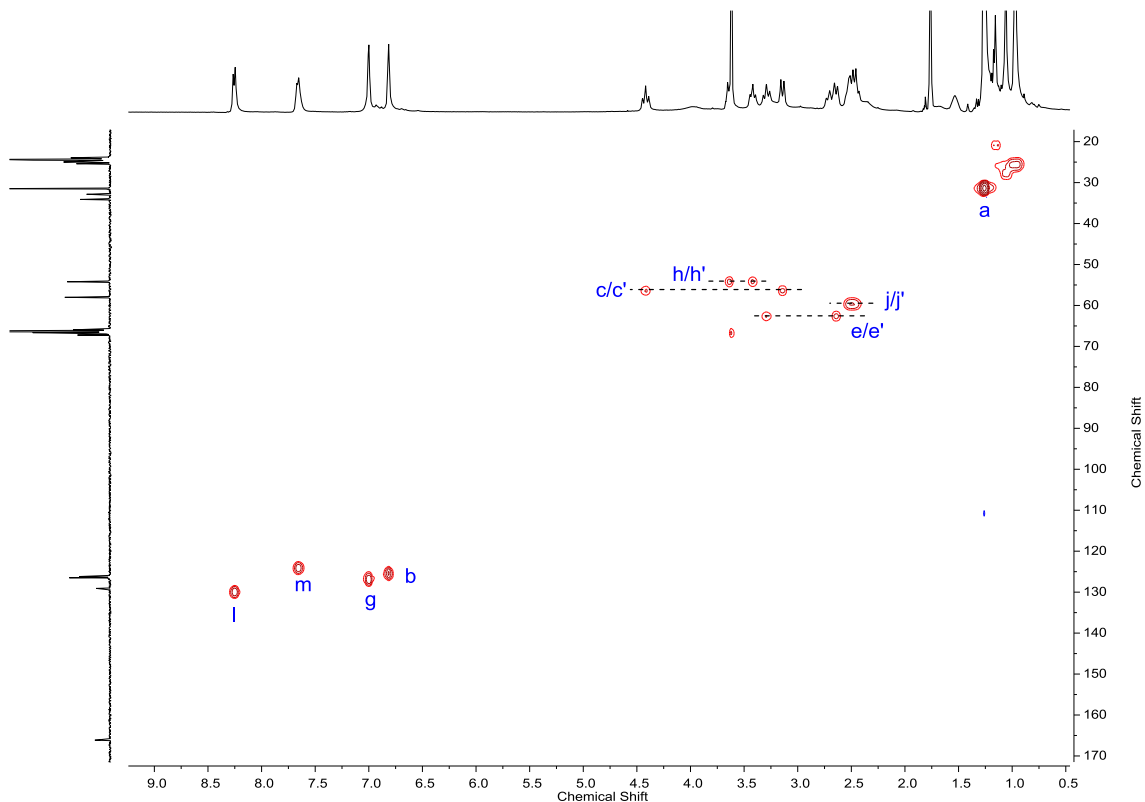


Figure S46: HSQC NMR of complex **7b** (d_8 -THF, 298 K).

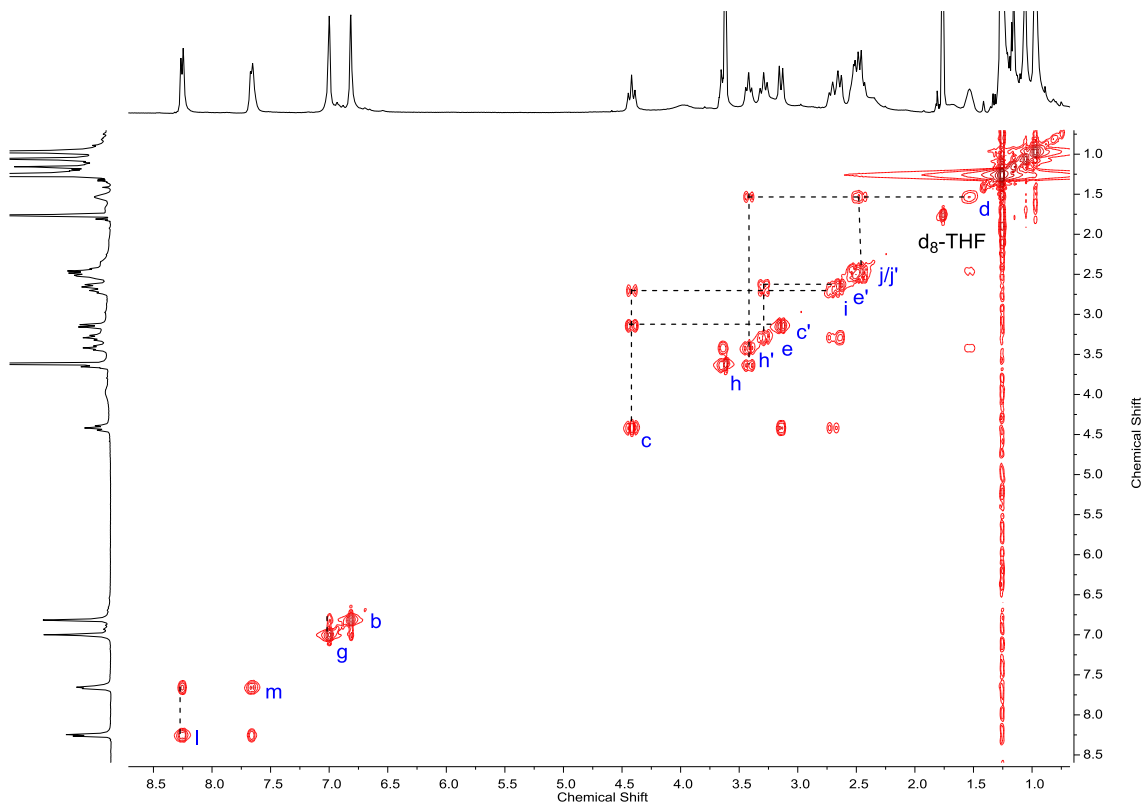


Figure S47: COSY NMR of complex **7b** (d_8 -THF, 298K).

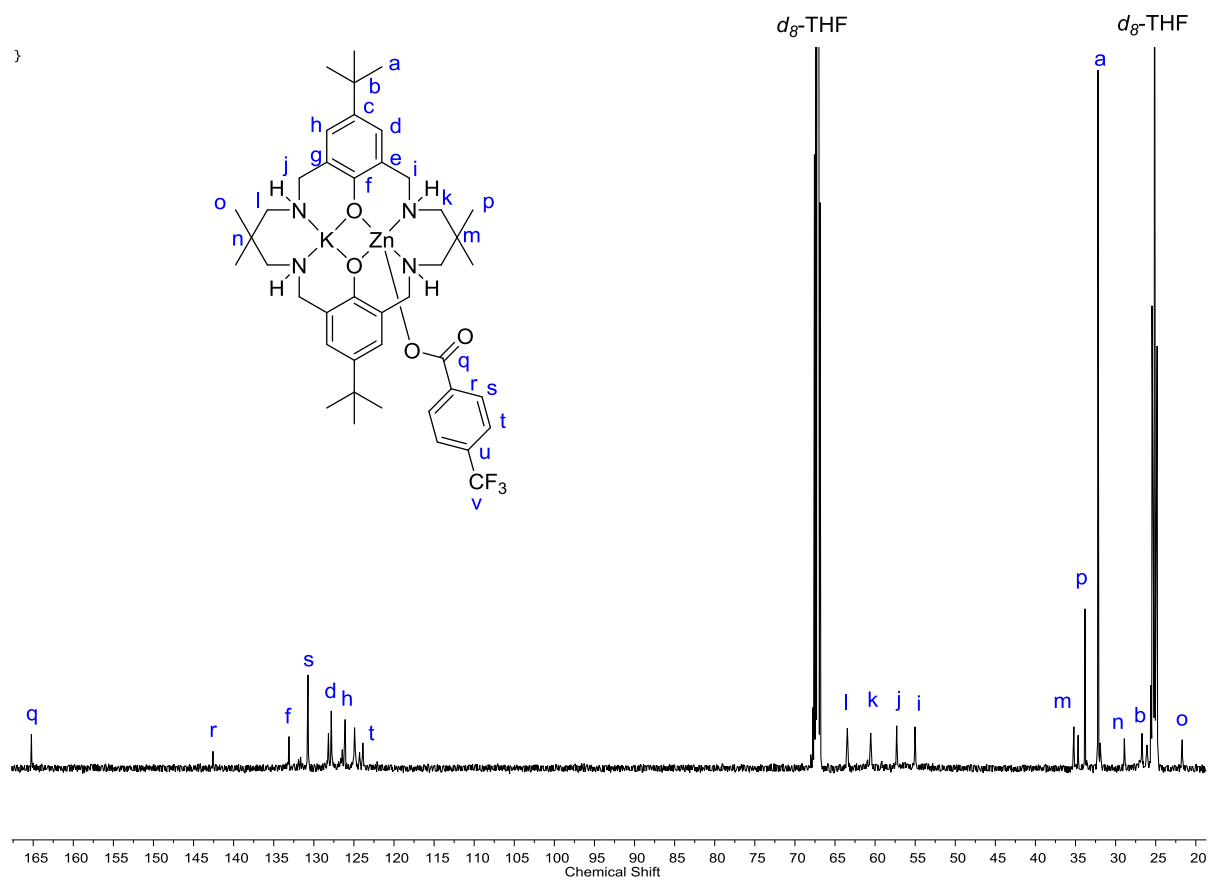


Figure S48: ^{13}C NMR of complex **7b** ($d_8\text{-THF}$, 298 K).

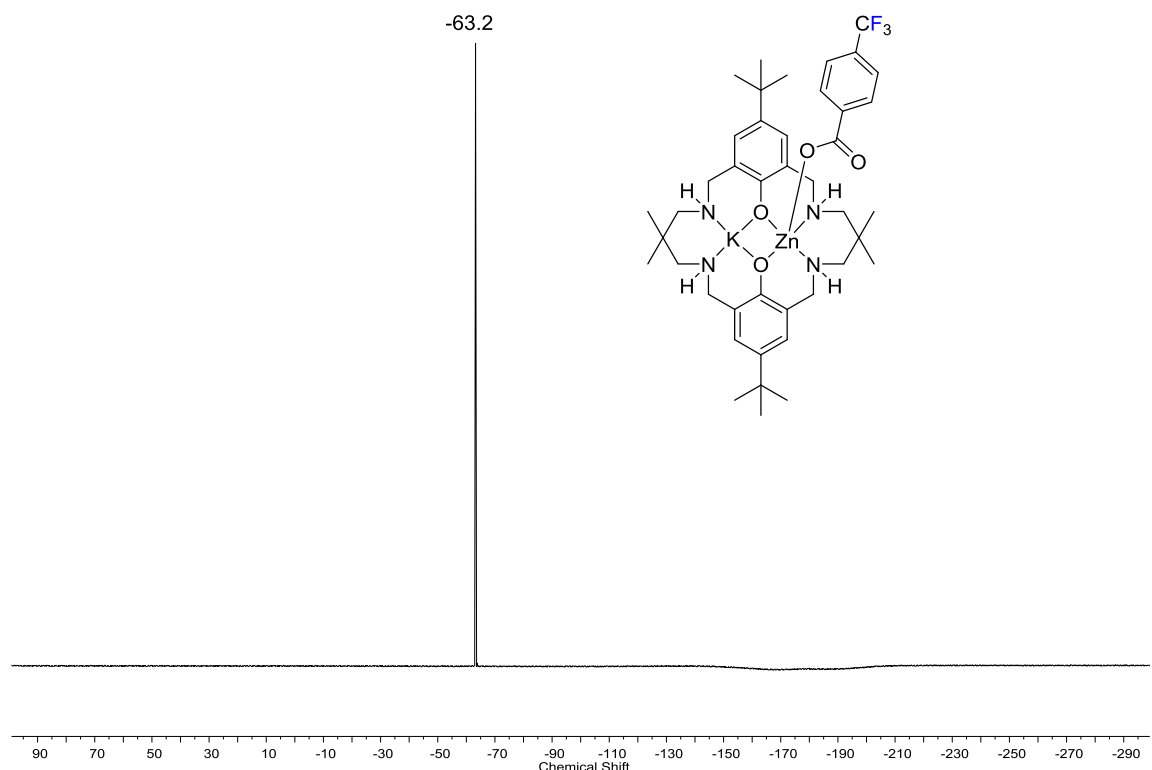


Figure S49: ^{19}F NMR of complex **7b** ($d_8\text{-THF}$, 298 K).

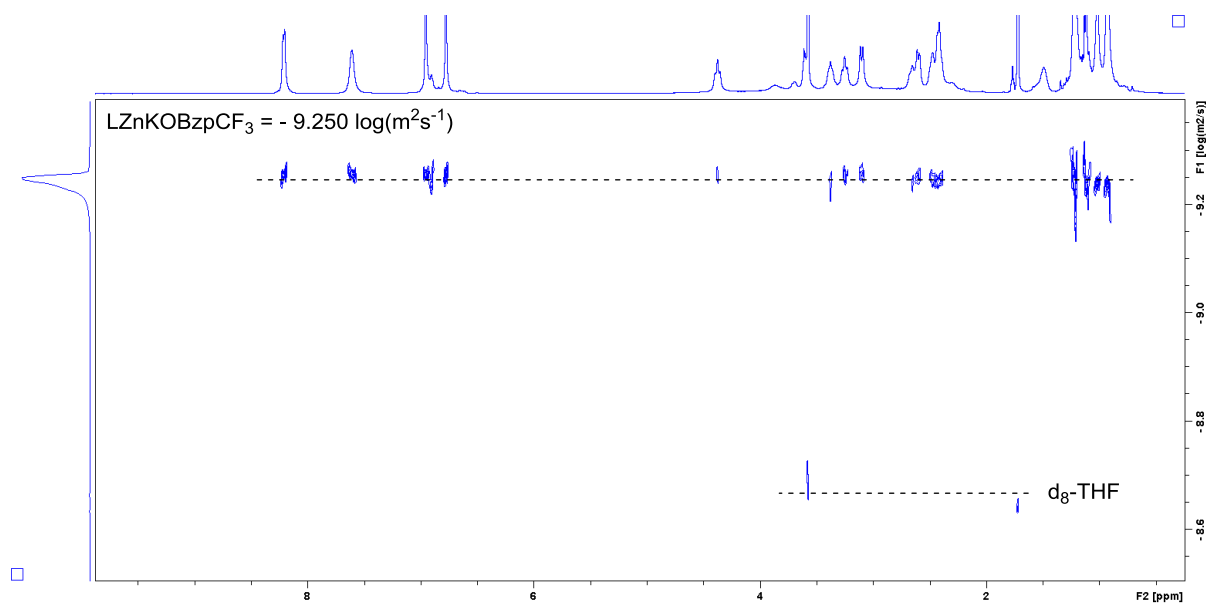


Figure S50: 2D DOSY NMR of complex **7b** (d_8 -THF, 298 K).

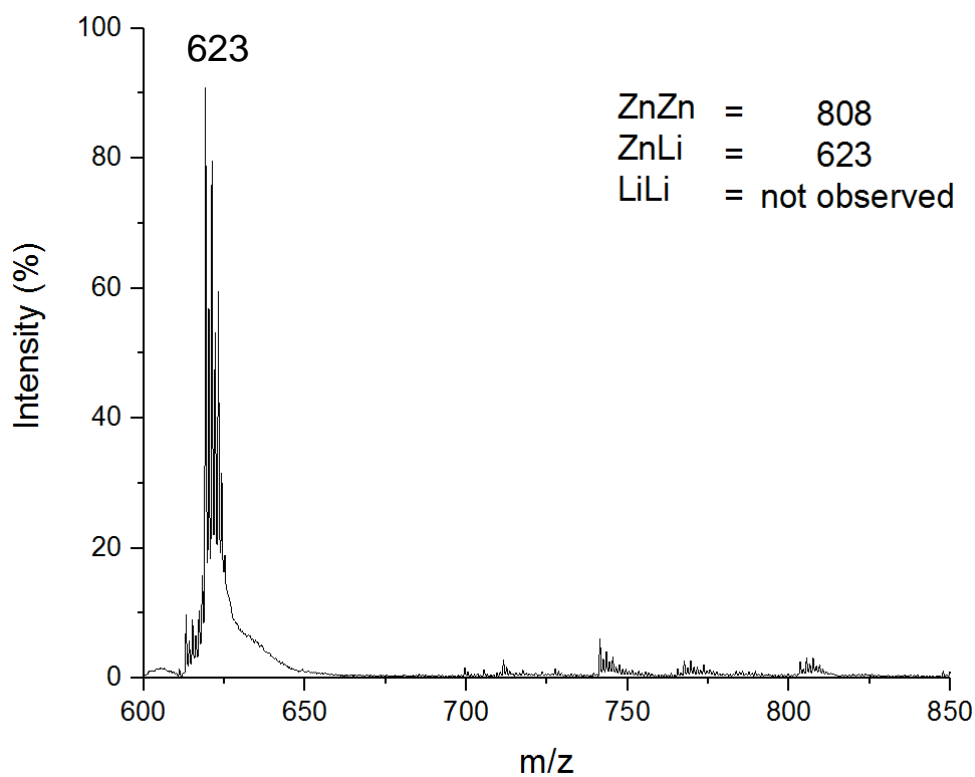


Figure S51: MALDI-ToF mass spectrum of complex **5a**

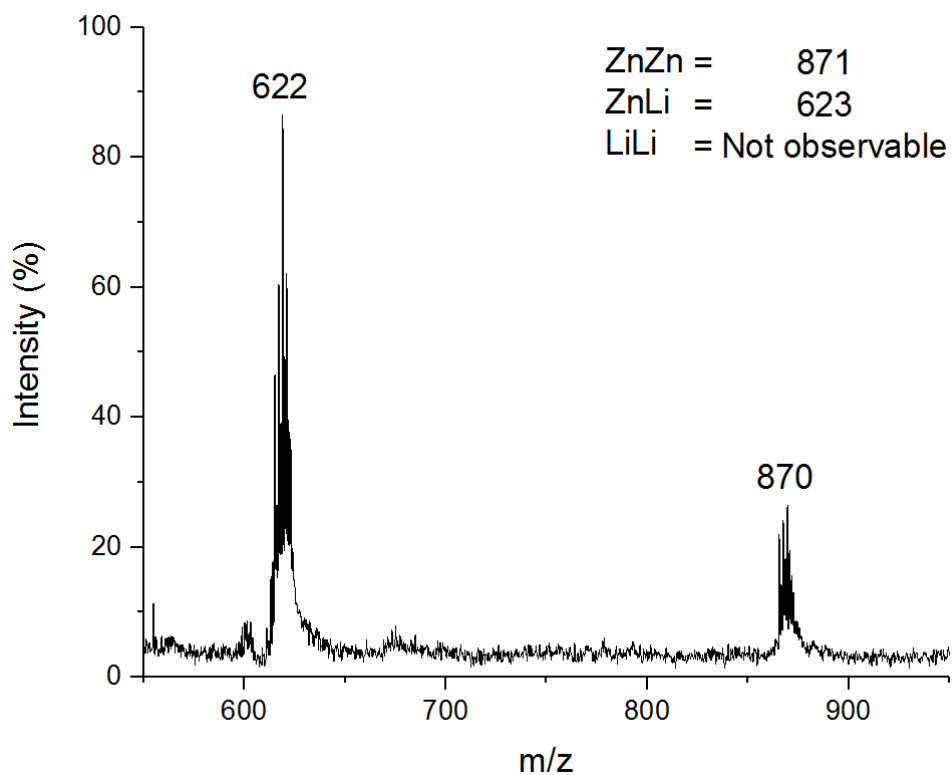


Figure 52: MALDI-ToF mass spectrum of complex **5b**.

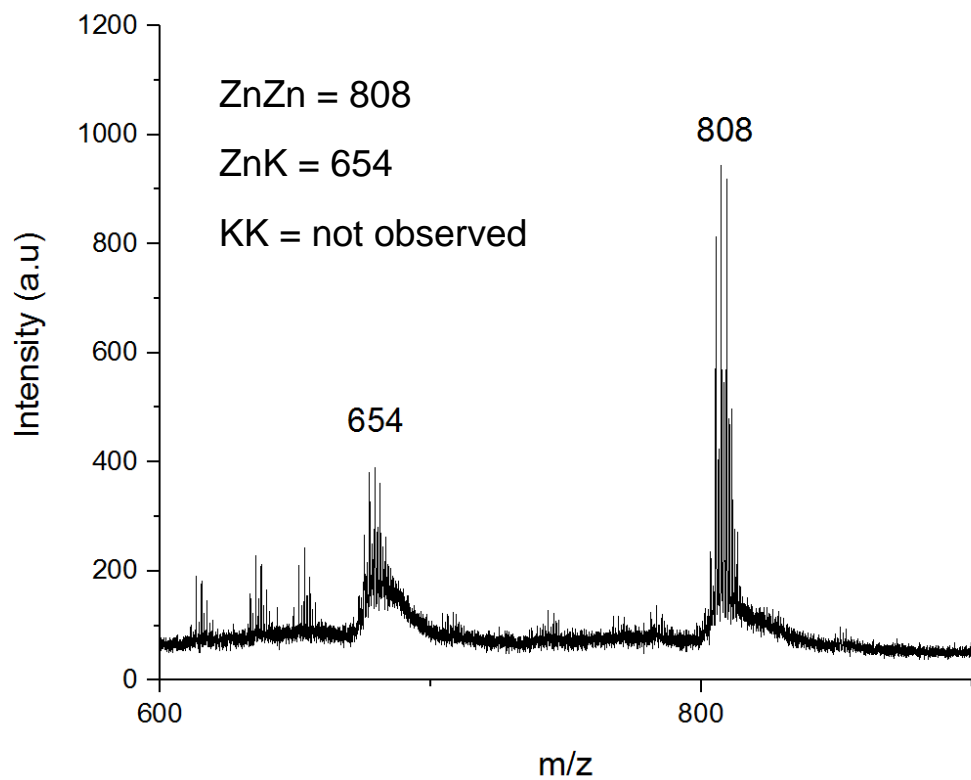


Figure S53: MALDI-ToF mass spectrum of complex **7a**.

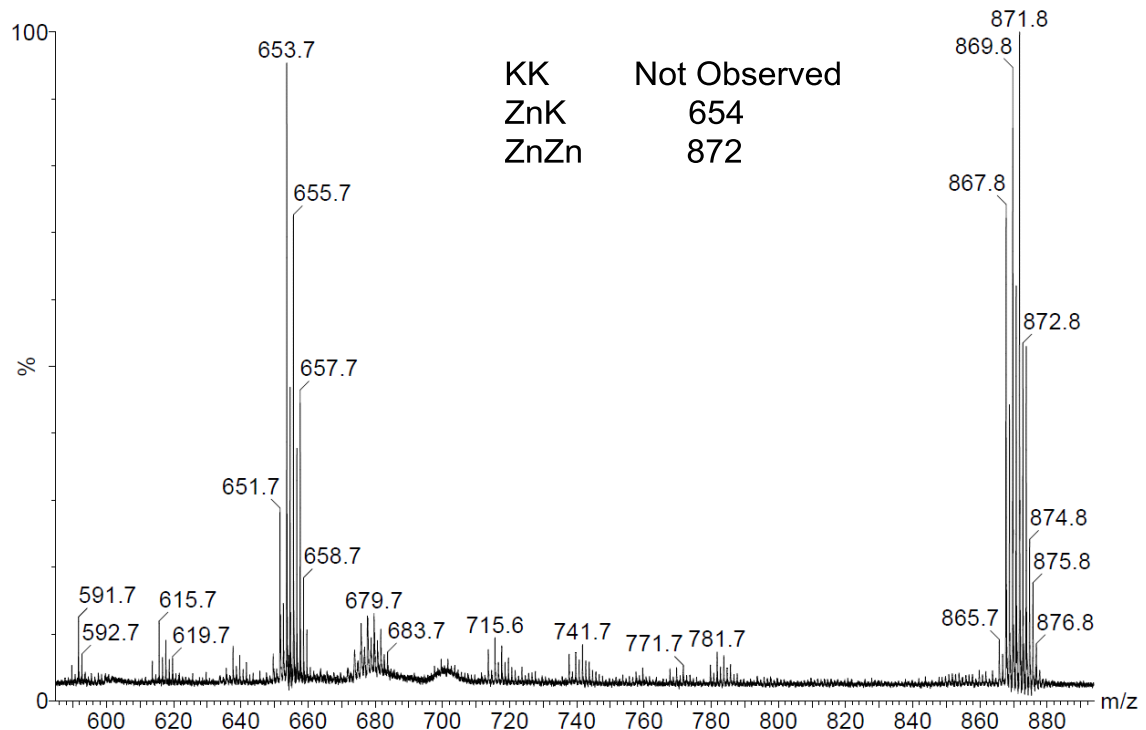


Figure S54: MALDI-ToF mass spectrum of complex **7b**.

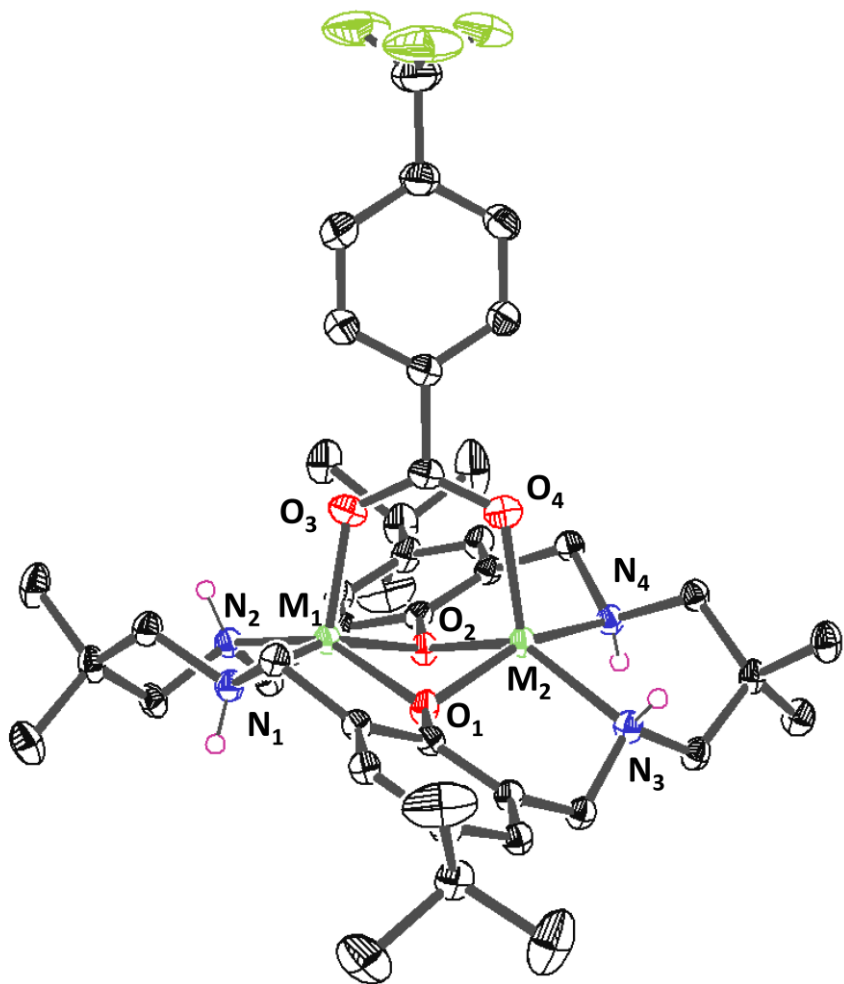


Figure S55: ORTEP representation of the molecular structure of **5b**, with disorder and hydrogen atoms (excluding N-H) omitted for clarity with thermal ellipsoids represented at 30 %.

Bond	Bond Length (Å)	Bond	Bond Angle (°)
N (1) – M (1)	2.16(5)	N (1) – M (1) – O (2)	157.9(5)
N (2) – M (1)	2.14(5)	N (2) – M (1) – O (1)	147.4(6)
O (1) – M (1)	1.98(4)	O (1) – M (1) – O (3)	100.0(1)
O (2) – M (1)	2.00(3)	N (3) – M (2) – O (2)	142.9(3)
O (3) – M (1)	1.99(3)	N (4) – M (2) – O (1)	155.9(3)
N (3) – M (2)	2.22(5)	O (1) – M (2) – O (4)	99.6(1)
N (4) – M (2)	2.15(2)	Metal – Metal	
O (1) – M (2)	1.98(8)	M (1) – M (1)	
O (2) – M (2)	1.99(1)	Distance (Å)	
O (4) – M (2)	2.03(5)	2.86(1)	

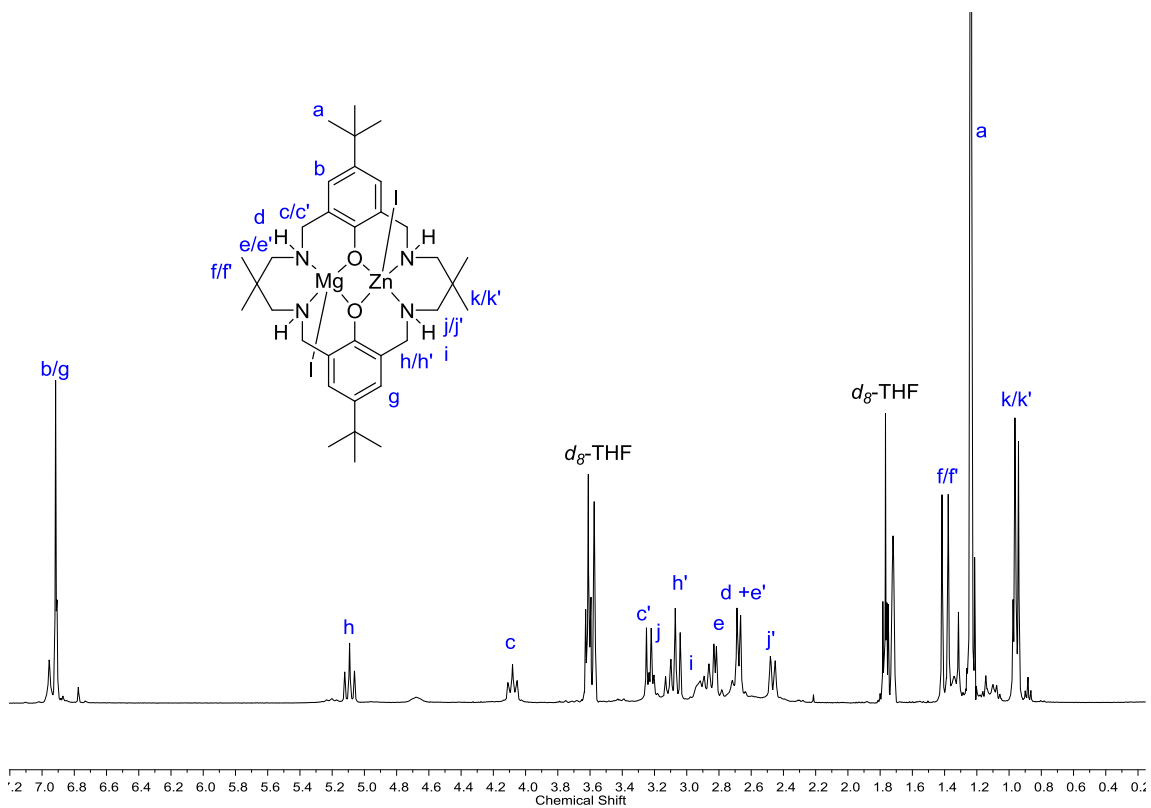


Figure S56: ^1H NMR of **8a** ($d_8\text{-THF}$, 298 K).

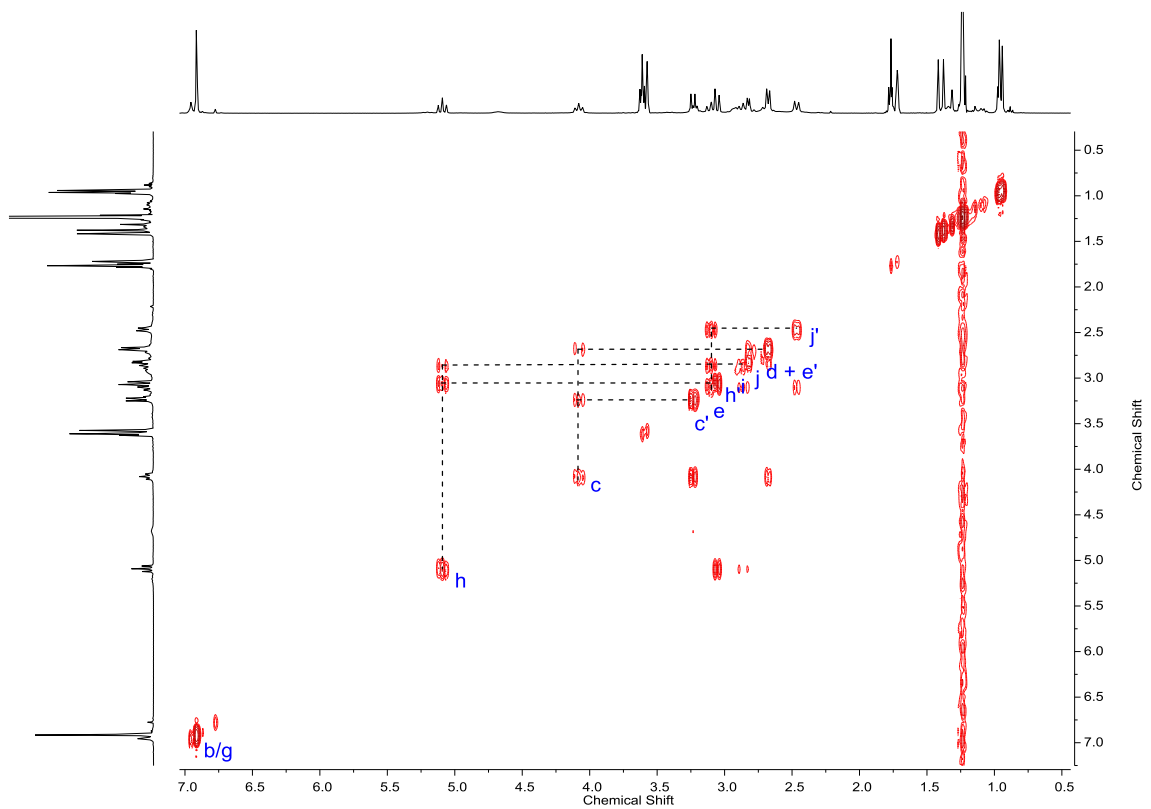


Figure S57: 2D COSY NMR of **8a** ($d_8\text{-THF}$, 298 K).

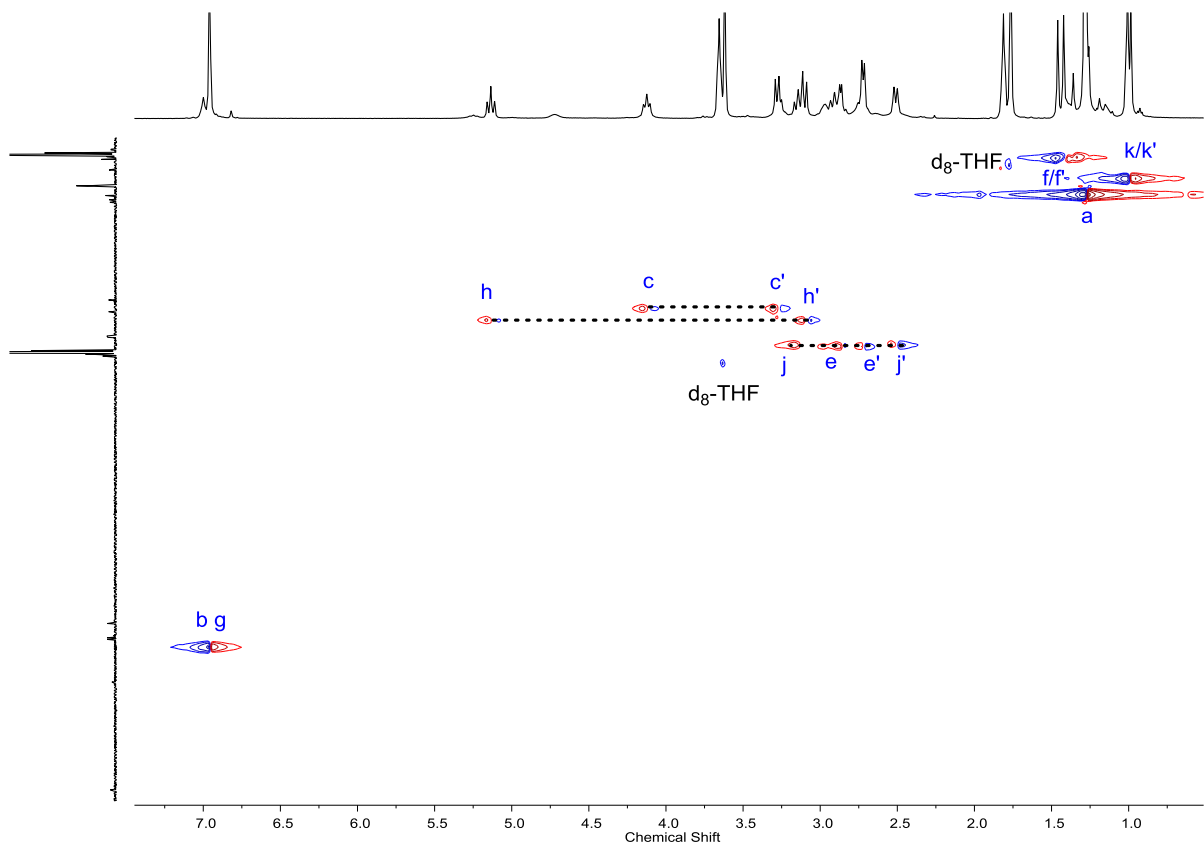


Figure S58: HSQC NMR of complex **8a** (d_8 -THF, 298 K).

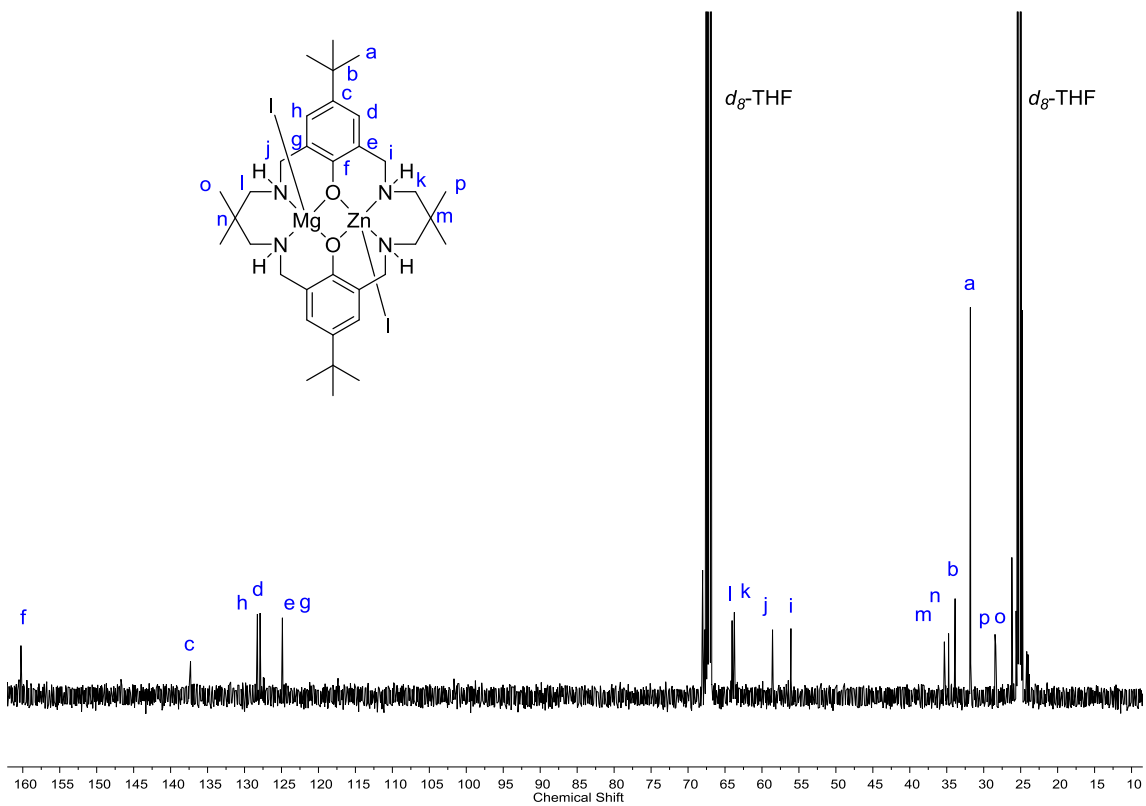


Figure S59: ^{13}C NMR of **8a** (d_8 -THF, 298 K).

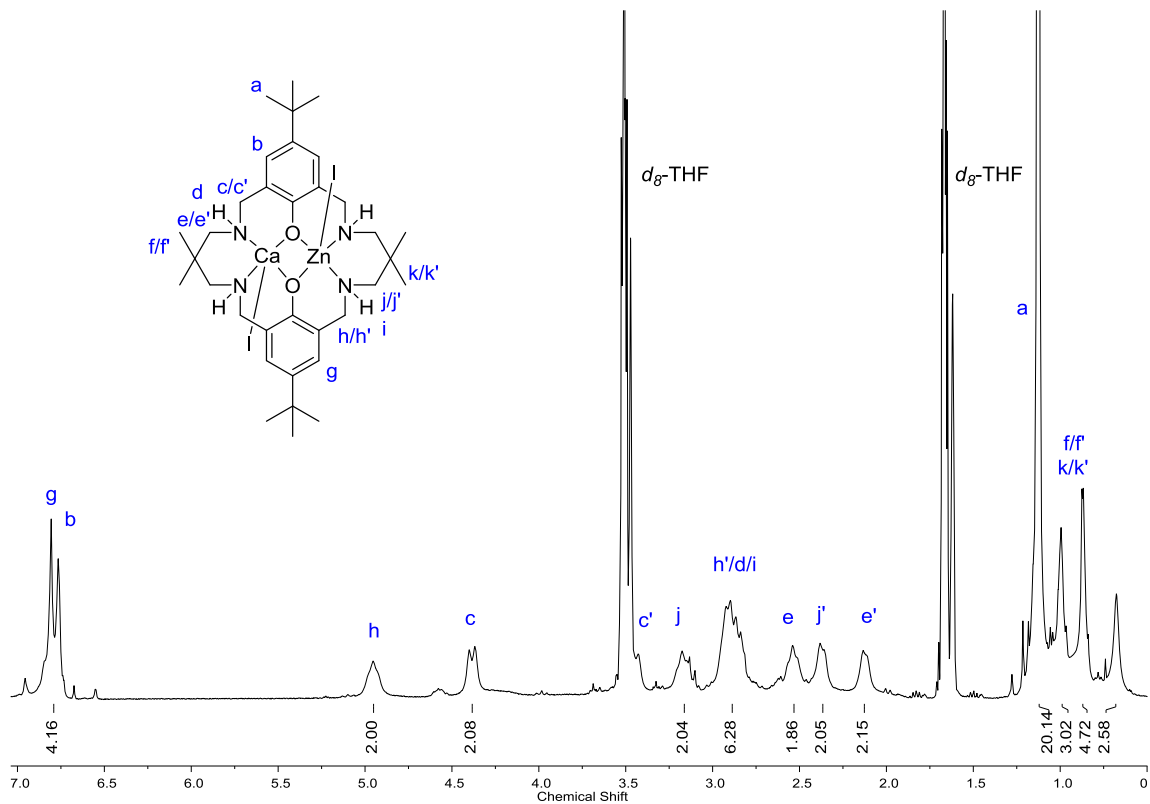


Figure S60: ^1H NMR of **9a** ($d_8\text{-THF}$, 298 K).

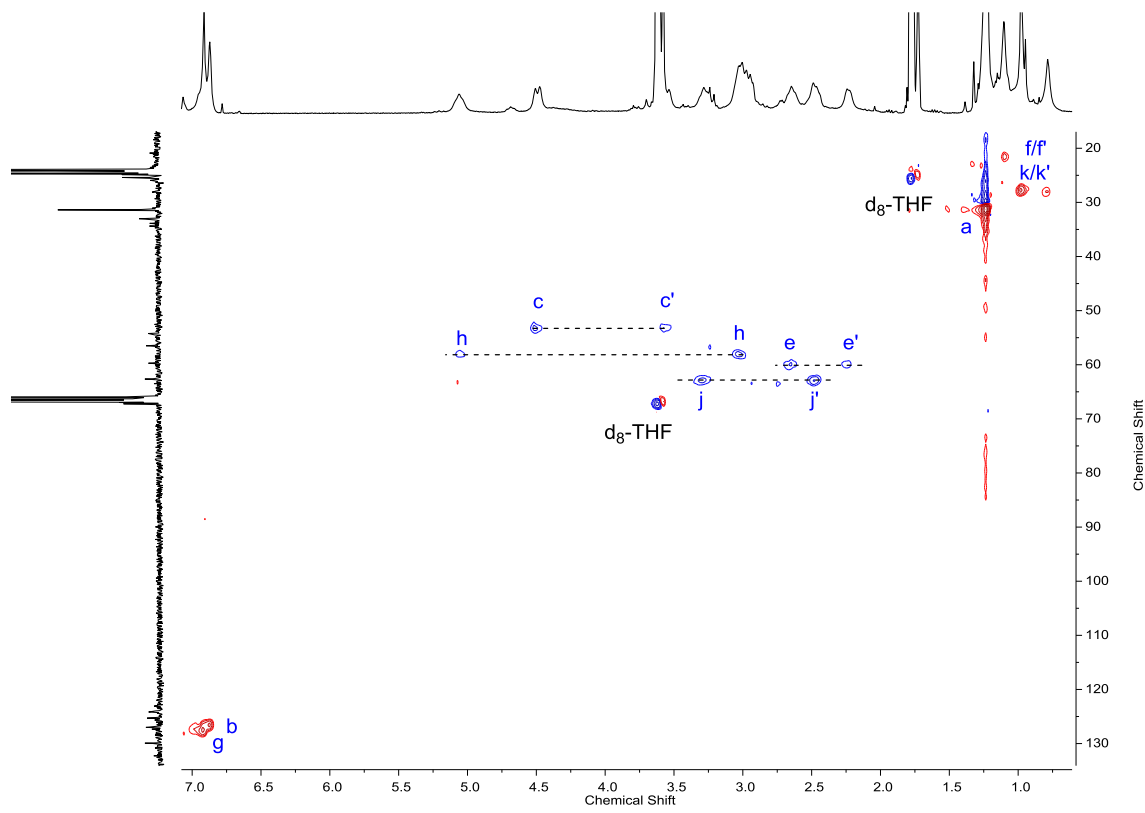


Figure S61: 2D HSQC NMR of **9a** ($d_8\text{-THF}$, 298 K).

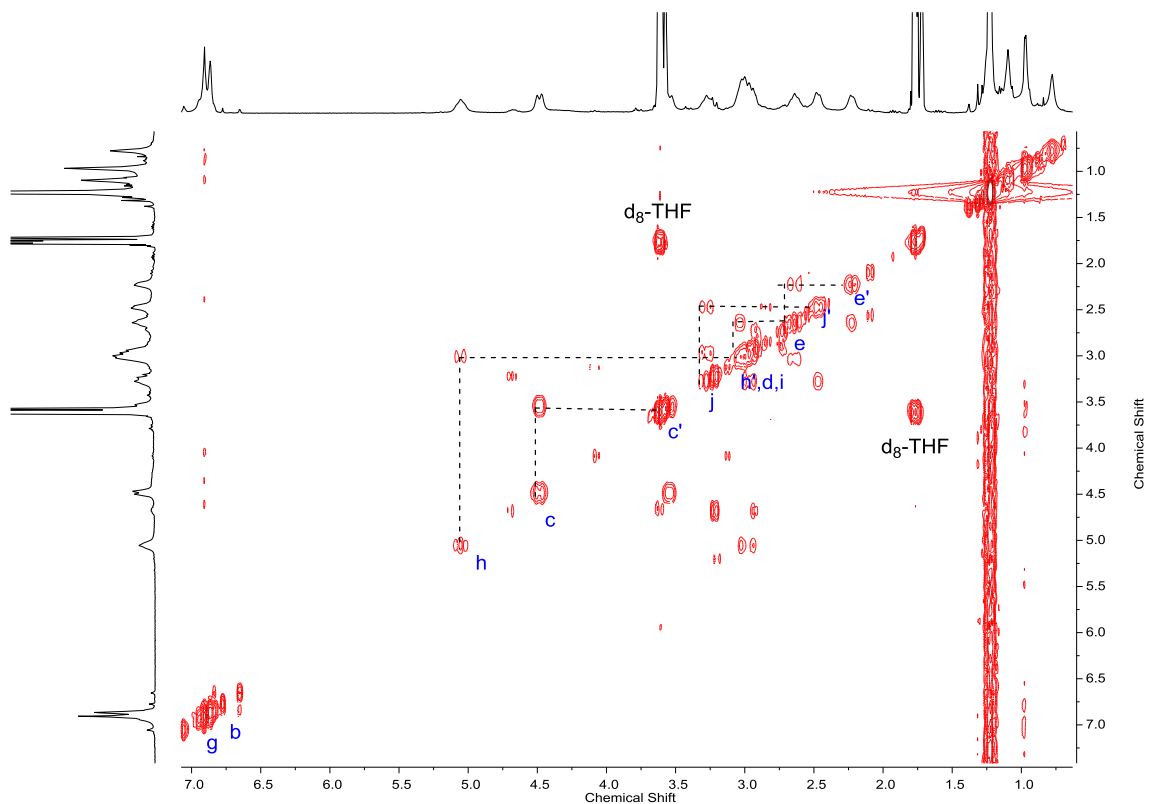


Figure S62: 2D COSY NMR of **9a** (d_8 -THF, 298 K).

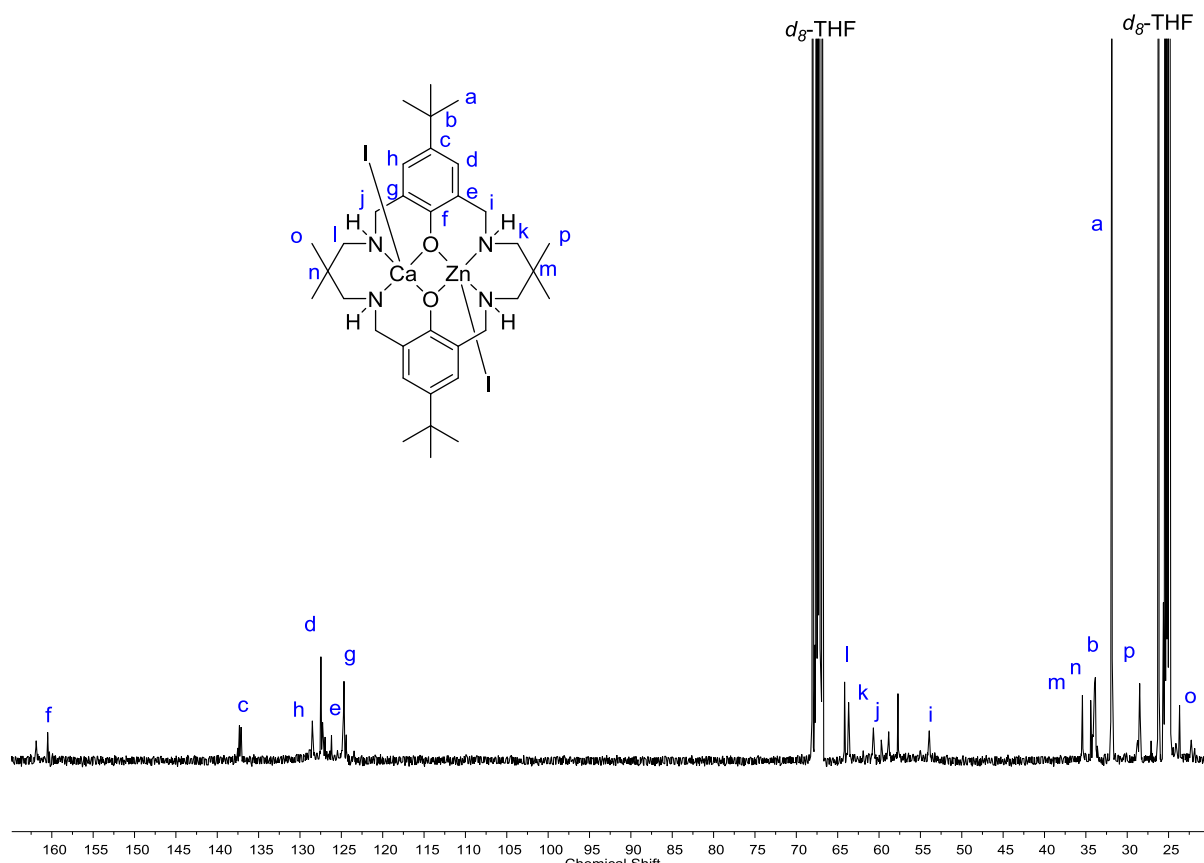


Figure S63: ^{13}C NMR of complex **9a** (d_8 -THF, 298 K).

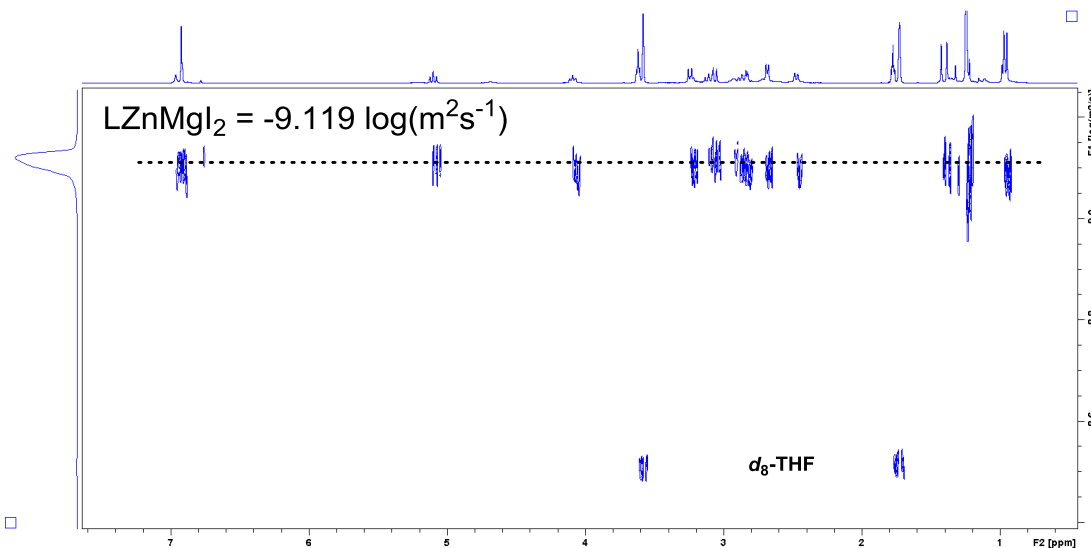


Figure S64: 2D DOSY NMR of **8a** (d_8 -THF, 298 K).

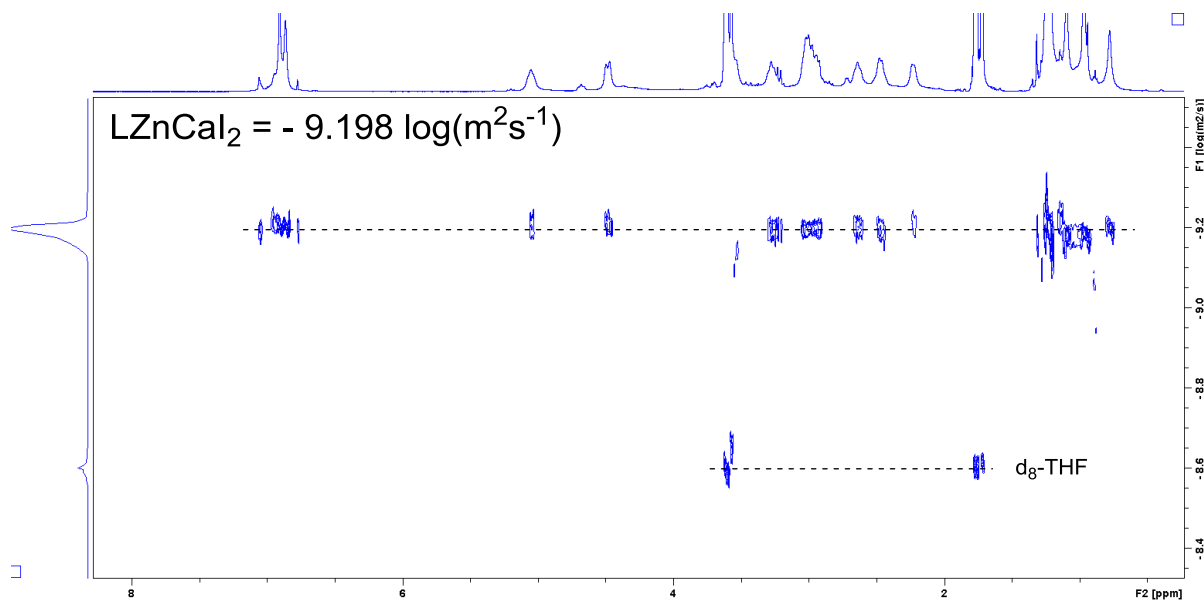


Figure S65: 2D DOSY NMR of **9a** (d_8 -THF, 298 K).

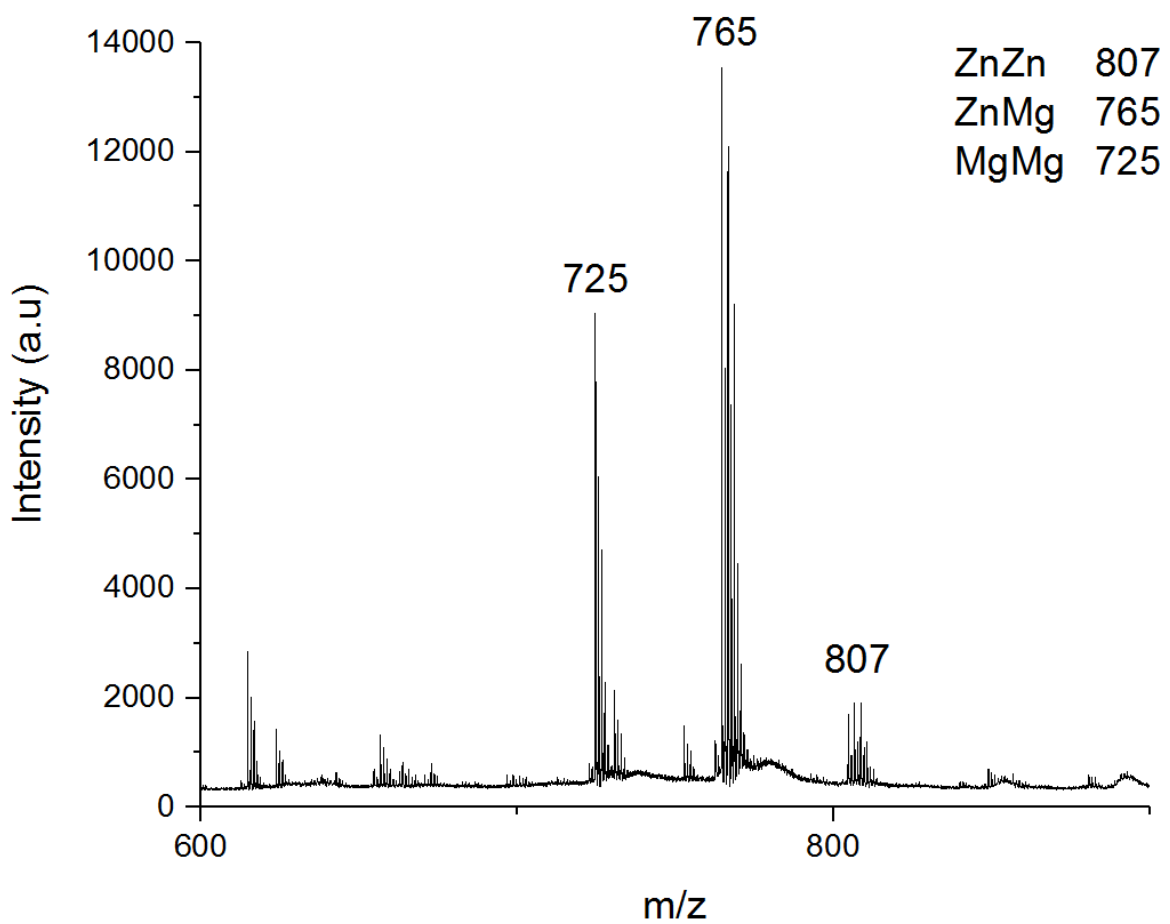


Figure S66: MALDI-ToF of complex **8a**.

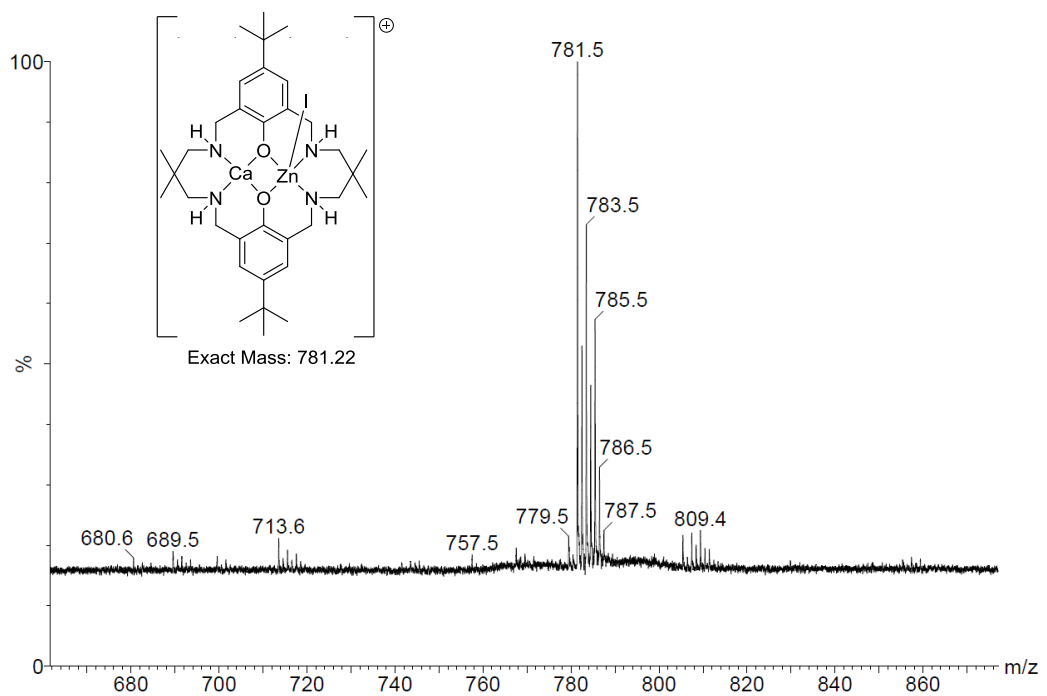


Figure S67: MALDI-ToF mass spectrum of **9a**.

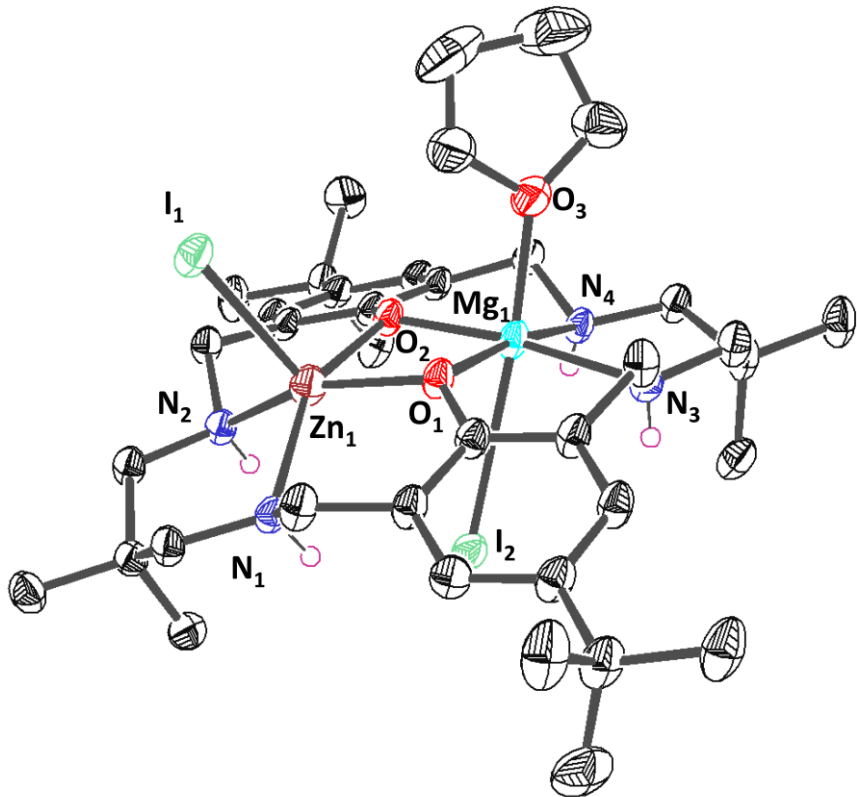


Figure S68: ORTEP representation of the molecular structure of **8a**, with disorder and hydrogen atoms (excluding N-H) omitted for clarity with thermal ellipsoids represented at 30 %.

Table S5: Selected bond lengths (\AA) and angles ($^{\circ}$) for complex **8a**.

Bond	Bond Length (\AA)	Bond	Bond Angle ($^{\circ}$)
N (1) – Zn (1)	2.13(6)	N (1) – Zn (1) – O (2)	150.0(5)
N (2) – Zn (1)	2.13(4)	N (2) – Zn (1) – O (1)	155.1(8)
O (1) – Zn (1)	2.08(9)	I (1) – Zn (1) – O (1)	103.7(6)
O (2) – Zn (1)	2.10(4)	N (3) – Mg (1) – O (2)	172.8(9)
I (1) – Zn (1)	2.68(2)	N (4) – Mg (1) – O (1)	169.5(5)
I (2) – Zn (1)	3.59(9)	O (3) – Mg (1) – O (1)	93.8(3)
N (3) – Mg (1)	2.14(8)	I (2) – Mg (1) – O (1)	172.8(4)
N (4) – Mg (1)	2.15(6)	Metal – Metal	
O (1) – Mg (1)	2.04(0)	Zn (1) – Mg (1)	3.06(2)
O (2) – Mg (1)	2.01(8)		
O (3) – Mg (1)	2.13(7)		
I (2) – Mg (1)	3.21(6)		

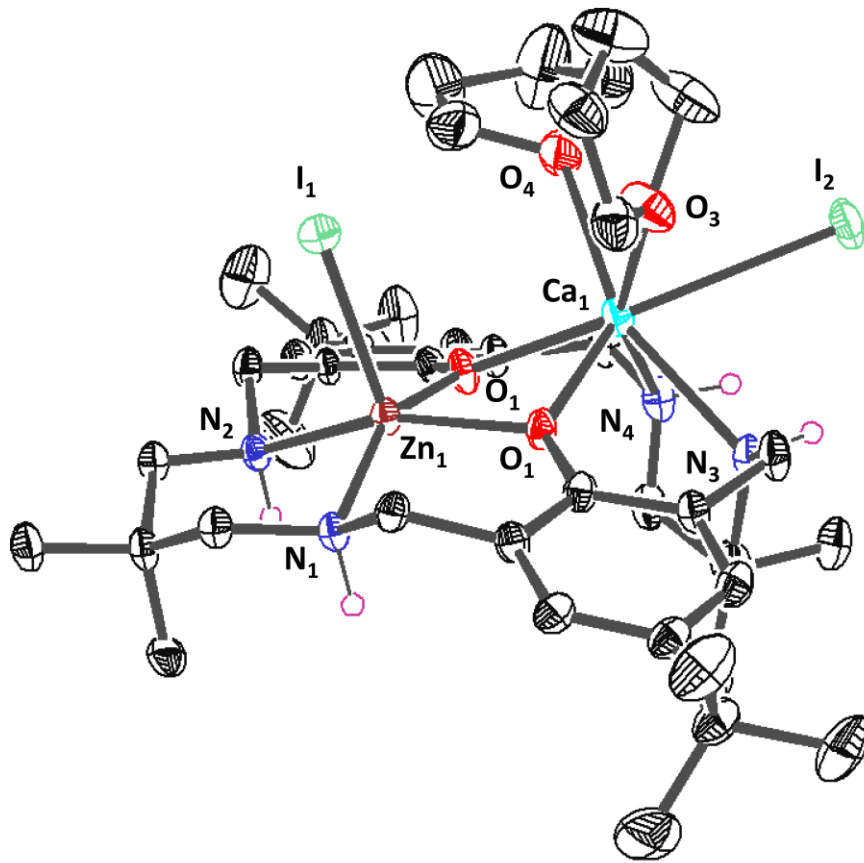


Figure S69: ORTEP representation of the molecular structure of **9a**, with disorder and hydrogen atoms (excluding N-H) omitted for clarity with thermal ellipsoids represented at 30 %.

Table 6: Selected bond lengths (\AA) and angles ($^\circ$) for complex **9a**.

Bond	Bond Length (\AA)	Bond	Bond Angle ($^\circ$)
N (1) – Zn (1)	2.12(6)	N (1) – Zn (1) – O (2)	153.4(5)
N (2) – Zn (1)	2.14(2)	N (2) – Zn (1) – O (1)	157.2(5)
O (1) – Zn (1)	2.10(1)	I (1) – Zn (1) – O (1)	101.8(0)
O (2) – Zn (1)	2.07(4)	N (3) – Ca (1) – O (2)	114.6(8)
I (1) – Zn (1)	2.68(2)	N (4) – Ca (1) – O (1)	114.1(2)
N (3) – Ca (1)	2.49(5)	O (3) – Ca (1) – O (1)	81.7(4)
N (4) – Ca (1)	2.49(0)	I (2) – Ca (1) – O (1)	140.5(3)
O (1) – Ca (1)	2.32(7)	Metal – Metal	
O (2) – Ca (1)	2.31(4)	Distance (\AA)	
O (3) – Ca (1)	2.42(9)	Zn (1) – Ca (1)	3.35(3)
O (4) – Ca (1)	2.49(3)		
I (2) – Ca (1)	3.36(7)		

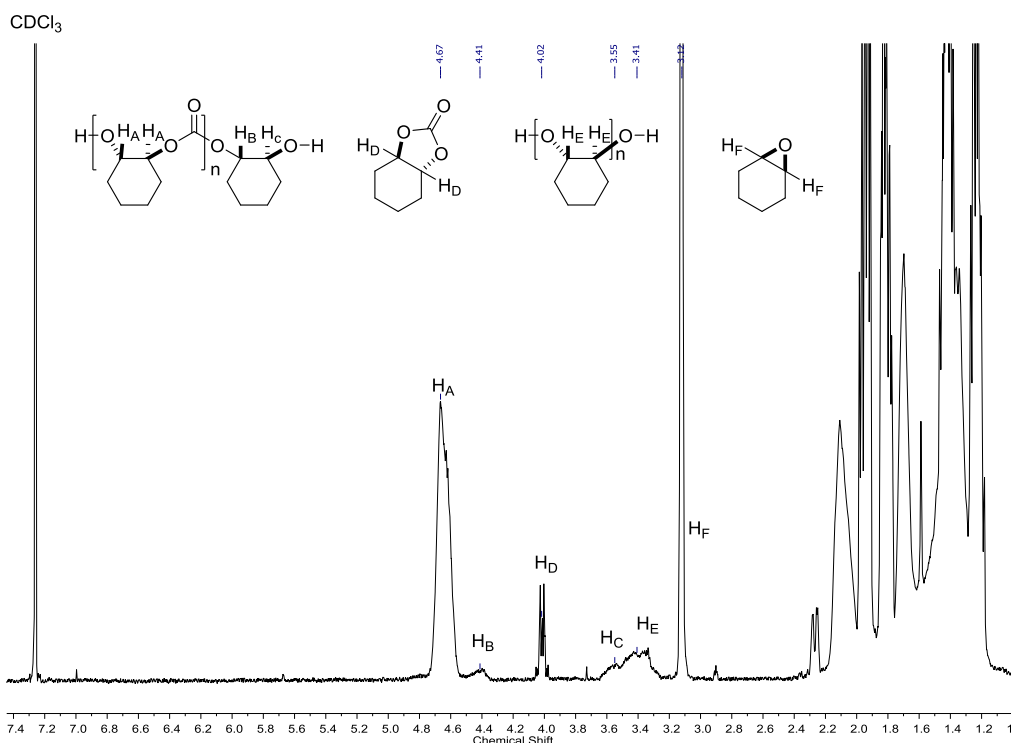


Figure S70: Representative example of ¹H NMR spectrum of a typical CO₂-CHO ring opening copolymerisation forming both poly(cyclohexene oxide) and *trans*-cyclic carbonate (CDCl₃, 298 K).

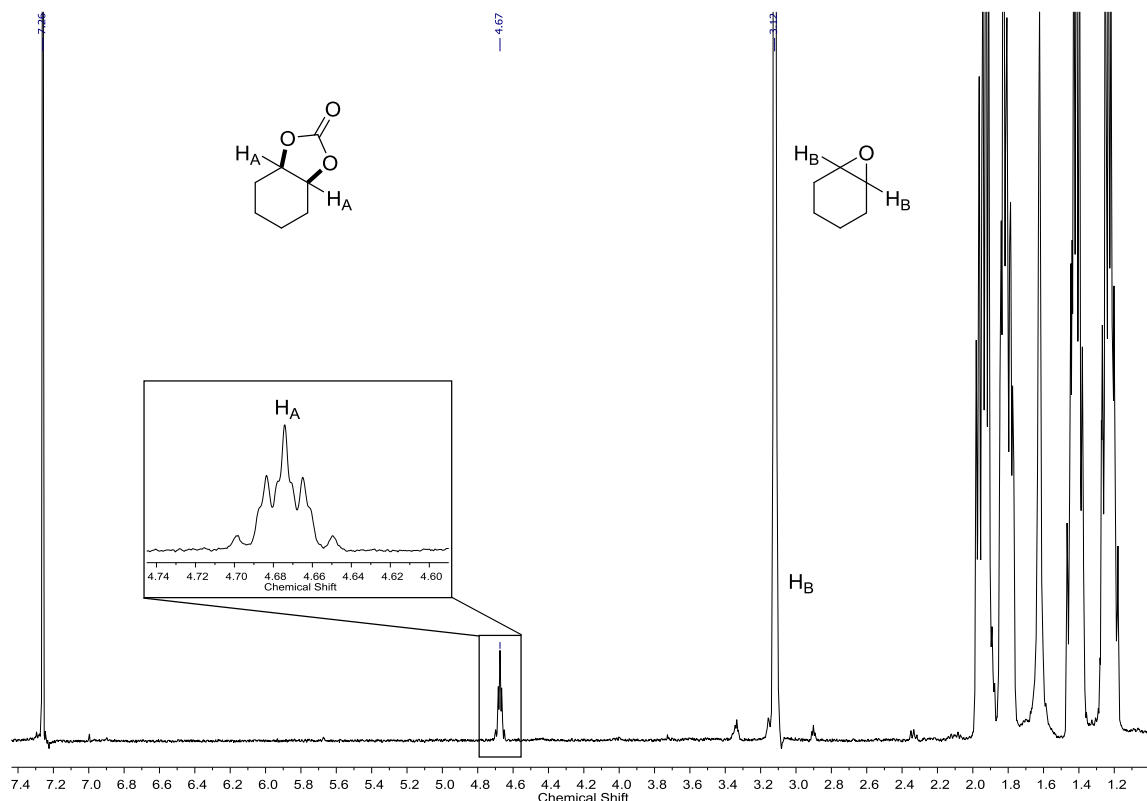


Figure S71: Representative example of ¹H NMR spectrum of a typical CO₂-CHO reaction forming the *cis*-cyclic carbonate (CDCl₃, 298 K).

Compound	1	2	4a	4b
Chemical formula	C ₆₈ H ₁₀₈ Li ₄ N ₈ O ₄	C ₆₈ H ₁₀₈ N ₈ Na ₄ O ₄	C ₃₄ H ₅₄ I ₂ N ₄ O ₂ Zn ₂	C ₇₄ H ₁₁₀ F ₆ N ₄ O ₁₂ Zn ₂
Formula weight	1129.38	1193.58	999.43	1492.39
Temp (K)	173(2)	150(2)	173(2)	150(2)
Space group	Monoclinic, C 2/c	Monoclinic, P2 ₁ /n	Monoclinic, P2 ₁ /n	Triclinic, P-1
<i>a</i> (Å)	13.65176(11)	13.2851(4)	9.74571(17)	10.5918(4)
<i>b</i> (Å)	20.53347(18)	24.2490(7)	18.8597(3)	12.9538(4)
<i>c</i> (Å)	23.7113(2)	29.4852(10)	22.6200(5)	14.8712(6)
α (°)				106.271(3)
β (°)	92.7089(7)	93.115(3)	92.3499(19)	104.316(4)
γ (°)				91.429(3)
V (Å ³)	6639.29(10)	9484.6(5)	4154.08(14)	1888.08(13)
<i>Z</i>	4	4	4	1
D _{calcd} (Mg/m ³)	1.130	0.836	1.598	1.313
Crystal size (mm)	0.23 X 0.13 X 0.05	0.20 X 0.18 X 0.05	0.22 X 0.13 X 0.05	0.18 X 0.18 X 0.10
Theta range for data collection (°)	3.732 to 73.725	3.512 to 76.932	2.340 to 28.256	3.210 to 75.910
μ (mm ⁻¹)	(Cu, K α) 0.531	(Cu, K α) 0.563	(Mo, K α) 2.681	(Cu, K α) 1.411
Reflections collected	19802	76624	14387	19260
Unique reflections	6547 [R _{int} = 0.0207]	19706 [R _{int} = 0.0793]	8344 [R _{int} = 0.229]	7787 [R _{int} = 0.0501]
Data Completeness to [θ]	99.8% [67.684]	100.0% [67.684]	99.0% [25.242]	100.0% [67.684]
Data/restraints/parameters	6547 / 4 / 405	19706 / 132 / 833	8344 / 61 / 483	7787 / 72 / 506
R1 (all data)	0.0394 (0.0445)	0.1002 (0.1411)	0.0333 (0.0503)	0.0629 (0.0758)
wR2 (all data)	0.1051 (0.1094)	0.2740 (0.3245)	0.067 (0.0658)	0.1720 (0.1873)
Goodness-of-fit on F ²	1.046	1.039	1.014	1.080
Largest diff. peak and hole (e Å ⁻³)	0.451 and -0.207	1.002 and -0.489	0.765 and -0.427	0.698 to -0.668

Compound	5b	8a	9a
Chemical formula	C ₄₆ H ₇₀ F ₃ LiN ₄ O ₆ S ₂ Zn	C ₄₆ H ₇₈ I ₂ MgN ₄ O ₅ Zn	C ₆₂ H ₁₁₀ CaI ₂ N ₄ O ₉ Zn
Formula weight	968.49	1110.60	1414.78
Temp (K)	150(2)	150(2)	150(2)
Space group	Triclinic, P-1	Triclinic, P-1	Monoclinic, P2 ₁ /n
<i>a</i> (Å)	12.1745(4)	12.7937(3)	12.0447(2)
<i>b</i> (Å)	13.4531(4)	15.2136(5)	19.3383(4)
<i>c</i> (Å)	16.6606(6)	15.7314(6)	29.1641(7)
α (°)	107.876(3)	70.554(3)	
β (°)	91.914(3)	67.441(3)	94.498(2)
γ (°)	103.978(3)	73.188(2)	
V (Å ³)	2502.97(15)	2620.08(16)	6772.1(2)
<i>Z</i>	2	2	4
D _{calcd} (Mg/m ³)	1.285	1.408	1.388
Crystal size (mm)	0.30 X 0.25 X 0.15	0.20 X 0.15 X 0.05	0.25 X 0.05 X 0.02
Theta range for data collection (°)	2.806 to 76.642	3.807 to 76.271	3.804 to 76.343
μ (mm ⁻¹)	(Cu, K α) 1.952	(Cu, K α) 10.358	(Cu, K α) 8.746
Reflections collected	21139	27471	49977
Unique reflections	10383 [R _{int} = 0.0308]	10794 [R _{int} = 0.0507]	14037 [R _{int} = 0.0626]
Data Completeness to [θ]	100.0% [67.684]	100.0% [67.684]	99.9% [67.684]
Data/restraints/parameters	10383 / 205 / 709	10794 / 0 / 558	14037 / 433 / 789
R1 (all data)	0.0467 (0.0525)	0.0545 (0.0719)	0.0599 (0.0750)
wR2 (all data)	0.1209 (0.1249)	0.1402 (0.1586)	0.1514 (0.1602)
Goodness-of-fit on F ²	1.081	1.024	1.083
Largest diff. peak and hole (e Å ⁻³)	0.635 and -0.444	1.931 and -1.718	1.152 and -0.848

References

1. Zhu, Y.; Romain, C.; Williams, C. K., Selective Polymerization Catalysis: Controlling the Metal Chain End Group to Prepare Block Copolyesters. *J. Am. Chem. Soc.* **2015**, *137* (38), 12179-12182.